Identification and Targeting of Collagen in the Capsule of Rat Knees with Immobilization-Induced Flexion Contractures

By Kayleigh Wong

A thesis submitted in partial fulfillment of the requirements for the degree of Master of Science, Biochemistry

Submitted: February 2015
Defended: April 7, 2015
Final Submission: April 2015

University of Ottawa
Faculty of Medicine
Department of Biochemistry, Microbiology and Immunology

Supervisor: Dr. Odette Laneuville

ABSTRACT

Immobility causes joint contractures, loss in range of motion (ROM), notably in elderly and bed-ridden patients. In a rat knee immobilization flexion contracture (FC) model, the posterior capsule contributes to irreversible limitation of ROM. Through microarray, extracellular matrix and collagen pathways were identified as differentially expressed in the posterior capsule of knees with FC. We hypothesized that intra-articular injection of collagenases in rats with knee FC will interfere with collagen in the capsule and allow increased ROM. After four weeks of hind-limb immobilization, rats develop knee FC; two weeks of remobilization with collagenase treatment showed increased ROM compared to buffer injected knees of 8.043° (p-value=0.046). Histological analysis of knee sections revealed changes in collagen content of the extracellular matrix in posterior capsule. *In vitro* incubation of rat capsules with collagenases confirmed changes in collagen. Along with current rehabilitation methods, treatment with collagenase may augment ROM recovery from knee joint contractures.

ACKNOWLEDGMENTS

First I'd like to thank my thesis supervisor Dr. Odette Laneuville for her mentorship, direction, and patience.

My thesis advisory committee, Dr. Martin Pelchat and Dr. Guy Trudel, for their guidance.

My thesis examiners Dr. Guy Trudel and Dr. Mary Alice Hefford for their time and constructive criticisms.

Members of the Bone and Joint Lab: Winnie Nie, Dr. Mark Campbell, and Dr. Hans Uhthoff for their contributions and advice.

Collaborators: Génome Québec, Dr. Paola Sebastiani and Dr. Fangui Sun, Dr. Ana Giassi and the uOttawa Histology Core Facility, Eileen Franklin and the uOttawa Animal Care Facility

Funding for my graduate studies was provided by grants from the University of Ottawa and the Government of Ontario in the form of OGS, QEII-GSST, and Excellence scholarship awards. Funding for this project was provided by a grant from the Canadian Institutes of Health Research awarded to Dr. Odette Laneuville and Dr. Guy Trudel.

My loved ones for their encouragement and support.

Table Of Contents

LIST OF ABBREVIATIONS

AGEs	advanced glycation end products
AGPAT-9	1-acylglycerol-3-phosphate O-acyltransferase 9
B-Inj	buffer-injected
CAGED	Cluster Analysis of Gene Expression Dynamics
cDNA	cloned deoxyribonucleic acid
CHAD	chondroadherin
ColG	collagenase G (type 1) from *Clostridium histolyticum*
ColH	collagenase H (type 2) from *Clostridium histolyticum*
COLI	collagen type 1
COLIII	collagen type 3
ConLat	contralateral
cRNA	cloned ribonucleic acid
CTGF	connective tissue growth factor
CYR61	cysteine-rich angiogenic inducer 61
DAB	diaminobenzidine
DAVID	Database for Annotation, Visualization, and Integrated Discovery
EDTA	ethylenediaminetetraacetic acid
H&E	hematoxylin and eosin
HSP47	heat shock protein 47
ICU	intensive care unit
IHC	immunohistochemistry
GO	gene ontology
KEGG	Kyoto Encyclopedia of Genes and Genomes
knee FC	knee flexion contracture
MMP	matrix metalloproteinase
mRNA	messenger ribonucleic acid
MT	Masson trichrome
OA	osteoarthritis
P4HB	prolyl 4-hydroxylase, beta peptide
PCK1	phosphoenolpyruvate carboxykinase 1
PCR	polymerase chain reaction
PGHS	prostaglandin endoperoxide H synthase
RGB	red green blue
ROM	range of motion
RT-PCR	reverse transcription polymerase chain reaction
SDS-PAGE	sodium dodecyl sulfate polyacrylamide gel electrophoresis
SEM	standard error of the mean
SRY-box *9*	sex determining region Y-box 9
TBS	tris-buffered saline
TGFβ	transforming growth factor beta
TIMP	tissue inhibitor of metalloproteinases
TKA	total/tri-compartmental knee arthroplasty
X-Inj	Xiaflex®-injected

LIST OF FIGURES

LIST OF TABLES

1 INTRODUCTION

1.1 Joint Contractures

A joint contracture is defined as a limitation in the passive range of motion (ROM) of a joint [1,2]. Passive range of motion describes movement initiated from an outside force, such as a physiotherapist, where active range of motion describes movement without assistance and initiated by the patient [2]. Contractures are characterized as stiffness around a joint that prevents joint mobility and full ROM [1,2]. Joint contractures are a complication of heterogeneous disorders that are multifactorial and occur through a variety of etiologies. They can arise from congenital or neurological disorders [3,4], joint injury or be secondary to other diseases such as rheumatoid arthritis and osteoarthritis (OA) [5], and they are known to occur secondary to immobility [1,6,7,8,9].

Many different joint structures can be involved in limiting ROM, including changes in the articular structures (bone, cartilage, capsule) and non-articular structures (muscle, tendon, and skin) [1]. Joint contractures occur in patients of all ages, from newborns with congenital diseases that cause contractures, to the elderly, especially those who have limited mobility such as Alzheimer's disease or Parkinson's patients [1]. Contractures can occur post-injury, and even minor losses in range of motion can disadvantage active or athletic individuals [10]. Injuries like burns can lead to contractures caused by limitation from scarred skin [1]. Patients with congenital disorders such as arthrogryposis multiplex congenita, which occurs in approximately 1/3000 live births, will often have more than one non-progressive joint contracture [3]. Contractures are common in people with neurological problems such as patients with spinal cord or brain injury and cerebral palsy [2]. A myogenic cause of contractures in these patients is spasticity (muscle stiffness) caused by changes in the motor neurons [1]. While spasticity can be treated, other structures can be affected through disuse and a contracture can still remain [1]. Another type of contracture occurs in Dupuytren's disease, where a fibrotic transformation of the palmar fascia (connective tissue) in the hand causes contractures in fingers and thumb [11]. It is difficult to associate a joint contracture with a single type of tissue as there are often multiple

factors involved in the loss of ROM. Joint contractures, especially in multiple limbs, leaves patients bedridden or requiring full-time care, can cause pressure sores or ulcers due to immobility, or can lead to infection if patients are unable to practice standard hygiene [1].

1.2 Knee Flexion Contractures

Any mobile joint can develop a contracture, which is diagnosed through physical examination by a physician. A universal goniometer, similar to a protractor, is the diagnostic instrument used to compare passive range of motion of the affected joint with the ROM of the contralateral joint or known normal values [1]. Joint contractures are named for the joint involved and the direction opposite to the lack of range of motion. For example, an elbow extension contracture is "stuck" in extension and is unable to reach full flexion. A knee flexion contracture (knee FC) is defined as lacking full extension of the knee [1]. As little as 5° in lack of knee extension can cause a limp [7]. When a healthy knee is fully extended, the joint is able to bear weight efficiently [12]. If the knee is unable to fully extend, the energy required for stabilization during standing or walking increases, which causes normal daily activities to be tiring and cumbersome, or even dangerous due to falls [13]. Along with a limp and disability, contractures can also cause pain, pressure ulcers, and disfigurement [2]. There are economic consequences to disability from joint contractures, including compensation benefits [14], loss of productivity, and increased hospital stays [8].

Knee flexion contractures can be caused by multiple factors and can involve multiple tissues, but it is agreed that they can arise secondary to immobility [1,6,7,8,9,15,16,17]. Restricting movement is an ancient treatment for musculoskeletal diseases, and is a natural and instinctive treatment for pain [1,15]. Disuse of a joint, however, induces structural changes of the tissues [1], which can be irreversible [14,18]. In institutionalized elderly, one study reported that over 70% of those who were immobile had at least one contracture in a major joint, compared to mobile patients who had none [19]. In the intensive care unit (ICU), where there is prolonged immobility due to critical illness, a stay of two weeks or longer was associated with at least one functionally significant contracture in a third of patients [8]. A follow up study conducted 3.3 years after discharge reported that over 70%

of those with contractures in the ICU still had self-reported issues with mobility [20], suggesting potential irreversibility with immobility-associated contractures. Immobility is prevalent and is a burden in nursing homes, hospitals, and outpatient communities, and as the global population becomes older, more people are at risk for developing contractures [18].

A knee contracture can arise from a variety of genetic (arthrogryposis multiplex congenita) and environmental (immobility) factors, or often from a combination of the two [3,21]. There is evidence that immobility is a factor in the development of a joint contracture in patients with genetic diseases. For example, neuromuscular diseases commonly have joint contractures as a symptom, including Duchenne, Becker, and Emery Dreifuss muscular dystrophies [21]. Static positioning of the limbs is an important cause of contracture formation in these patients [21]. Arthrogryposis multiplex congenita is a heterogeneous group of genetic disorders defined by two or more joint contractures at birth [3]. A common pathway in this group is a lack of fetal joint movement, highlighted by the observation of higher prevalence in multiple births [3].

Contractures can develop with direct injury to the joint, however they can also occur with other injuries such as fracture, joint dislocation, or burns [1]. Trauma to the knee can induce a contracture, such as a tear in ligament or tendon, or trauma caused by surgery. A 3.6% incidence rate in patients undergoing total knee arthroplasty (TKA) has been reported at 2 years postoperative [12]. While this may seem to be a low percentage, every year there are 130,000 knee replacements performed in the United States alone for patients with disabling arthritis [12]. This corresponds to more than 4630 new patients who develop flexion contractures each year in the USA [12]. Contractures post-TKA corresponds with lower patient satisfaction, mostly due to pain and lack of mobility, and may require additional revision surgery which risks postsurgical complications [22].

1.3 Current Treatments for Knee Flexion Contractures

Preventing joint contractures is the best course of action, however most contractures are diagnosed when they are chronic, at which point it is too late to induce a

response with current treatments. Contractures develop slowly over time, and preventing contractures can only be employed with early diagnosis. For patients who have undergone joint surgery, by keeping pain under control and actively and/or passively exercising joints at full ROM, the formation of joint contractures can be avoided [1,7]. Once a contracture has developed, rehabilitation with physiotherapy is the most common treatment [1]. Rehabilitation includes stretching and exercise; heating the soft tissue around the joint (i.e. with Ultrasound) can improve elasticity when stretching [1]. Dynamic bracing can be used, which involves maximal stretching held in place with a splint. However, with this strategy there is a risk of breaking skin, ulcer formation, joint dislocation, and pain [1]. Although progress can be made with physiotherapy, it is not clear if passive movements are generally effective for the treatment or prevention of contractures [2]. Stretch is also less effective for people with neurologic conditions (stroke, spinal cord, brain injury, or cerebral palsy) [4].

As a last resort and only if the contracture is severe, joint capsule release surgery is an option [1,7]. Although it can be effective, the surgery is reported as technically demanding [7]. Sectioning of the posterior capsule in patients with knee FC also involves risk of creating instability in the joint and potential damage to the neurovasculature structures running through the back of the knee [5]. In children with cerebral palsy, posterior capsulotomy has a failure rate of over 35% [23]. Overall, current treatments are not effective and the disease permanently impairs the physical function of individuals.

1.4 Animal Models

A rat model has been developed by the Bone and Joint Laboratory at the University of Ottawa in order to study the pathophysiology of joint contractures secondary to immobilization (**Figure 1a**) [24]. Methodological differences in duration and manner of immobilization (plaster cast, internal fixation, injury to the joint), species used (rabbits, dogs, rats), and which joint is studied (shoulder, knee, ankle) makes comparisons between studies difficult and may explain divergent results [15,24,25,26]. The rat knee flexion

a

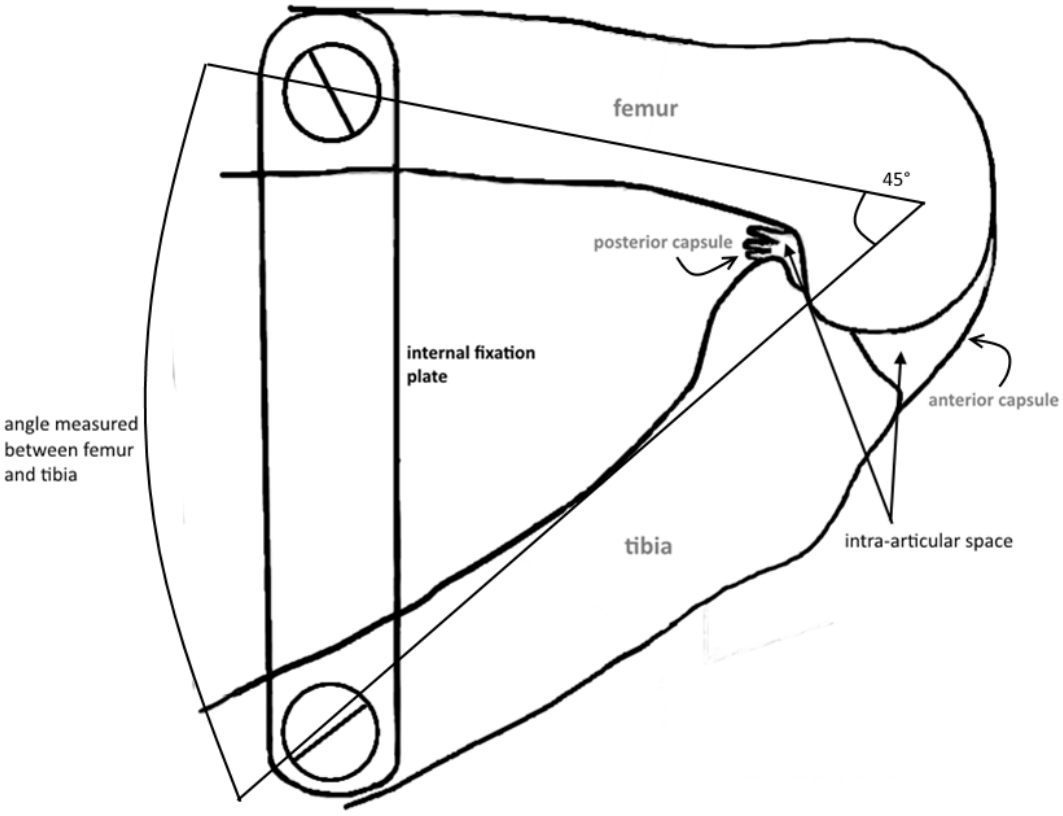
femur
45°
posterior capsule
internal fixation plate
anterior capsule
angle measured between femur and tibia
tibia
intra-articular space

b

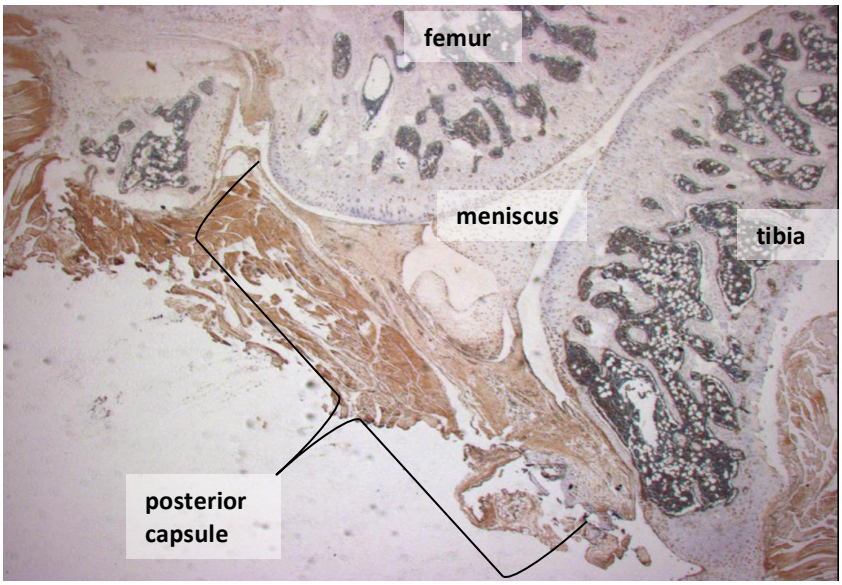
femur
meniscus
tibia
posterior capsule

Figure 1. Rat Model for Knee Flexion Contractures Induced by Immobilization with an Internally Fixed Plate. a) In the rat knee FC model, screws are surgically inserted through the proximal femur (thigh bone) and distal tibia (shin bone) to hold the Delrin® plate which is placed internally under skin and muscle, but away from the joint itself. The knee joint is therefore immobilized at a 45° angle between the femur and tibia. In flexion, the anterior capsule of the knee joint is stretched while the posterior capsule is folded. Sham-operated animals have the screws inserted with no plate. In the following research project, four weeks of immobilization is followed by surgical removal of the plate and injection of collagenase or buffer into the intra-articular space. ROM in extension of the knee is reported as the angle between the femur and tibia measured at four increasing torques. **b)** Image of a stained (DAB and hematoxylin) sagittal section of a rat knee joint (3.3X), not in flexion, highlighting the position of the posterior capsule. The dense, fibrous connective tissue is lined with synovium (containing synoviocytes) and has nerves and blood vessels passing through. While consisting mostly of fibroblasts, the capsule is composed of other types of cells including adipocytes, synoviocytes, and endothelial cells.

contracture model uses a sturdy internal fixation device composed of a plate fixed with screws in the proximal femur and distal tibia of one of the hind limbs. This model does not directly interfere with or violate the joint and therefore allows for examination of the changes in joint structures strictly due to immobilization. The control rats for this model are sham-operated; the surgery is performed with screws inserted but the plate is omitted. The knee is immobilized at a 45° angle between the femur (thigh bone) and tibia (shin bone). Post-surgery rats are unable to move the immobilized knee, but they are able to load the joint with their weight. A study of 250 rats that were immobilized for up to 32 weeks and left to spontaneously recover (remobilized) for up to 48 weeks revealed relative articular and muscular contributions to contracture and the minimal potential for spontaneous reversibility [27]. Up to eight weeks of immobilization, there was a gradual loss of ROM that thereafter plateaued [27]. Fixation periods of less than two weeks caused knee FCs that were mostly due to muscular limitation, and contractures were reversible with remobilization [27]. With four or more weeks of immobilization, articular structures contributed more to the limitation of ROM and these contractures were irreversible after all tested durations of recovery [27]. Immobility is known to cause muscle atrophy [28,10], but the nature of muscle tissue allows recovery through exercise [10]. Articular structures such as the knee capsule do not recover as easily.

Previous studies have shown that the main articular structure that prevents full ROM in contractures is the posterior capsule [7,14,18,29,30,31,32,33,34], connective tissue located at the back of the knee that is attached to the femur and tibia a few centimeters (in humans) above and below the joint space (**Figure 1b**) [35]. In the rat model, contractures following immobilization of eight weeks failed to recover after four weeks of remobilization [34]. Sectioning of the musculature around the joint did not allow full ROM and it was only after cutting the posterior capsule that full ROM was regained [34]. From these results, the posterior capsule has become a focus point and investigation of the molecular mechanisms involved in the capsule during immobilization was pursued.

1.5 The Capsule in Joint Contractures

Changes in the capsule associated with joint contractures have been reported in many different animal models and in humans. Structurally, the capsule forms a sleeve around synovial joints (such as knees, shoulders, elbows, etc.) and keeps synovial fluid in place in the intra-articular space between the bones [36]. It is dense and fibrous connective tissue composed mostly of bundles of collagen fibers (80% collagen type I and some collagen type III) in extracellular matrix [37], however it is also a through point for nerves and blood vessels [36]. The capsule is lined with synovium that contains Type A (macrophage-like) and Type B (fibroblast-like) synoviocytes [16]. Immobilization in flexion stretches the anterior part of the capsules and loosens the posterior part of the capsule, creating folds (**Figure 1a**).

Disruptions in collagen synthesis, organization, and post-translational modifications have been reported by multiple groups as associated with joint contractures caused by immobilization and/or trauma to the joint [14,18,38]. In the internal-fixation rat model, immunohistochemistry (IHC) experiments showed higher type I collagen levels and lower type III collagen levels in capsule cells of immobilized legs compared to sham-operated legs, suggesting that the contractures were caused by fibrosis (excess fibrous connective tissue) [38]. An older study in rats and dogs provided evidence for an increase in collagen synthesis in the articular tissue after immobilization [14]. In a rat model from a different group, there was a significant increase in biochemical reduction of cross-links of collagen in the form of advanced glycation end products (AGEs) [18]. These post-translational cross-links are known to increase stiffness in connective tissue [18,39]. There is a prevalence of several rheumatologic conditions in patients with diabetes mellitus, thought to be caused by an excess of AGEs because of the increased availability of glucose [40]. The previous rat study noted disorganization of collagen fibers in the posterior capsule compared to non-immobilized joints and a decrease in glycosaminoglycans was also reported in immobilized capsule [18]. These long polysaccharide chains retain water and their loss may allow further collagen crosslinking [41]. Other changes in the posterior capsule include fewer proliferating synoviocytes and a decrease in synovial intimal length [33]. A shortening of the

posterior capsule combined with fibrosis may be contributing to the irreversibility of knee flexion contractures.

1.6 Gene Expression Changes in Joint Contractures

Changes in gene expression have been associated with the development of joint contractures in both human diseases and animal models. More than 150 specific disorders under the classification of arthrogryposis multiplex congenita (multiple contractures at birth) have been associated with mutations in specific genes [42]. The genes identified are part of myopathic pathways, neuropathic pathways, and/or are involved in connective tissues [42]. Using the rat knee contracture model, changes in gene expression in the chondrocytes of articular cartilage have been identified. In immobilized cartilage there were increases in prothrombin expression [43], protein levels of cyclooxygenases (PGHS-1 and PGHS-2) [44], mRNA levels of chitinase like-3 [45], and myeloid cell leukemia-1 transcript [46]. Experiments using different inbred rat strains provided evidence of a genetic contribution to immobilization-induced contractures. Dark Agouti and Fisher 344 rat strains developed more severe contractures than Augustus Copenhagen Irish and Brown Norway strains [47], indicating that there are intrinsic genetic factors that influence susceptibility to and severity of contractures.

There is evidence of changes in gene expression in the posterior capsule in the development of contractures. Genome-wide gene expression analysis of posterior capsule in patients with OA and knee FC showed an expression decrease in casein mRNA, and increases in chondroadherin (*CHAD*), angiogenic inducer *CYR61*, and *SRY*-box 9; four genes that have been associated with tissue fibrosis [5]. Protein levels of cyclooxygenases (PGHS-1 and PGHS-2) decreased in the synovial lining of capsule of immobilized rat knees [44]. Changes in gene expression in the anterior capsule of post-traumatic human elbow contractures have been studied using reverse transcription polymerase chain reaction (RT-PCR). Researchers found increased expression of collagen types I, III, and V, biglycan, matrix metalloproteinases (MMPs) -1, -2, -9, -13, and -15, and a decrease in tissue inhibitors of MMPs (TIMPs) [48]. In another similar study, the same group showed that mRNA levels

were increased for transforming growth factor-β1 (TGF- β1), connective tissue growth factor (CTGF), and α-smooth muscle actin [25]. Increases in TGFβ-1 and CTGF mRNA were also identified in rat immobilized posterior knee capsule using *in situ* hybridization [49]. These growth factors have been identified as fibrogenic as well as myofibroblast up-regulators, and actin is a myofibroblast marker [25]. An Increase in myofibroblasts has been correlated with fibrotic diseases [11,32,50,51].

Based on these genetic results and the apparent duration-dependence of joint contracture development, a time-series genome-wide microarray experiment was designed and conducted before I joined the lab. Microarray is a high-throughput method of quantifying mRNA expression and can be used to examine the entire transcriptome. The benefit of using genome-wide expression analysis, compared to PCR techniques, is that it is an unbiased approach that examines all possible pathways that may be involved. In a brief summary of microarray technology, RNA is extracted from samples and a cDNA library is created. *In vitro* transcription is used to produce biotin-labelled cRNA that is then fragmented and hybridized with an array. The array contains probes sets of known hybridization sequences (and negative controls) for each known mRNA transcribed from the genome. Occasionally there is more than one probe set per gene. Arrays are visualized, normalized against spike-ins and/or negative controls, and the amount of expression for each probe set is quantified. [52]

A microarray experiment was conducted for the posterior capsule of rat knee joints over a time course in order to examine the dynamic changes in gene expression over the development of a contracture secondary to immobilization [publication under review]. Rats were either immobilized or sham-operated and posterior capsule was harvested at 1, 2, 4, 8, or 16 weeks post-operation. Since there is an apparent point of no return for reversibility of immobilization-induced contractures that occurs at around four weeks, this indicates that there is a dynamic and time-dependent process. This was the rationale for using a time-series expression experiment in order to detect temporal changes in gene expression. This decision created a statistical problem, given that a static comparison would not be appropriate in analysis of genome-wide expression over a time series. The Cluster Analysis

of Gene Expression Dynamics (CAGED) algorithm was chosen to determine which genes were differentially expressed based on patterns of expression and to take all time points into consideration [53]. A summary of the work previously done is included in this text. My work begins with analysis of the microarray results, specifically with functional analysis in pursuit of a hypothesis for a pharmacological intervention for joint contractures.

1.7 Collagen

Collagen constitutes one third of proteins in humans [54], with type I collagen as the most abundant protein in higher organisms [54,55]. There are 28 identified members of the collagen family [39] and they are found in virtually every type of tissue [55]. Of the main collagens, types I, II, III, and V are fibrillar and provide structure [56]. Collagen type I is abundant in most connective tissues (skin, bone, tendon, etc.) and type II is the major component of cartilage [55]. Type IV collagen composes basal lamina and is critical in the structure of neurovasculature [56]. Collagen is an insoluble extracellular matrix protein that provides tensile strength due to its highly organized structure [55]. The amino acid sequence of collagen is highly repetitive; every third residue is a glycine and approximately 20% of the residues are proline or hydroxyproline (post-translational modification of proline by the enzyme prolyl hydroxylase) [55,57]. The most common amino acid residue triplet is Pro-Hyp-Gly occurring at about 10% [39]. With a high percentage of proline, fibrillar collagen has a triple helical structure. Collagen type I, the most abundant type in the joint capsule, is a heterogeneous triple helix, composed of two α1(I) and one α2(I) molecule; collagen types II and III are homogeneous helices composed of three α1(II) or α1(III) polypeptide chains, respectively. A single molecule of collagen with its three polypeptide chains is called tropocollagen; tropocollagen type I is a rigid, rod-shaped, right-handed superhelix, 300nm in length by 1.5nm in diameter [39].

The fibrillar collagens assemble into quaternary banded fibrils often composed of several different types of collagen [55]. Studies on type I collagen structure reveal fibrils packed in hexagonal arrays that are 2μm in length and 300nm in diameter [55]. Hydrogen bonds and hydrophobic interactions support this highly stable conformation lending to a

long half-life of over 100 years for collagen II molecules in cartilage tissue [39]. Collagen fibrils are also highly intramolecularly and intermolecularly cross-linked, derived from the lysine and histidine side chains [55]. It is possible that the organized pattern of a collagen "weave" is what provides the rigid rods with elasticity, similar to a nylon stocking [14,15]. Genetic diseases involving collagen including osteogenesis imperfecta diseases, Ehlers-Danlos syndromes, and Marfan syndromes are caused by inherited abnormal collagen structure that induces helical relaxation and hyper-flexibility in joints [58].

1.8 Collagenases and Other Fibrotic Contractures

Contractures due to fibrosis occur throughout the body and not just at synovial joints. Dupuytren's disease is a common (about 5% of Caucasian populations), benign, fibroproliferative disorder of palmar fascia of the hands, which results in contractures in fingers [11]. In the fibrotic cord that forms in the hand, there is an increase in collagen and an increase in collagen cross-links [11,59]. Peyronie's disease is another connective tissue disorder characterized by the formation of a fibrous collagen scar in the tunica albuginea, which results in penile curvature [60]. A pharmacological protein drug treatment of collagenase injections has recently been approved for Dupuytren's and Peyronie's diseases. These injectable collagenases, under the brand name Xiaflex® (Auxillium Pharmaceuticals), are also in clinical Phase 2 trial for treatment of frozen shoulder [61], which is characterized by fibrosis in the connective tissue of the shoulder joint and loss of ROM [51]. Aside from contractures, Xiaflex® has also been proposed as a potential treatment for uterine fibroids, one of the most common tumours in reproductive age women, which contain abundant and disordered collagens [62].

In humans, highly specific matrix metalloproteinases (MMPs) are the only proteases that degrade the collagen triple helix [63]. There are over 20 MMPs that are responsible for collagen turnover in the extracellular matrix [63]. Human MMPs have a preference for fibrillar collagens and only cleave at specific sites [61]. Bacterial collagenases, specifically from the Clostridia family, are notably non-specific and have a broad substrate spectrum [54, 55]. Clostridia are anaerobic, sporulating, gram-positive bacteria [54,56]. The

pathogenic strains of the bacteria use collagenases for host colonization, to spread into tissues, and for toxin diffusion [54,57]. *Clostridium histolyticum* has been known to cause gas gangrene [64]. Its collagenases have been purified into a pharmacologic preparation in Xiaflex®. There are two types of collagenases from *C. histolyticum*, each from two different genes. *ColG* (type 1 collagenase) has two calcium binding domains, hypothesized as collagen binding domains, and *ColH* (type 2 collagenase) has one calcium-binding domain [54,57,65]. A mixture of these two collagenases has been shown to degrade type I collagen into small peptides through cleavage at multiple sites [54,57,66]. ColG preferentially makes its first cleavage near the termini while ColH cleaves closer to the center of the molecule [66]. The calcium binding domain has been shown to bind to types I, II, III, and IV collagens *in vitro* [56] and the collagenases have been shown to degrade most collagen types, with one notable exception [57]. Purified collagenases in Xiaflex® spare type IV collagen, the main collagen of neurovasculature, which makes it suitable in clinical treatments where it is important to maintain these structures, particularly in the posterior knee capsule [59].

1.9 Goal, Objectives, and Hypothesis

The overall goal is to discover a target for pharmacological treatment of knee FC, and to test the treatment in the rat knee immobilization model.

1) A time series microarray experiment comparing immobilized and sham-operated rat knee posterior capsule has been completed and identified a list of differentially expressed genes. My first objective was to complete the functional analysis of this microarray experiment and to deduce the possible pathways and molecular mechanisms involved in the development of a knee flexion contracture. A hypothesis for a molecular target and a direction for pharmacological intervention were sought from these results.
2) Test the effectiveness of intra-articular Xiaflex® injections for increasing range of motion in rat knees with flexion contractures and determine through histological analysis the effect of Xiaflex® on collagen I and III in posterior capsule.

3) Complete *in vitro* tests of the effect of Xiaflex® on collagen in posterior capsule samples from rat and human knees.

Hypothesis: If, in the rat model, extracellular collagen content and organization in the knee posterior capsule is a contributor to restricted range of motion, then knee flexion contracture can be improved with collagenase treatments.

2 MATERIALS AND METHODS

2.1 Genome-Wide Gene Expression: Microarray and Analysis

2.1.1 Abbreviated Summary of Previous Work by Dr. Odette Laneuville and the Bone and Joint Laboratory (manuscript under review)

Male adult Dark Agouti rats were immobilized at the knee joint of one hind limb with an internal plate and screw system at 45° flexion (**Figure 1a**). Sham-operated animals with screws but no plate constituted as controls (see below for more details on surgery). Sixteen rats were used for each time point: 1, 2, 4, 8, and 16 weeks; 8 immobilized and 8 sham-operated. At the end of the immobilization period, animals were euthanized and posterior knee capsules were harvested for RNA extraction with Trizol according to the protocol provided by the supplier. Sham-operated rat knees and immobilized rat knees with 2, 4, 8, and 16 weeks of immobilization that were not used for RNA extraction were fixed in formalin (10%) overnight and decalcified over 60 days in 10% ethylenediaminetetraacetic acid (EDTA) solution. These knees were embedded in paraffin and sectioned into 7µm sagittal slides for immunohistochemistry (IHC) (see below for details on cutting and IHC).

Based on quality and quantity of extracted RNA using a 2100 BioAnalyzer, samples from 4 sham-operated and 4 immobilized rats at each time point were selected for analysis using Affymetrix GeneChip microarrays (Rat Genome 230 2.0 Array). Microarray experiments were conducted at Génome Québec in Montreal and results were provided as .CEL files. Analysis of the microarray data followed the pipeline shown in **Figure 2**. Analyses

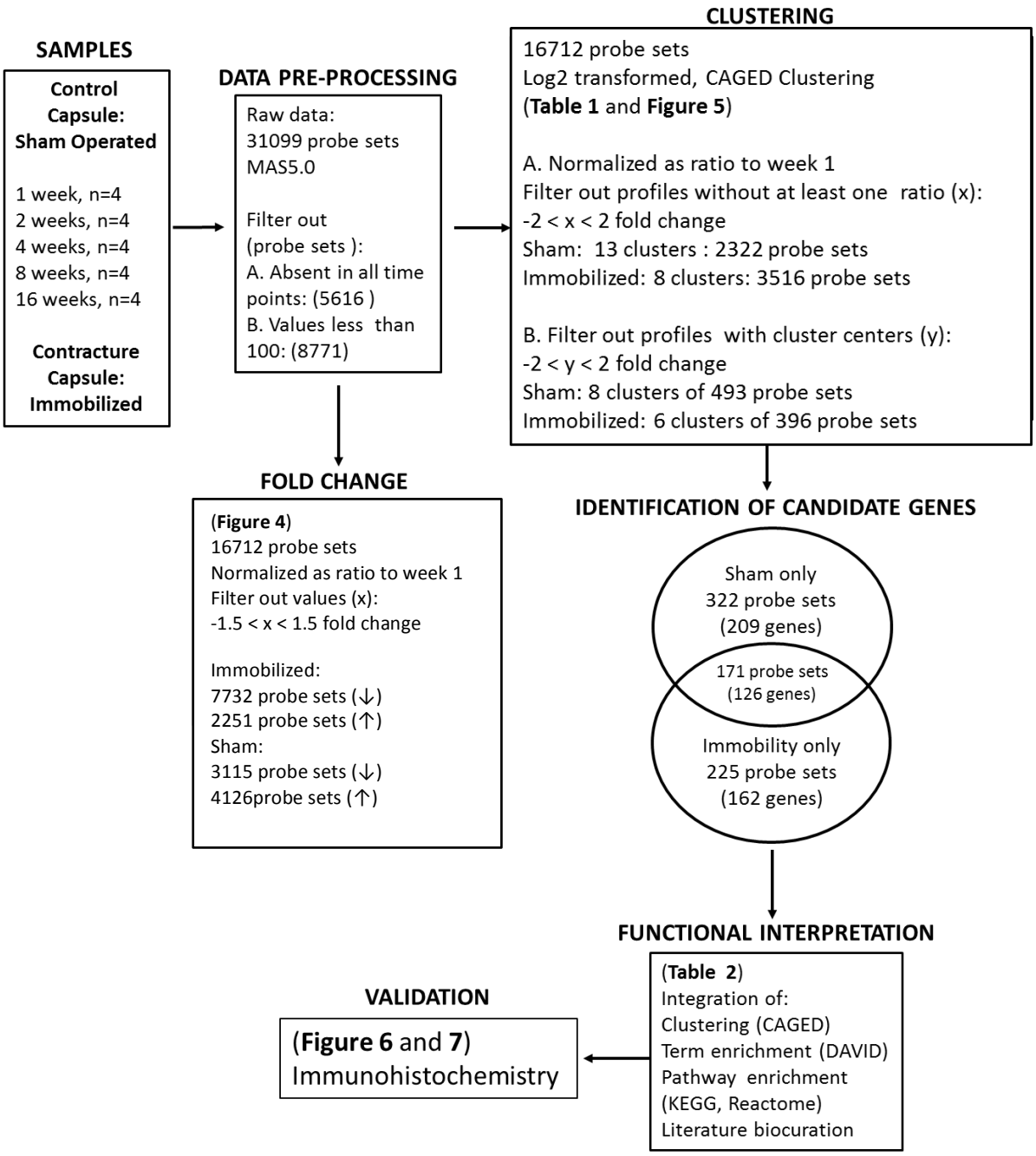
SAMPLES
Control Capsule: Sham Operated
1 week, n=4
2 weeks, n=4
4 weeks, n=4
8 weeks, n=4
16 weeks, n=4
Contracture Capsule: Immobilized
DATA PRE-PROCESSING
Raw data:
31099 probe sets
MAS5.0
Filter out
(probe sets):
A. Absent in all time points: (5616)
B. Values less than 100: (8771)
CLUSTERING
16712 probe sets
Log2 transformed, CAGED Clustering
(Table 1 and Figure 5)
A. Normalized as ratio to week 1
Filter out profiles without at least one ratio (x):
-2 < x < 2 fold change
Sham: 13 clusters : 2322 probe sets
Immobilized: 8 clusters: 3516 probe sets
B. Filter out profiles with cluster centers (y):
-2 < y < 2 fold change
Sham: 8 clusters of 493 probe sets
Immobilized: 6 clusters of 396 probe sets
FOLD CHANGE
(Figure 4)
16712 probe sets
Normalized as ratio to week 1
Filter out values (x):
-1.5 < x < 1.5 fold change
Immobilized:
7732 probe sets (↓)
2251 probe sets (↑)
Sham:
3115 probe sets (↓)
4126probe sets (↑)
IDENTIFICATION OF CANDIDATE GENES
Sham only
322 probe sets
(209 genes)
171 probe sets
(126 genes)
Immobility only
225 probe sets
(162 genes)
FUNCTIONAL INTERPRETATION
(Table 2)
Integration of:
Clustering (CAGED)
Term enrichment (DAVID)
Pathway enrichment
(KEGG, Reactome)
Literature biocuration
VALIDATION
(Figure 6 and 7)
Immunohistochemistry

Figure 2. Experimental Design for Identification of Rat Knee Posterior Capsule Transcripts Associated with Immobilization-Induced Flexion Contractures. Posterior knee capsule samples from either sham-operated or immobilized rats were collected at immobilization time points of 1, 2, 4, 8, and 16 weeks and were processed for RNA extraction. Gene expression was measured using microarray technology and data were analyzed via two pipelines: examining fold changes in expression compared to week one, and time-series clustering analysis with the CAGED algorithm. CAGED analysis was applied to both sham-operated and immobilized data sets and transcripts unique to the immobilized group were further analyzed for functional analysis using a variety of online tools including DAVID, Reactome, and literature biocuration. Expression levels of selected genes were validated with IHC. This figure is modified from a figure conceived by Dr. Odette Laneuville (manuscript under review). n=4 sham-operated rats; n=4 immobilized rats in each group at each time point.

of .CEL files were performed in the R software environment. The "affy" package was used to execute "mas5" and "mas5calls" to generate expression values and detection calls. The initial 31099 probe sets were filtered by removing those determined to be "absent" or with expression values less than 100 across all time points for the same group (immobilized or sham-operated). The sham-operated data set and the immobilized data set were analyzed separately by Cluster Analysis of Gene Expression Dynamics (CAGED) [53]. Expression values at each time point were compared to week 1 data and were log2 transformed (representing fold change) to create expression profiles for each probe set. Only those probe sets with at least one observation above a 2 fold increase or below a 2 fold decrease were further considered in the analysis. Expression profiles are represented as fold change at each time point compared to week 1. Probe sets with similar profiles of expression were clustered together using CAGED, which uses a Bayesian clustering algorithm. Clusters with cluster centre values (i.e. average expression values) between 2 and -2 fold change across the four ratios were eliminated.

End work previously completed; begin work done by Kayleigh Wong

2.1.2 Microarray Data Analysis

From the data analyzed by CAGED, common probe sets were identified between the sham and immobilized data sets. By removing these common probe sets from the immobilized list, an immobilized-only probe set list was identified and considered in functional analysis.

Along with CAGED analysis, global fold changes represented as ratios of expression values of week 2, 4, 8 or 16 over week 1 values were calculated for each data set (immobilized and sham). Ratios with a minimum of 1.5 fold change were counted and plotted into bins (up 1.5-2 fold, up over 2 fold, down 1.5-2 fold, and down more than 2 fold).

2.1.3 Functional Interpretation of Identified Genes

The list of probes identified by CAGED analysis as differentially expressed in the immobilized capsules were subject to the bioinformatics research tool DAVID (Database for Annotation, Visualization, and Integrated Discovery) [67] for enrichment analysis to identify clusters of Gene Ontology (GO) terms and Kyoto Encyclopaedia of Genes and Genomes (KEGG) pathways. DAVID was also used to convert the list of probe sets into a list of genes (since multiple probe sets can be used for the same gene). Pathways enriched in the immobilization candidate gene list were identified using the online Reactome database [68].

2.1.4 Immunohistochemistry

The differential expression of selected genes was confirmed by IHC on rat knee sections. Medial mid-condylar sagittal sections were stained for the selected proteins. The following dilutions (in water) were used for the primary antibodies: 1:750 for PCK1 (bs5001R, Bioss, Woburn, MA, US) and AGPAT-9 (GTX87708, GeneTex, Irvine, CA, US), 1:2000 for HSP47 (LS-C137998, LifeSpan Biosciences, Seattle, WA, US), and 1:5000 for P4HB (LS-B3137, LifeSpan Biosciences). Sections of sham and immobilized rats at every time point were stained at the same time for each antibody. Unless otherwise specified, steps were performed at room temperature. Sections were deparaffinized with five-minute incubations in xylenes (twice) and brought to water with 10 dips each into 100% (twice), 70%, and 50% ethanol. Slides were rinsed in water and Tris-buffered saline (TBS) for 5 minutes each. Endogenous peroxidase was removed with a 10-minute incubation with 3% peroxide. After another two rinses in TBS for 5 minutes each, slides were incubated for 20 minutes in Background Sniper blocking solution (Biocare Medical, Concord, CA, US). For each antibody, sections were incubated overnight at 4°C, except for HSP47 for which sections were incubated for two hours at 4°C. After rinsing with TBS, sections treated with P4HB primary antibody were incubated with MACH 4 Mouse Probe (Biocare Medical) for 5 minutes to allow for detection of mouse epitopes. All sections were incubated with MACH 4 HRP-Polymer (Biocare Medical) for 10 minutes and then developed with a Liquid DAB

Substrate Pack (HK103-5K, BioGenex, Fremont, CA, US) for 5 min at room temperature with tin foil used over the slide holder to block light. Slides were rinsed in water and counterstained with Shandon Instant Hematoxylin (Thermo Scientific Corporation, Pittsburgh, PA, US) for one minute. Excess hematoxylin was removed with 10 dips in acid alcohol, a rinse in water, and incubation in ammonia water for one minute. Sections were dehydrated with four dips each in 50%, 70%, and 100% (twice) ethanol and four dips in xylenes (thrice). Permount (Thermo Scientific Corporation) was used to mount and preserve slides. Negative controls corresponded to the omission of the primary antibodies (just water) and performing all other steps of the staining protocol.

Areas of posterior capsule in the stained sections were visualized with an Olympus BH-2 light microscope and a Marlin F080C digital camera (Allied Vision Technologies) with AVT Smartview 1.5.1 software at 132X at four fields: near the femoral attachment, near meniscus on the femoral side, near meniscus on the tibial side, and near the tibial attachment. Fields with approximately 50-100 fibroblasts while minimizing adipose cells and vessels were chosen. From two independent examiners, the average number of cells stained positively with DAB was calculated as percentage of total cells, and data was plotted using the R environment [69].

2.2 Collagenase Intervention in the Rat Model

Figure 3a outlines the experimental protocol used to test the effect of Xiaflex® on the rat knee FC model.

2.2.1 Animals and Surgery

The following protocols are compliant with Canadian Council on Animal Care guidelines and were submitted for review and approved by the University of Ottawa's Animal Care Committee. A total of 45 male adult Sprague Dawley rats (Charles River Laboratories, St-Constant, Quebec, Canada) had one hind knee surgically immobilized at a 45° flexion angle between the femur and tibia for four weeks (**Figure 1**) [9]. Under halothane anesthesia and with sterile conditions, two 1cm incisions were made at the

a

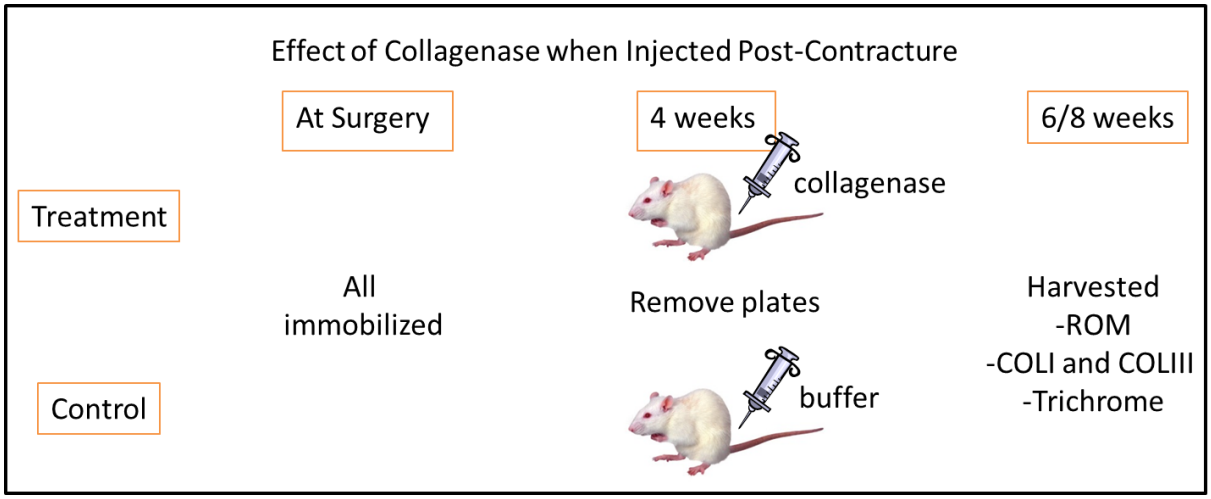
Effect of Collagenase when Injected Post-Contracture
At Surgery
4 weeks
6/8 weeks
Treatment
collagenase
All immobilized
Remove plates
Harvested
-ROM
-COLI and COLIII
-Trichrome
Control
buffer

b

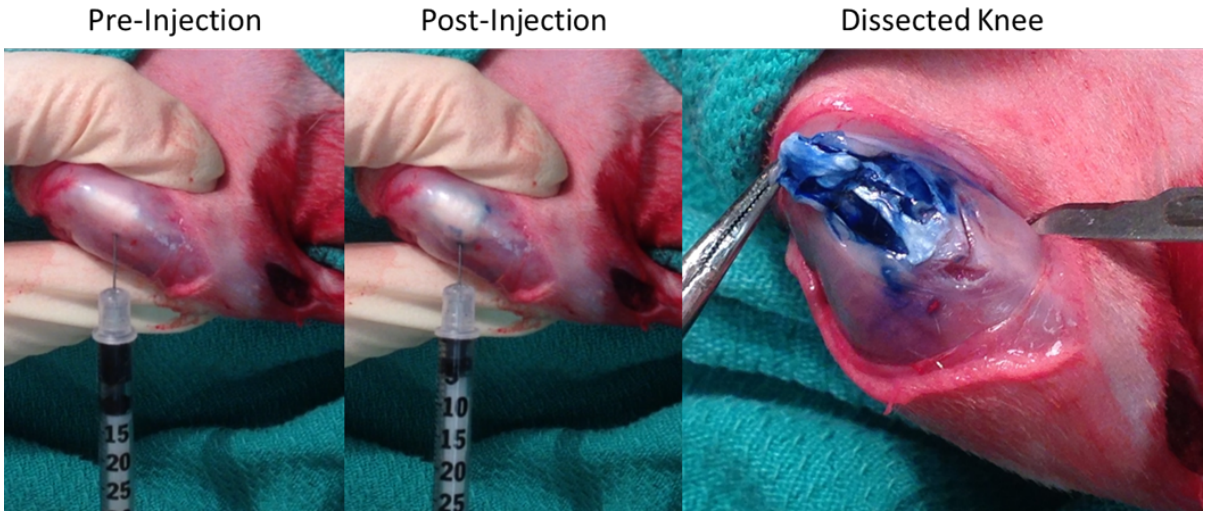
Pre-Injection
Post-Injection
Dissected Knee

Figure 3. **Experimental Design and Feasibility of Xiaflex® (Collagenase) Intra-Articular Injection in the Rat Contracture Model. a)** To evaluate the use of Xiaflex® in knee flexion contractures, rats were immobilized as previously described for four weeks. At remobilization, the plate was removed and experimental knees were injected with either Xiaflex® (collagenase) or saline buffer. After two or four weeks of remobilization, rats were euthanized and outcome measures ROM, collagen IHC, and Masson trichrome staining were evaluated. **b)** Evan's blue solution (50 µL) was injected intra-articularly into the knee joint of a euthanized rat using a lateral approach to show that injection into this small, intra-articular area is possible. Pre-injection and post-injection images are shown, followed by dissection of the knee, removing skin, patella, and connective tissues to show injection localization into the joint space.

lateral side of the proximal femur and distal tibia. The bone was exposed and a drill was used to create holes for the steel screws used to attach a Delrin® plate (DuPont Engineering Polymers, Wilmington, DE). The plate was inserted with an internal, but extra-articular, submuscular course that passed laterally between the peronei and lateral gastrocnemius muscles of the leg and distal to the greater trochanter of the femur at the thigh. After an approximate total surgery time of 20 minutes, the incisions were closed with staples and animals woke up after removal of anesthesia. The side of surgery was alternated between rats. After four weeks of immobilization, rats were again under anesthesia for removal of screws and plates by opening the same incisions as the first surgery. Xiaflex® (Auxillium Pharmaceuticals PA) was suspended in the provided saline-calcium buffer according to the medication guide. After plate removal, the knee was intra-articularly injected with a sterile 27 gauge needle using a lateral approach (**Figure 3b**) with either 50µL of 0.6mg/mL Xiaflex® or 50µL of buffer. Incisions were stapled closed and rats were removed from general anesthesia. After each surgery, rats were subcutaneously administered buprenorphine topically for pain relief, and had unrestricted movement in cages and free access to food and water. A total of 16 rats out of 45 were euthanized before end point due to broken legs at surgeries or loosening of the immobilization device and subsequent mobility.

2.2.2 Range of Motion of the Knee

Two weeks after plate removal and spontaneous remobilization of the animals, ten rats injected with Xiaflex® (X-Inj) and eleven rats injected with buffer (B-Inj) were euthanized with carbon dioxide inhalation. The remaining eight rats (four with Xiaflex® and four with buffer) were euthanized four weeks after remobilization. Rats were euthanized one at a time and ROM was measured immediately after death. ROM was measured by using an automatic arthrometer developed by the Bone and Joint Laboratory at the University of Ottawa [27]. The femur of the surgical leg was clamped onto the arthrometer and a rotating arm displaced the tibia at four pre-determined torques: 2.5N·cm, 7.5N·cm, 12.5N·cm, and 23.4N·cm. At each torque, a picture was automatically captured along with a video. The skin and musculature surrounding the knee joint was then cut with scissors and the arthrometer again captured images at each of the four different torques. This process

was repeated on the contralateral leg. ROM data from one rat was eliminated due to a leg broken by the arthrometer.

Images were imported into ImageJ software [70] and the angle between the femur and tibia was measured. Knowing that the femur runs through the middle of the clamp and the real distance between the end of the clamp and the centre of rotation, an angle is drawn between the femur and the tibia. The centre of rotation (the knee) was the apex of the angle and the posterior side of the lateral malleolus (a protruding boney structure at the proximal region of the foot, part of the ankle) was a tibial landmark. The angle was measured by using ImageJ and the R environment was used for statistical analysis and creation of graphs.

2.2.3 Range of Motion Statistics

Using the "lme4" package in R [71], we constructed linear mixed effect models of ROM as a function of the independent variables in order to assess the statistical significance of the results. This approach was chosen in order to account for each of the independent variables; fixed variables including type of injection, torque, muscle on or off, and leg (experimental or contralateral), and the random variable of Rat ID. The p-values for the relationship between injection and ROM were obtained by likelihood ratio tests of the full model against the model without the effect of injection.

2.2.4 Tissue Processing and Sectioning

After functional testing with the arthrometer, rat knee joints were wrapped in gauze and soaked in 10% formalin overnight at 4°C. Knees were then transferred to 10% EDTA for decalcification and kept at 4°C with fresh solution changes 3 times per week, for approximately 60 days until bone was easily cut with scissors. Decalcified knees were then processed to paraffin by the Histology Laboratory of the Pathology Department at the University of Ottawa. Knees were embedded in paraffin and a microtome was used to slice 7µm sagittal sections at the medial mid-condylar level in order to visualize the posterior capsule.

2.2.5 Immunohistochemistry: Collagen I and Collagen III

All steps were performed at room temperature unless otherwise specified. Slides were rinsed twice in xylene for 5 minutes and were then hydrated via 10 dips each in 100% (twice), 75%, and 50% ethanol and washing in cold running water for 5 minutes. Slides were rinsed in TBS for 5 minutes and endogenous peroxidase was removed in a 10-minute incubation with 3% H_2O_2. After 2 rinses in TBS for 5 minutes, slides were incubated Background Sniper (Biocare Medical) solution for blocking for 20 minutes. Primary antibody for COLI (GTX20292, GeneTex) and COLIII (bs-0549R, Bioss Inc.) were diluted in water to 1:300 and 1:500, respectively. Slides were incubated overnight at 4°C. After rinsing with TBS twice for 5 minutes sections were incubated with MACH 4 HRP-Polymer (Biocare Medical) for 10 minutes and again rinsed in TBS twice for 5 minutes. Slides were developed with a Liquid DAB Substrate Pack (HK103-5K, BioGenex, Fremont, CA, US) for 5 minutes at room temperature. After rinsing in water, sections were counterstained with Shandon Instant Hematoxylin (Thermo Scientific Corporation, Pittsburgh, PA, US) for 30 seconds, rinsed in water, dipped 10 times in acid alcohol, rinsed in water again, and incubated in ammonia water for one minute. Sections were dehydrated with four dips each in 50%, 70%, and 100% (twice) ethanol and four dips in three xylene solutions. Permount (Thermo Scientific Corporation) was used for mounting with a coverslip. Negative controls corresponded to the omission of the primary antibodies (just water) and performing all other steps of the staining protocol.

Areas of posterior capsule in the stained sections were visualized with an Olympus BH-2 light microscope and a Marlin F080C digital camera (Allied Vision Technologies) with AVT Smartview 1.5.1 software at 66X at four fields: near the femoral attachment, near meniscus on the femoral side, near meniscus on the tibial side, and near the tibial attachment. Fields with fewer adipose cells and vessels were chosen. ImageJ was used to quantify the intensity of extracellular matrix staining. The image was converted to an RGB stack and the blue channel was chosen to eliminate intensity from the hematoxylin staining. The “Plot Profile” function was used, which displays a graph of the average intensities of each column of vertical pixels against horizontal distance. The area under the graph was

measured as “intensity of staining” and the four fields were averaged per knee. Results were graphed using Excel and a Student’s t-test was used to test for significant differences.

2.2.6 Masson Trichrome

Slides were also stained with Masson Trichrome (MT) by the Histology Laboratory in the Pathology Department at the University of Ottawa. With MT, collagen stains blue, cytoplasm stains red, and nuclei stain black [72]. Stained slides were imaged with an Olympus BH-2 light microscope and a Marlin F080C digital camera (Allied Vision Technologies) with AVT Smartview 1.5.1 software at 66X at four fields: near the femoral attachment, near meniscus on the femoral side, near meniscus on the tibial side, and near the tibial attachment. Fields with fewer adipose cells and vessels were chosen. ImageJ was used to quantify the amount of collagen staining. The number of blue pixels (threshold colour “blue”, between 115-195) was counted and divided by the total area. Percentages of blue pixels were calculated; the four fields were averaged and graphed using Excel with a Student’s t-test used to test for significant differences.

2.2.7 Hematoxylin and Eosin Staining

All steps were performed at room temperature unless otherwise specified. Paraffin sections were rinsed twice in xylene for 5 minutes and were then hydrated via 10 dips each in 100% (twice), 75%, and 50% ethanol and washed in cold running water for 5 minutes. Sections were stained for ten minutes with Shandon Instant Hematoxylin (Thermo Scientific Corporation, Pittsburgh, PA, US), rinsed in water, dipped 10 times in acid alcohol, rinsed in water again, and rinsed in ammonia water for one minute. Slides were soaked in 50% ethanol for 2 minutes and subsequently counterstained with eosin for 20 seconds. Slides were rinsed in water and dehydrated in with four dips each in 50%, 70%, and 100% (twice) ethanol and four dips in three xylene solutions. Permount (Thermo Scientific Corporation) was used for mounting with a coverslip. Stained slides were imaged with an Olympus BH-2 light microscope and a Marlin F080C digital camera (Allied Vision Technologies) with AVT Smartview 1.5.1 software at 3.3X and 13.2X to visualize the articular cartilage on the femur and tibia.

2.3 Collagenase *in vitro* Incubations

In order to examine the effect of Xiaflex® on posterior capsule, rat and human capsule samples were incubated in either Xiaflex® or buffer for 24 hours at 37°C. The tissue and supernatant were analyzed for protein content, including collagen.

2.3.1 Posterior Knee Capsule Incubations

Normal posterior rat knee capsule was harvested from three unoperated Sprague Dawley rats. Human posterior knee capsule samples were obtained from Dr. Mark Campbell from osteoarthritis patients undergoing total knee arthroplasty [5]. Three samples were from patients with knee FC and one sample was from a patient without contracture. All capsules were frozen at -80°C in RNAlater® (Life Technologies, Austin, TX, US) until ready for use. Five to 10mg of each capsule sample was incubated at 37°C with 50µL Xiaflex® (1µg/µL) or 50µL of saline buffer for 24 hours. Tissue was then processed and embedded in agar by the Histology Laboratory in the Pathology Department at the University of Ottawa and sliced into 7µm sections on slides.

2.3.2 Immunohistochemistry: Collagen I and Collagen III

All steps were performed at room temperature unless otherwise specified. Slides were rinsed twice in xylene for 5 minutes and were then hydrated via 10 dips each in 100% (twice), 75%, and 50% ethanol and washed in cold running water for 5 minutes. Slides were rinsed in TBS for 5 minutes and endogenous peroxidase was removed with a 10-minute incubation with 3% H_2O_2. After two more rinses in TBS for 5 minutes, slides were incubated for 20 minutes with Background Sniper (Biocare Medical, Concord, CA, US) solution for blocking. For the rat samples, primary antibody for COLI (GTX20292, GeneTex) and COLIII (bs-0549R, Bioss Inc.) were diluted in water to 1:150 and 1:200, respectively, and slides were incubated for four hours at 4°C. For human capsule samples, primary antibody for COLI (GTX20292, GeneTex) and COLIII (bs-0549R, Bioss Inc.) were diluted in water to 1:300 and slides were incubated for two hours at room temperature and 4°C, respectively. After rinsing with TBS twice for 5 minutes sections were incubated with MACH 4 HRP-Polymer

(Biocare Medical) for 10 minutes and again rinsed in TBS twice for 5 minutes each. Slides were developed with a Liquid DAB Substrate Pack (HK103-5K, BioGenex, Fremont, CA, US) for 5 minutes at room temperature. After rinsing in water, sections were counterstained with Shandon Instant Hematoxylin (Thermo Scientific Corporation, Pittsburgh, PA, US) for 30 seconds, rinsed in water, dipped 10 times in acid alcohol, rinsed in water again, and incubated in ammonia water for one minute. Sections were dehydrated with four dips each in 50%, 70%, and 100% (twice) ethanol and four dips in three xylene solutions. Permount (Thermo Scientific Corporation) was used for mounting with a coverslip.

IHC stained sections were visualized with an Olympus BH-2 light microscope and a Marlin F080C digital camera (Allied Vision Technologies) with AVT Smartview 1.5.1 software. The entire sample was imaged at 6.6X. ImageJ was used to quantify the intensity of ECM staining. The image was converted to an RGB stack and the blue channel was chosen to eliminate intensity from the hematoxylin staining. The "Plot Profile" function was used, which displays a graph of the average intensities of each column of vertical pixels against horizontal distance. The area under the graph was measured as "intensity of staining". Total tissue area was measured by adjusting the threshold to exclude cutting artefacts, adipocytes, and other "empty" spaces. Total "intensity of staining" was divided by total amount of ECM and graphed using Excel. A paired t-test was used to detect significant differences between means.

2.3.3 Masson Trichrome

Slides of the rat and human capsule samples were also stained with MT (done by uOttawa Histology Department) for which collagen stains blue, cytoplasm stains red, and nuclei stain black [72]. The entire sample sections were imaged with an Olympus BH-2 light microscope and a Marlin F080C digital camera (Allied Vision Technologies) with AVT Smartview 1.5.1 software at 6.6X. ImageJ was used to quantify the amount of blue (collagen) staining. The number of blue pixels (threshold colour "blue", between 115 and 195) was counted and divided by the total tissue area, measured by adjusting the threshold to exclude tears, adipocytes, and other "empty" spaces. A percentage of blue pixels was

calculated and graphed using Excel. A paired t-test was used to detect differences between means.

2.3.4 Protein Gels

The supernatant remaining from the incubations were analyzed for protein content using sodium dodecyl sulfate polyacrylamide gel electrophoresis (SDS-PAGE). Freshly poured 12% polyacrylamide gels were used. The ladder used was 10µL of BLUeye prestained protein ladder (PM007-0500, FroggaBio, North York, ON, CAN), and 20µL (the maximum volume possible to use) of each supernatant sample was loaded with 20µL of Laemmli loading buffer (BioRad, Mississauga, ON, CAN). Gels were under 120V electrophoresis for one hour and stained with BioSafe Coomassie Stain (BioRad). Gels were imaged with a BioRad gel doc system. ImageJ was used to determine migration distance of each protein band and Excel was used to create a standard curve to determine the sizes of the protein bands in the samples.

3 RESULTS

3.1 Identification of Genes Associated with Immobilization-Induced Knee Flexion Contracture in Rat Knee Posterior Capsule

The results of the microarray experiments completed by Génome Québec were received as .CEL files for each group (immobilized and sham-operated at time points of 1, 2, 4, 8, and 16 weeks, the average of four rats per group). A raw total of 31099 probe sets were pre-processed with MAS5.0 and filtered to 16712 probe sets by removing 5616 absent probe sets and 8771 probe sets with expression values of less than 100 at every time point. Multiple probe sets are sometimes used for the same gene, for example, while over 30000 transcripts are analyzed, these correspond to just over 28000 genes [73].

3.1.1 Gene Expression –Fold Change

For the immobilized and sham time-series, week 1 was used as a reference point to evaluate fold change in expression at weeks 2, 4, 8, and 16. Ratio values with a minimum of a 1.5 fold change up or down were binned in four categories; 1.5 to 2.0 and 2.0 or more, up-regulated or down-regulated. The direction and number of probe in each bin are shown in **Figure 4**. Note that if the same probe set displays a decreased amount of expression across multiple weeks, it will be present in multiple bars in the figure.

The data set for the immobilized group was dominated by a reduction in gene expression: a total of 7622 unique probe sets decreased by at least 1.5 fold in expression compared to week 1 and 2252 unique probe sets increased by at least 1.5 fold. Changes in expression were different over time as a decrease in expression occurred more frequently at week 8 with 92.5% (=7047/7622 probe sets) of the total probe sets decreased at any time point. Increases in expression were observed mostly at weeks 2 and 4, for 1921 probe sets or 85.3% (1921/2252). A total of 9549 unique probe sets were identified with a 1.5 fold change in expression, with 325 unique probe sets fluctuating over time between >1.5 fold increase and decrease, or 3.4% (325/9549).

The data set for the sham-operated group displayed more probe sets increasing in expression with 4126 unique probe sets compared to 3115 unique probe sets decreasing in expression. Most increases occurred at week 4 with 72.6% (2996/4126) of unique increasing probe sets. The most important decrease occurred during weeks 8 and 16 with 92.2% (2871/3115) of unique decreasing probe sets at these time points. A total of 7051 unique probe sets were identified, with 190 fluctuating between being up and down regulated over time, or 2.7% (190/7051).

In comparing the two data sets, across all time points, 1751 common probe sets decreased, or 19.5% (1751/8986) and 929 common probe sets increased, or 17.0% (929/5449). A total of 1816 probe sets increased in immobilized data set while the same probe sets decreased in the sham-operated one, and 529 probe sets increased in sham-operated data set while they decreased in immobilized data set.

a

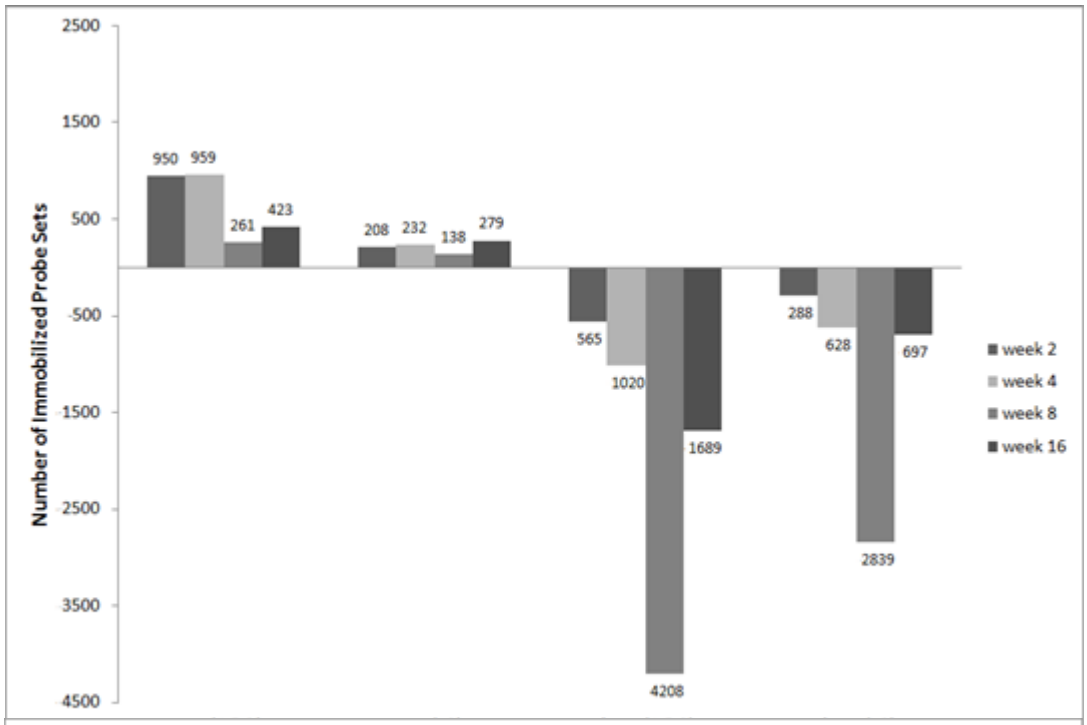
Number of Immobilized Probe Sets
2500
1500
500
-500
-1500
-2500
-3500
-4500
950
959
261
423
208
232
138
279
565
1020
4208
1689
288
628
2839
697
week 2
week 4
week 8
week 16

b

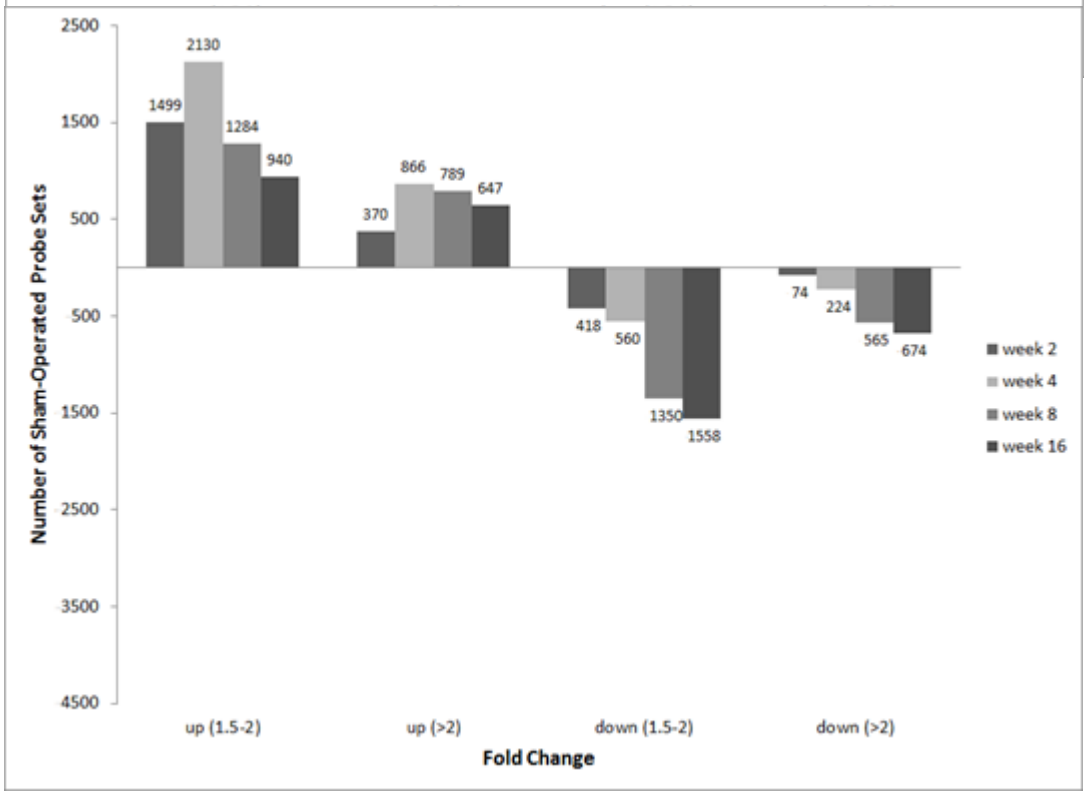
Number of Sham-Operated Probe Sets
2500
1500
500
-500
-1500
-2500
-3500
-4500
1499
2130
1284
940
370
866
789
647
418
560
1350
1558
74
224
565
674
week 2
week 4
week 8
week 16
up (1.5-2)
up (>2)
down (1.5-2)
down (>2)
Fold Change

Figure 4. Fold Changes in Gene Expression in the Posterior Capsule of Immobilized and Sham-Operated Knee Joints. After preprocessing raw microarray data, intensity values of probe sets measured at 2, 4, 8, and 16 weeks were compared to results measured at week 1 for each of the **a)** immobilized and **b)** sham-operated groups, to determine the fold change in expression. Probe sets were counted into four bins: up-regulated by a fold change of 1.5 to 2.0 or above 2.0, and down-regulated by a fold change of -1.5 to -2 or more than -2. The immobilized data set had more down-regulated probe sets and the sham-operated data set had more up-regulated probe sets. In the immobilized data set, a total of 7622 unique probe sets decreased in expression compared to week 1 and 2252 had increased. In the sham data set, 3115 had decreased and 4126 had increased. n=4 sham-operated rats and n=4 immobilized rats at each time point.

3.1.2 Time Series Analysis of Gene Expression

Pre-processed and log2 transformed data were analysed using the CAGED algorithm with week 1 expression data of each series as a reference point. Only probe sets with a fold change observation above 2 fold for at least one time point were considered, which summed to a total of 2322 probe sets for the sham-operated group and 3516 for the immobilization group. The number of probes in each cluster and average log2 values (cluster centers) over the time course is provided in **Table 1**.

CAGED analysis of the immobilization gene-expression time series identified 8 profiles of expression; clusters 2 and 3 were eliminated as all cluster centers (each time point's expression median in log2 base), were neither higher than 1 or lower than -1 (a two- fold change). This value was arbitrarily chosen for data reduction. For the immobilization group, a total of 396 probe sets corresponding to 288 genes were included in 6 clusters. Clusters 1 and 7 displayed up regulation, clusters 4 and 8 displayed down regulation, and clusters 5 and 6 were variable. (**Figure 5a**)

Clustering analysis of sham-operated data recognized 13 expression profile clusters, 8 of which had cluster centers that exceeded a two-fold change and were used in further analysis. The total 493 probe sets included in the 8 sham-operated clusters corresponded to 335 different genes. (**Figure 5b**)

The 171 probe sets common to both experimental conditions (corresponding to 126 genes) were eliminated from the immobilized-only list, leaving 225 probes set (162 genes). These 162 genes displayed dynamic changes of expression in the posterior capsule over a 16-week time course of immobilization-induced knee FC.

3.1.3 Functional Analysis

The list of 162 genes with differential expression in the posterior knee capsule over the development of immobilization-induced knee FC was analyzed to discern biological significance. Results of GO term, KEGG pathway, and Reactome pathway analyses are presented in **Table 2**. Using the online tool DAVID [74], GO term enrichment in the

a Immobilized - Cluster Centers: Average $\log_2$ values

	Cluster							
	1	2	3	4	5	6	7	8
# Probes	87	376	2744	113	176	6	12	2
2 weeks	1.03	0.52	-0.19	-0.47	-0.95	1.03	2.50	-0.41
4 weeks	1.80	0.50	-0.32	-1.31	-1.20	2.14	2.41	-2.29
8 weeks	0.61	0.27	-0.90	-1.48	-2.02	-0.97	1.59	-3.61
16 weeks	1.59	0.51	-0.39	-1.52	-0.12	-0.32	3.00	-3.36

b Sham - Cluster Centers: Average $\log_2$ values

	Cluster												
	1	2	3	4	5	6	7	8	9	10	11	12	13
# Probes	14	11	128	97	109	161	647	97	85	110	796	47	20
2 weeks	1.62	-0.95	0.14	0.80	0.42	0.05	0.56	0.38	0.66	-0.54	-0.27	0.94	1.39
4 weeks	2.82	-1.22	0.38	0.99	0.65	0.37	0.73	0.93	1.41	-0.73	-0.35	1.86	3.11
8 weeks	3.15	-1.26	-0.26	0.56	0.97	0.64	0.61	1.45	1.91	-1.01	-0.68	2.53	0.83
16 weeks	3.27	-2.28	-0.16	0.90	1.08	0.76	0.33	1.66	2.16	-1.56	-0.75	2.79	1.13

Table 1. CAGED Clustering Results of Posterior Capsule Gene Expression in Immobilized and Sham-Operated Rat Knee Joints. After pre-processing of microarray raw data, the CAGED algorithm was used to cluster probe sets according to the similar profiles of expression; **a)** 8 expression profiles were identified for the immobilized group and **b)** 13 expression profiles were identified for the sham-operated group. Results at week 1 for each group were used as reference for comparison to weeks 2, 4, 8, and 16. The number of probes in each cluster is presented with cluster centers (median log2 change compared to week 1) for each time point. Tables composed by Dr. Odette Laneuville (manuscript under review). n=4 sham-operated rats and n=4 immobilized rats at each time point.

a

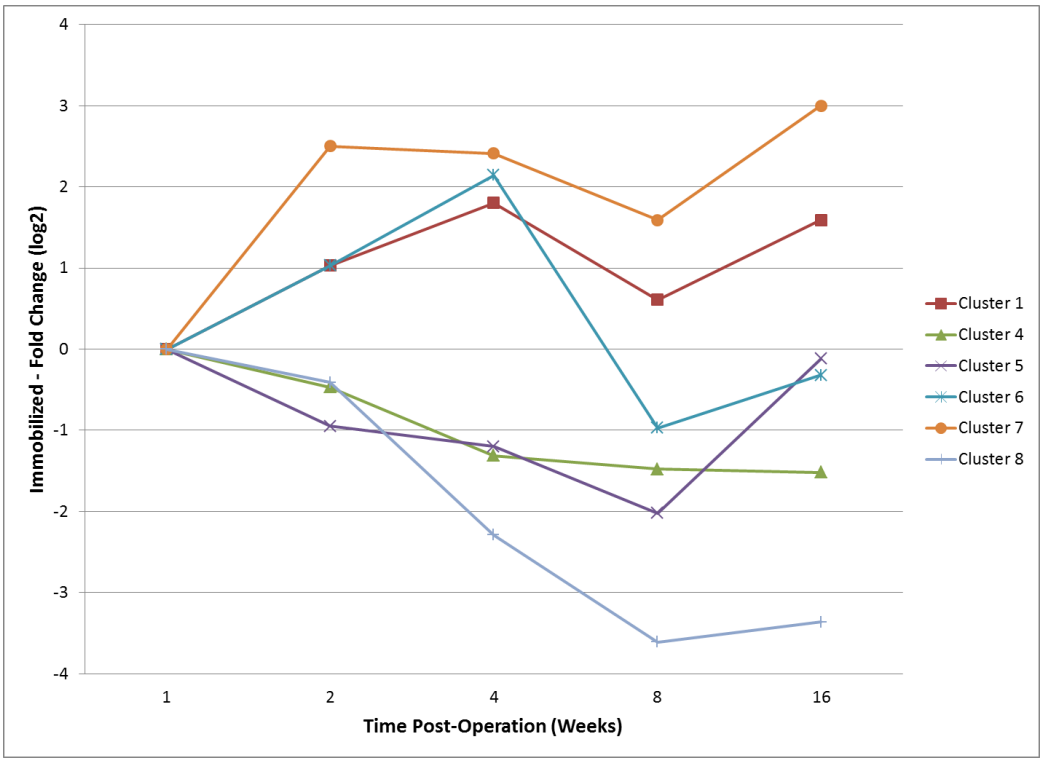
Immobilized - Fold Change (log2)
4
3
2
1
0
-1
-2
-3
-4
1
2
4
8
16
Time Post-Operation (Weeks)
Cluster 1
Cluster 4
Cluster 5
Cluster 6
Cluster 7
Cluster 8

b

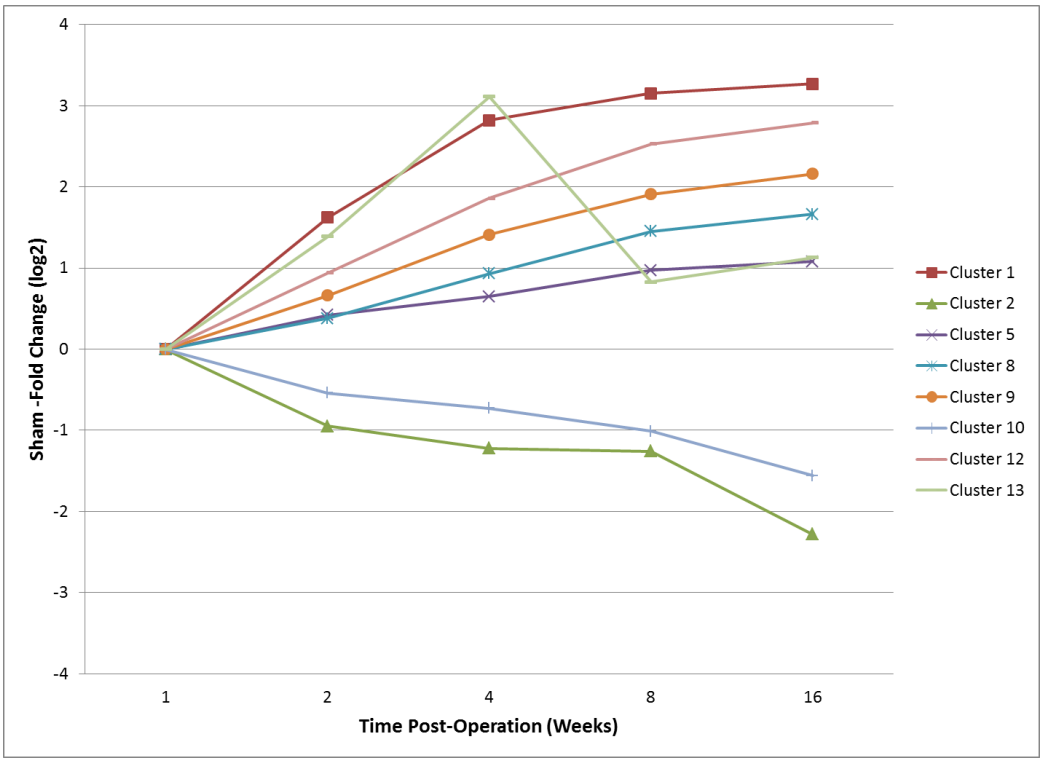
Sham -Fold Change (log2)
4
3
2
1
0
-1
-2
-3
-4
1
2
4
8
16
Time Post-Operation (Weeks)
Cluster 1
Cluster 2
Cluster 5
Cluster 8
Cluster 9
Cluster 10
Cluster 12
Cluster 13

Figure 5. CAGED-Identified Expression Profile Clusters of Probe Sets Associated with Immobilization or Sham-Operation. The CAGED algorithm on pre-processed microarray data clustered probe sets based on similar expression profiles which were evaluated by comparison of expression levels at each time point to week 1. Only expression profiles with all clusters centres at least doubled or halved compared to week 1 were kept. For each group, log2 values of cluster centers were plotted against time. **a)** Eight expression profile clusters were identified in immobilized capsule; clusters 2 and 3 had all four cluster centers with moderate fold change between log2 1 and -1 and were eliminated. **b)** Thirteen expression profiles were identified in sham-operated knee capsule; clusters 3, 4, 6, 7, and 11 had all cluster centers between log2 1 and -1 fold change and were eliminated. n=4 sham-operated rats and n=4 immobilized rats at each time point.

	GO Term	p-value	CAGED cluster (# of probes)	KEGG Pathways	p-value	CAGED cluster (# of probes)	Reactome Pathways	p-value	CAGED cluster (# of probes)
Biological Process	Extracellular structure organization	9.2E-7	1 (5) 4 (4) 5 (1) 6 (2)	Dilated cardiomyopathy	4.8E-4	1 (2) 4 (3) 5 (4) 8 (1)	Muscle contraction	5.0E-10	1 (3) 4 (3) 5 (4) 8 (1)
	Lipid biosynthetic process	1.9E-5	1 (3) 4 (12)	ECM-receptor interaction	2.0E-3	1 (2) 4 (1) 6 (3) 8 (1)	Triglyceride biosynthesis	3.6E-7	4 (9)
	Neutral lipid metabolic process	2.0E-5	1 (1) 4 (8)	Hypertrophic cardiomyopathy (HCM)	2.4E-3	1 (2) 4 (2) 5 (4) 8 (1)	Gelatin degradation by MMPs	3.8E-7	1 (2) 4 (3) 6 (2)
Cellular Component	Extracellular region part	8.6E-9	1 (7) 4 (15) 5 (1) 6 (4) 8 (1)	Cardiac muscle contraction	1.1E-2	4 (2) 5 (4) 8 (1)	Collagen type XI degradation by MMPs	9.7E-7	1 (2) 4 (2) 6 (1)
	Extracellular matrix	2.0E-8	1 (4) 4 (9) 6 (4) 8 (1)	Focal adhesion	2.2E-2	1 (3) 4 (1) 6 (3) 8 (1)	Degradation of collagen	1.3E-6	1 (2) 4 (5) 6 (2)
	Proteinaceous extracellular matrix	2.2E-8	1 (4) 4 (8) 6 (4) 8 (1)	Biosynthesis of unsaturated fatty acids	2.9E-2	4 (3)	Collagen type X degradation by MMPs	2.2E-6	4 (2) 6 (1)
Molecular Function	Vitamin Binding	2.9E-4	1 (1) 4 (6) 5 (2)	Complement and coagulation cascades	4.4E-2	4 (3) 5 (1)	ATP Hydrolysis by Myosin; Myosin Binds ATP; Calcium Binds Caldesmon; Release of ADP From Myosin	4.8E-6	1 (3) 4 (1) 5 (2) 8 (1)
	Cytoskeletal protein binding	4.4E-4	1 (6) 4 (3) 5 (5) 8 (1)	PPAR signalling pathway	4.5E-2	4 (5)	Degradation of the extracellular matrix	7.5E-6	1 (1) 4 (5) 6 (2)
	Actin binding	4.6E-4	1 (5) 4 (5) 5 (3)	Glycine, serine and threonine metabolism	5.0E-2	1 (1) 4 (2)	Smooth Muscle Contraction	7.9E-6	1 (3) 4 (1) 5 (2) 8 (1)

Table 2. Functional Interpretation of Rat Knee Posterior Capsule Genes Associated with Immobilization-Induced Knee Flexion Contractures. Differentially expressed genes in immobilized capsule only (225 probe sets converted to 162 genes) identified by CAGED were subjected to functional analysis by clustering using the online tools DAVID and Reactome. Genes were clustered according to GO Terms, KEGG Pathways, and Reactome Pathways. Results corresponding to biological terms are presented with p-values of functional clustering calculated by DAVID and Reactome and the CAGED expression profiles with the number of probe sets identified. Terms relating to the extracellular matrix were enriched in the gene list.

categories of Biological Process, Molecular Function, and Cellular Component was examined. GO terms relating to the extracellular matrix were the most significantly enriched in the gene list. Comparing the results with CAGED analysis, many of the probe sets belonged in profile 4, which displays down regulation over time.

The genes were also mapped to KEGG pathways using the DAVID software. The general terms identified were cardiomyopathy, extracellular matrix, and fatty acid pathways (**Table 2**). Comparing to the CAGED profiles of expression, no expression profile dominated the terms, as both up-regulated and down-regulated probes were present.

Enriched pathways were also discerned using another online tool, Reactome. The most represented Reactome pathways included: muscle contraction, triglyceride biosynthesis, and collagen degradation. The CAGED profiles present in the clustering include mostly down regulated (clusters 4 and 8) and variable expression (clusters 5 and 6). (**Table 2**)

In the most significant clusters of each category, which are shown in **Table 2**, 11 clusters are related to extracellular matrix and collagen, 8 clusters are related to muscle contraction, and 3 clusters are related to lipid biosynthesis.

The genes enriched in the immobilized capsule gene list that are related to the lipid biosynthesis included: *Fasn, Agpat2, Ggat2, Acaca, Gpd1, Elov1,* and *Acsl1*. These genes showed a reduction in expression over the immobilization time-course, all belonging to CAGED cluster 4. Genes relating to muscle contraction include *Myl3, Myl9, Myh11, Actg2, Acta2, Actc1, Tnnt1, Tnnt2,* and *Tpm3*. These genes showed variable expression and did not belong strongly to one CAGED cluster. The genes relating to extracellular matrix and collagen degradation included: *Mmp3, Mmp9, Mmp13, Col2a1, Col10a1, Col11a1, Agt, Alb, Cdh1, Cdh2, Cfd, Chad, Ibsp, Ky, Myh11, Obp3, Pcsk6, Tf, Tnfrsf11b, Tnn,* and *Vit*. The metalloproteinase genes (MMPs) all display a profile of decreased expression and the collagen genes displayed either variable or reduced expression over the time-course.

3.1.4 Immunostaining of Proteins Encoded by Candidate Genes

Four genes related to triglyceride biosynthesis and/or collagen synthesis were selected for validation of expression using IHC. An example of staining is shown in **Figure 6** with quantification and microarray results in **Figure 7**. Changes in protein levels were not determined at week 1 (specimens were not available) and mRNA expression values below each graph represent pre-processed microarray data. The genes measured included *Pck1* (phosphoenolpyruvate carboxykinase 1), *Agpat-9* (1-acylglycerol-3-phosphate O-acyltransferase 9), *P4hb* (prolyl 4-hydroxylase, beta peptide, subunit of the microsomal triglyceride transfer protein complex [75]and also involved in post-translational modification of collagens [55,76]), and *Hsp47* (heat shock protein, a collagen-specific molecular chaperone) [77].

For profiles of expression of *Pck1*, involved in lipid pathways, levels of protein and transcript did not match; mRNA levels decreased (CAGED cluster 4) while protein levels fluctuated over time (**Figure 7a**). *Agpat-9*, involved in triglyceride biosynthesis as identified by functional analysis, displayed a decrease in mRNA expression over the time course (CAGED cluster 4). *Agpat-9* protein and transcript levels varied with similar profiles (**Figure 7b**). *P4hb* and *Hsp47* were not identified by CAGED analysis as differentially expressed, but were identified as genes of interest by Dr. Odette Laneuville with an initial comparison of sham versus immobilized microarray data before focusing on time series analysis. The P4HB protein is involved in intracellular lipid exchange [75] and is also a collagen post-translational modifier, adding hydroxyl groups to proline to create hydroxyproline [55,76]. Levels of P4HB protein and the corresponding transcript decreased over the time-course in the immobilized capsule (**Figure 7c**). The protein HSP47 is a chaperone in the folding of collagens [77]. The levels of transcript and staining intensity of HSP47 decreased over the time-course of immobilization-induced knee FCs (**Figure 7d**). No statistical analysis was performed and levels of mRNA and protein in immobilized capsule were not corrected for control variation. Due high variability, only the trends in levels of proteins and transcripts were examined.

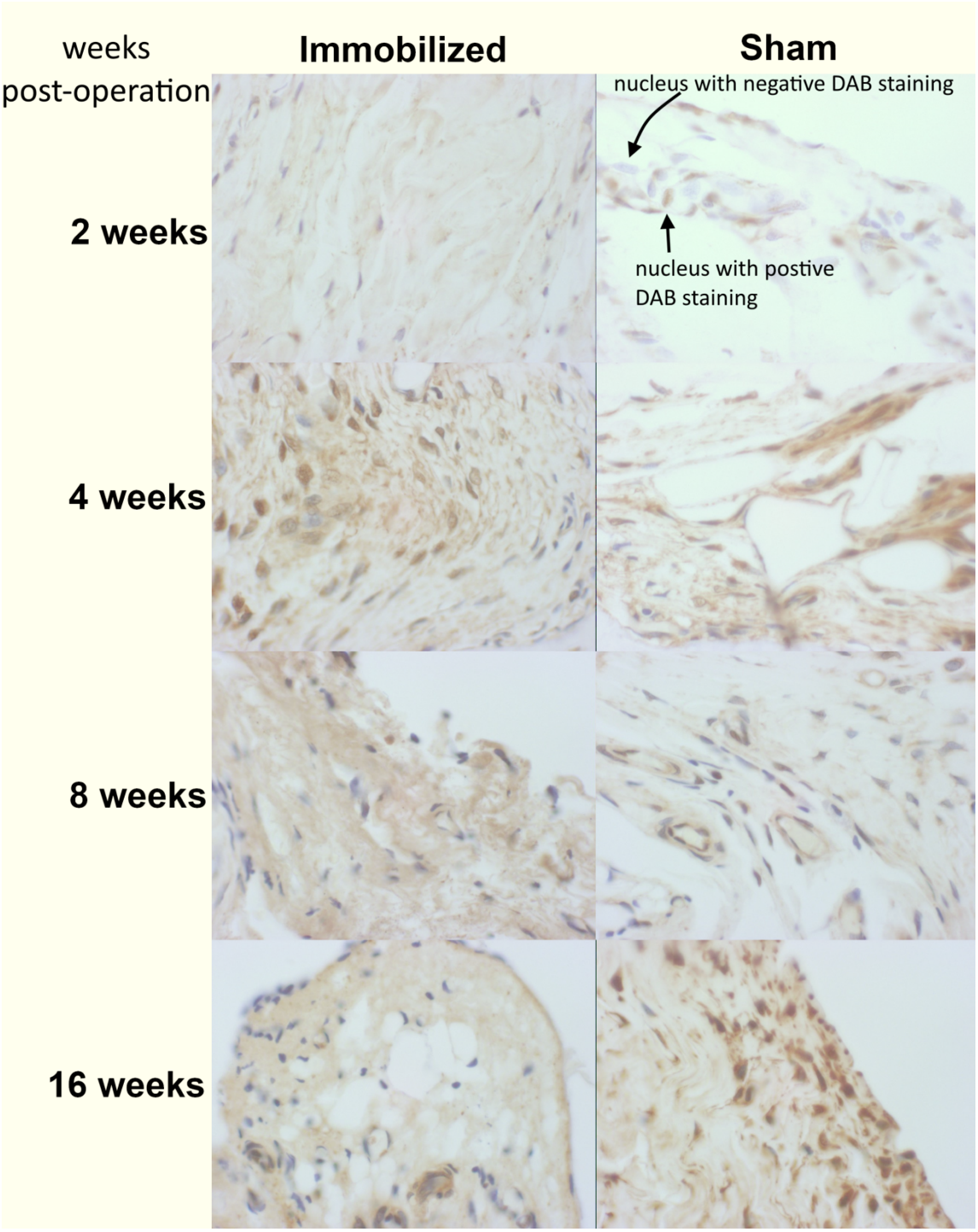
weeks
post-operation
Immobilized
Sham
nucleus with negative DAB staining
nucleus with postive
DAB staining
2 weeks
4 weeks
8 weeks
16 weeks

Figure 6. Immunostaining of AGPAT-9 Protein Levels in the Posterior Capsule of Immobilized and Sham-Operated Rat Knee Joints. Hematoxylin staining (nuclei) and IHC staining of AGPAT-9 in immobilized and sham-operated rat knee capsules at time points 2, 4, 8, and 16 weeks. Rat knees were harvested at end-point, fixed in formalin and decalcified in EDTA solution before paraffin embedding and sectioning into 7µm slides at the medial mid-condylar level in the sagittal plane. Sections were deparaffinized and immunostained by using primary antibody for AGPAT-9, HRP secondary antibody, and DAB substrate, resulting in a brown stain. Negative controls (not shown) corresponded to the omission of the primary antibodies. Cells stained brown were considered positively expressing AGPAT-9 protein. Images were captured with an Olympus BH-2 light microscope and a Marlin F080C digital camera (Allied Vision Technologies) with AVT Smartview 1.5.1 software, magnified to 132X.

a

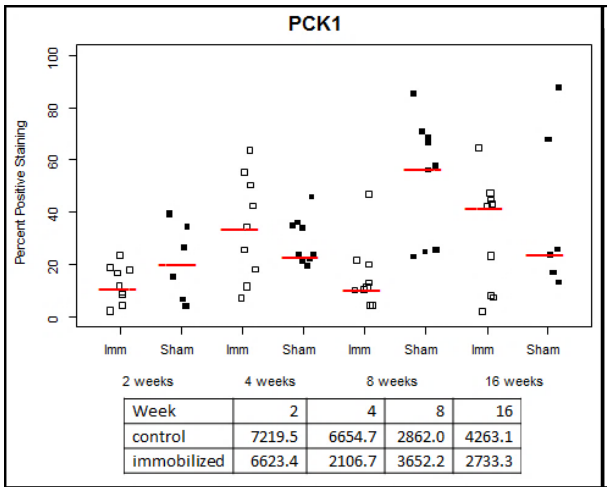

Week	2	4	8	16
control	7219.5	6654.7	2862.0	4263.1
immobilized	6623.4	2106.7	3652.2	2733.3

b

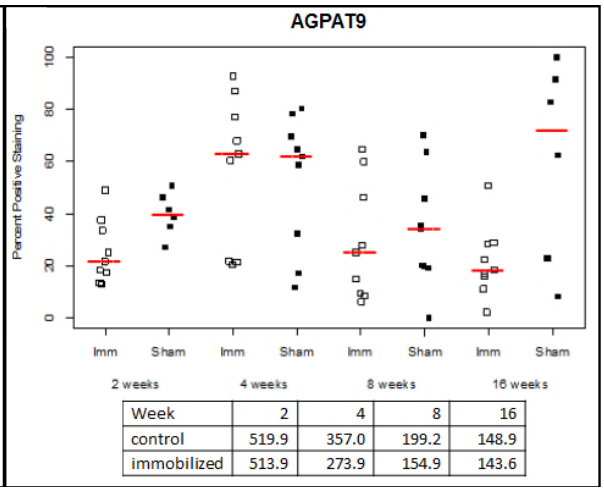

Week	2	4	8	16
control	519.9	357.0	199.2	148.9
immobilized	513.9	273.9	154.9	143.6

c

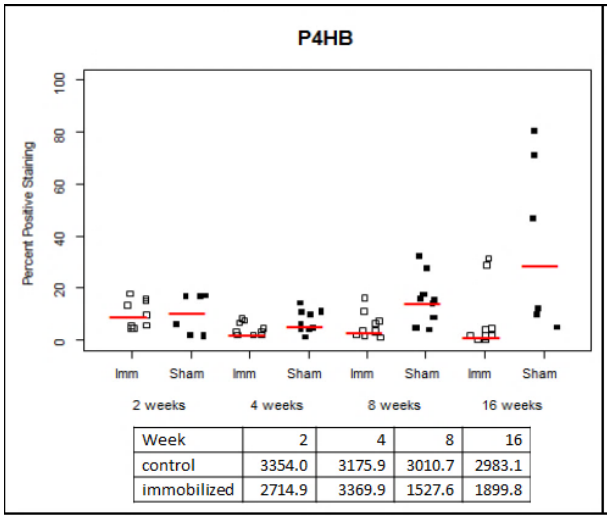

Week	2	4	8	16
control	3354.0	3175.9	3010.7	2983.1
immobilized	2714.9	3369.9	1527.6	1899.8

d

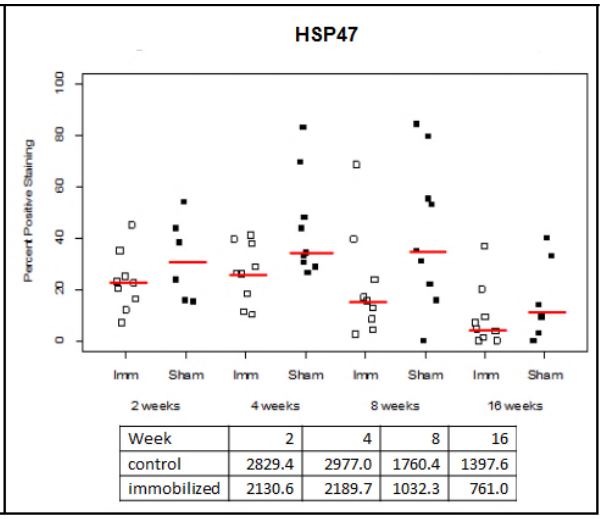

Week	2	4	8	16
control	2829.4	2977.0	1760.4	1397.6
immobilized	2130.6	2189.7	1032.3	761.0

Figure 7. Validation of Differential Expression for Immobilization Associated Genes in the Posterior Capsule with Immunostaining. Quantification of IHC staining of **a)** PCK1, **b)** AGPAT-9, **c)** P4HB, and **d)** HSP47 in the rat posterior knee capsule at 2, 4, 8, and 16 weeks post immobilization or sham operation. For each knee section stained via HRP-DAB for the desired protein, four fields of the posterior capsule at 132X were imaged and two independent examiners counted the percentage of positively stained cells. The average count of each field (4 fields per capsule) is plotted along with a median line for each experimental group. Tables present the preprocessed median mRNA levels from previous microarray data for the corresponding probe set of the protein. Patterns of mRNA and protein levels for *P4hb* and *Hsp47* loosely matched, while those for *Pck1* and *Agpat9* did not match. At 2 and 16 weeks n=2 sham-operated rats, n=3 immobilized rats; at 4 and 8 weeks n=3 sham-operated rats, n=3 immobilized rats.

3.2 Intra-articular Xiaflex® Injections for Rat Knee Flexion Contracture

Based on the gene expression results and the functional analysis of the differentially expressed genes, collagen pathways in the extracellular matrix appeared to be a potential pharmacological target in the treatment of joint contractures. Xiaflex®, collagenases in suspension, by Auxillium Pharmaceuticals is currently used in clinic for Dupuytren's contracture and Peyronie's disease, both fibrotic in pathophysiology. Xiaflex® was therefore chosen as a potential intervention in knee FC.

A total of 28 rats were used in biomechanical (ROM) and histological analyses after 17 rats were excluded due to bone breakage during surgery, loosening of the immobilization device resulting in mobility, or bone breakage while being tested on the arthrometer. A total of 20 rats (9 Xiaflex® and 11 Buffer) were remobilized for 2 weeks and 8 rats (4 Xiaflex® and 4 Buffer) were remobilized for 4 weeks. The contralateral legs of 6 rats were used for a separate project; therefore these legs are included in the ROM data but are not included in histology.

3.2.1 Range of Motion – Four Weeks Immobility Followed by Two Weeks Remobilization

ROM results of experimental and contralateral legs of rats immobilized for 4 weeks to induce a knee FC, intra-articularly injected with either Xiaflex® (X-Inj) or buffer (B-Inj), and remobilized for 2 weeks are presented in **Figure 8a**. Results presented include mean ROM +/- 1 SEM and sample size for each experimental group; nine rats were in the treated group and 11 rats were in the control group. Data is presented for all four torques and with muscle on and muscle off. Each leg group was assigned a letter for ease of reading the following figures, for example the letter 'a' indicates the experimental leg of Xiaflex®-injected rats with muscle on. ROM was always higher with increased torque and with removal of muscle indicating a contribution of muscles to the limitation of ROM. The contralateral leg was always more mobile than the immobilized leg. Immobilized legs injected with Xiaflex® have a higher ROM than those injected with buffer (see statistical analysis below). **Figure 8b** displays a graphical representation of the results of X-Inj legs versus B-Inj legs. **Figure 8c** is the calculated value of the difference in ROM between treated

a

		Xiaflex (n=9)						Buffer (n=11)					
		Immobilized			Contralateral			Immobilized			Contralateral		
Muscle	Torque	Mean	SEM	Name	Mean	SEM	Name	Mean	SEM	Name	Mean	SEM	Name
On	1	93.3	6.7	a	134.7	4.5	c	89.5	2.8	e	125.1	2.7	g
	2	98.4	7.2		143.8	4.3		95.7	3.2		134.5	2.6	
	3	116.2	7.7		156.3	3.0		105.6	3.7		145.4	2.4	
	4	133.4	6.4		169.4	2.6		119.1	4.1		157.0	2.3	
Off	1	128.5	6.4	b	156.0	2.1	d	111.8	8.8	f	147.2	2.3	h
	2	134.8	6.8		162.0	2.1		117.7	2.6		153.2	2.2	
	3	142.6	7.6		173.6	2.0		126.8	2.7		161.8	2.5	
	4	175.5	9.3		189.6	5.4		140.5	4.2		173.7	3.6	

b

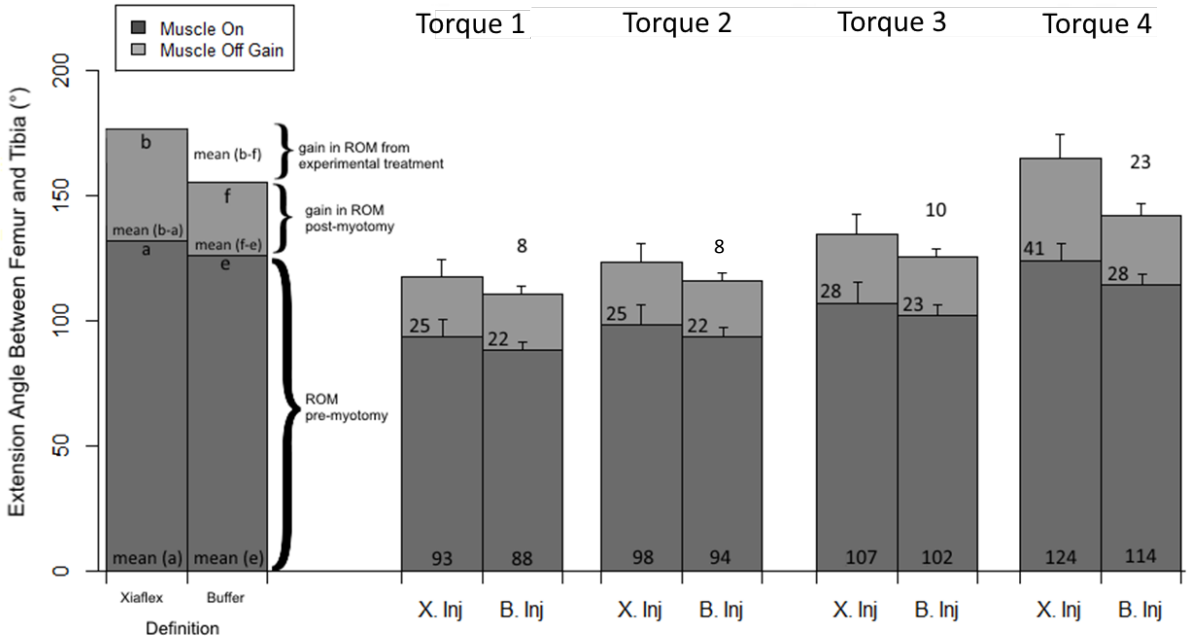

c

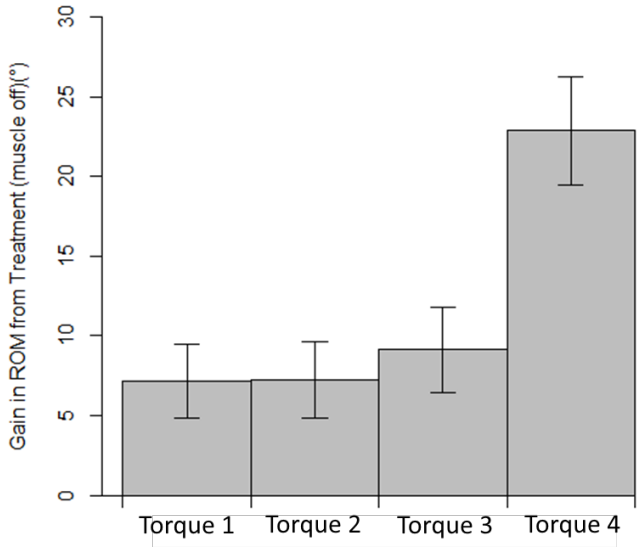

Figure 8. Direct and Calculated Measurements of the Range of Motion of Xiaflex®-Injected and Buffer-Injected Rat Knees After Four Weeks of Immobilization and Two Weeks Recovery at Four Torques. One hind leg of each rat was immobilized at 45° flexion with a plate and screws. After 4 weeks, legs were remobilized by surgically removing the immobilization device and knees were intra-articularly injected with either Xiaflex® (50µL, 0.6µg/µL) or buffer (50µL). Rats were brought to end point at 2 weeks post-injection and ROM in extension of both experimental and contralateral legs were measured, first with muscle on and then with the muscles around the joint sectioned. 'Muscle on' reflected the contribution of both muscles and posterior knee capsule in the limitation of ROM while 'muscle off' reflected the contribution of only the capsule. An automatic arthrometer was used at four different torques: 2.5N·cm, 7.5N·cm, 12.5N·cm, and 23.4N·cm. Pictures were captured at each torque and the angle between femur and tibia was measured using ImageJ. **a**) Mean extension angles are presented with standard error. Each group was assigned a letter for ease of interpreting the subsequent figures. **b**) Mean ROM values are given within each bar along with value of the differences between mean buffer-injected (B. Inj) and mean Xiaflex®-injected (X. Inj) extension with muscle off (number above B. Inj bar). Error bars present standard error of direct and calculated measurements. **c**) The difference in degrees between the mean ROM values of X-Inj legs and B-Inj legs without muscle against each of the four different torques shows that the ROM of X-Inj knees was higher than ROM of B-Inj knees.

Calculations:

Gain in ROM post-myotomy calculated by:

(Muscle Off ROM)-(Muscle On ROM); b-a, f-e

Gain in ROM from experimental treatment calculated by:

(Xiaflex® Muscle Off)-(Buffer Muscle Off); b-f

and untreated legs with muscle off, which compared the restriction of motion due to the posterior capsule. The difference between the groups was most noticeable at the higher torque, where ROM in the treated legs was higher than untreated.

In **Figure 8**, experimental (injected) legs of the two groups were compared. The experimental legs were also compared to the within-rat control of the contralateral legs, the difference between which can be interpreted as the amount of contracture. **Figure 9a and b** show the comparison for both groups. **Figure 9c** is a graphical representation of the amount of articular restriction remaining in the experimental legs when compared to the matching contralateral legs. Mean differences are presented with standard error. At the highest torque, articular restriction in the treated knees was noticeably less than in the untreated knees.

The statistical significance of the ROM measurements was evaluated using statistical linear modeling. The linear mixed effects model used took into account both fixed (experimental or contralateral; muscle on or off; Xiaflex® or buffer; torque) and random effects (random differences between rats; i.e. genetics, overall activity, etc.), and the repeated ROM measures made for the same knee at the four different torques. Boxplots presented in **Figure 10a and b** were generated in R with standard settings and show the median values and the interquartile range. Outliers, which lie outside 1.5 times the interquartile range, are shown as individual points. The X-Inj rats showed more variation in ROM compared to the B-Inj rats, even in the contralateral legs. Two of the nine X-Inj rats showed strikingly low ROM compared to the rest, but are only identified as mathematical outliers at the final torque. Overall median values in the X-Inj legs are higher than those of the B-Inj legs. The table in **Figure 10c** shows the results of the statistical analysis. Injection with Xiaflex® increases ROM by 8.043° (+/- 3.837°) with a p-value of 0.046.

a

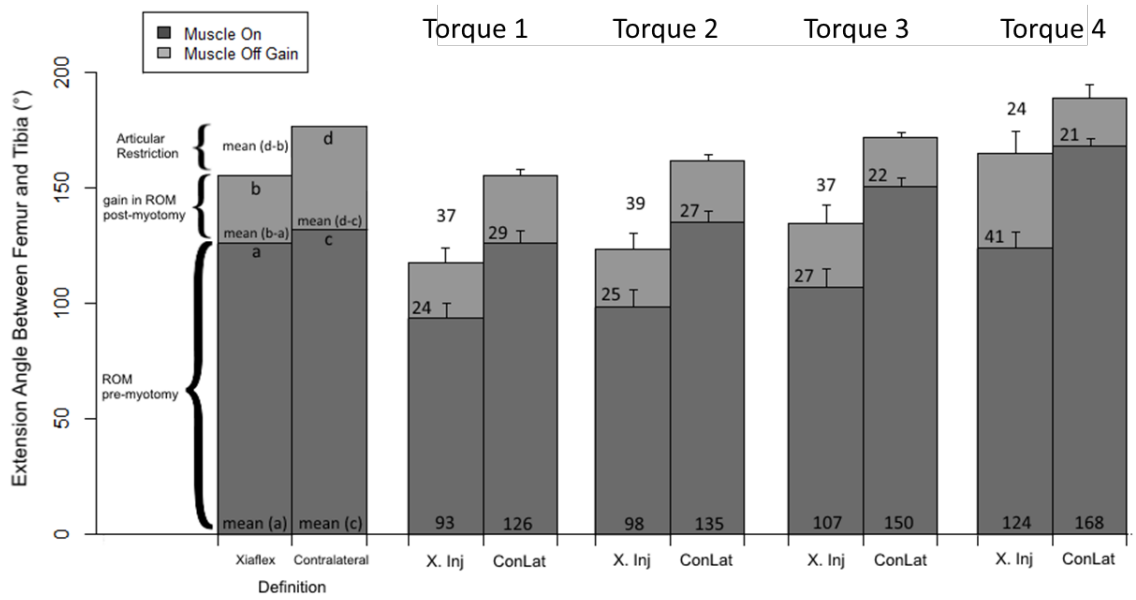
Muscle On
Muscle Off Gain
Torque 1
Torque 2
Torque 3
Torque 4
Extension Angle Between Femur and Tibia (°)
Articular Restriction
gain in ROM post-myotomy
ROM pre-myotomy
mean (d-b)
mean (d-c)
mean (b-a)
mean (a)
mean (c)
Xiaflex
Contralateral
X. Inj
ConLat
Definition

b

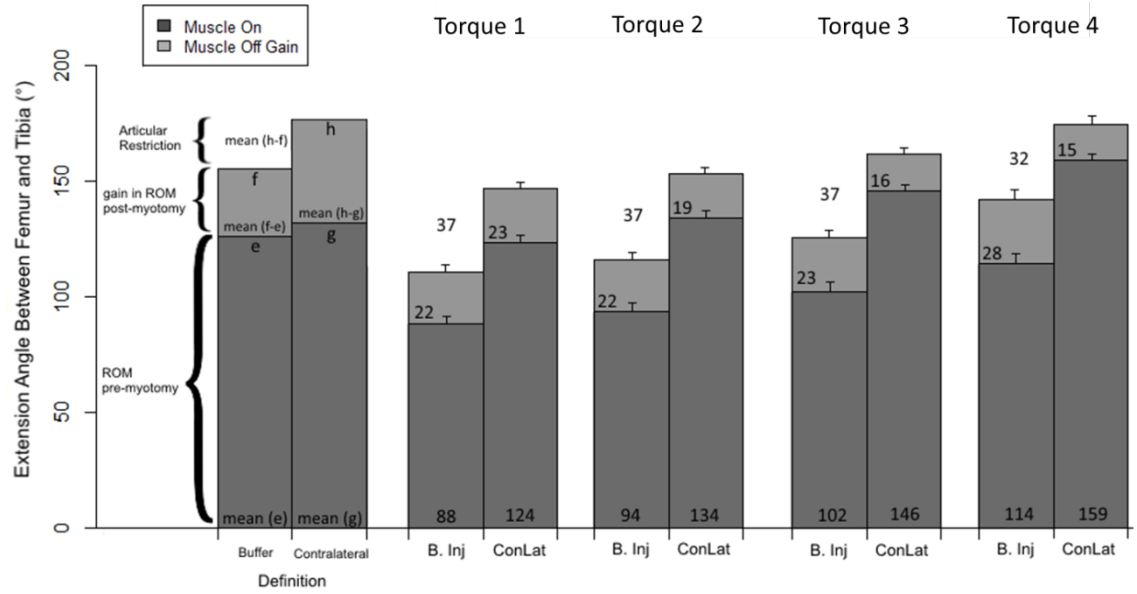
Muscle On
Muscle Off Gain
Torque 1
Torque 2
Torque 3
Torque 4
Extension Angle Between Femur and Tibia (°)
Articular Restriction
gain in ROM post-myotomy
ROM pre-myotomy
mean (h-f)
mean (h-g)
mean (f-e)
mean (e)
mean (g)
Buffer
Contralateral
B. Inj
ConLat
Definition

c

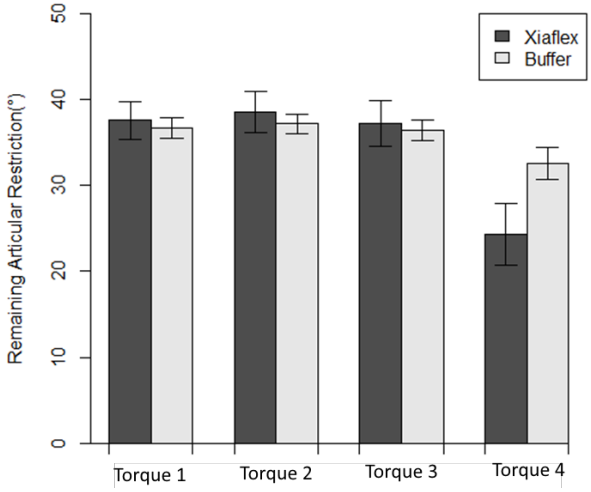
Xiaflex
Buffer
Remaining Articular Restriction(°)
Torque 1
Torque 2
Torque 3
Torque 4

Figure 9. Direct and Calculated Measurements of the Range of Motion of Xiaflex®-Injected and Buffer-Injected Rat Knees Against the Within-Rat Contralateral Knees After Two Weeks Post-Injection. Means of ROM are plotted with standard error. Mean ROM values are given within each bar along with value of the differences between mean immobilized (either **a)** X-Inj or **b)** B-Inj) and mean corresponding contralateral knee extension with muscle off (value above bar for injected knee). **c**) These differences are presented with standard error. At torque four, the X-Inj rats show less articular restriction than the B-Inj rats.

Calculations:

Gain in ROM post-myotomy calculated by:

(Muscle Off ROM)-(Muscle On ROM); b-a, d-c; f-e, h-g

Articular restriction in the diseased knee calculated by:

(Immobilized Muscle Off)-(Contralateral Muscle Off); d-b; h-f

a

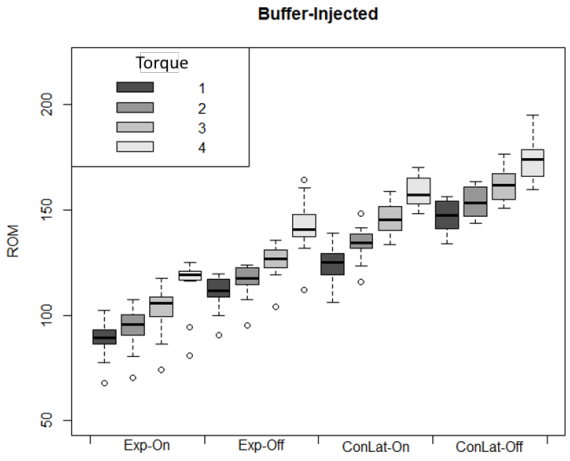

b

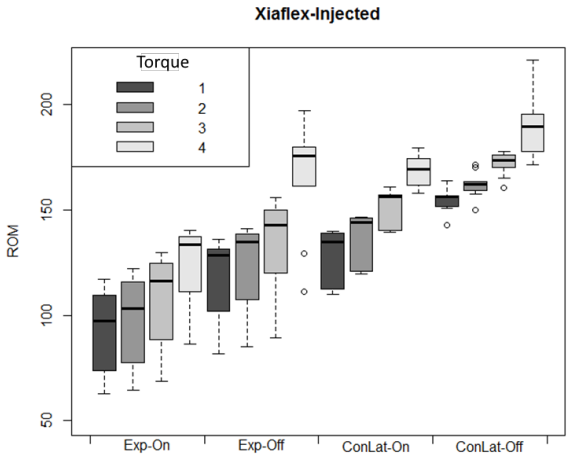

c

Linear model: ROM ~ Injection + Torque + Muscle + Leg + (1 | Rat.ID)

Buffer to Xiaflex®			Torque 1 to Torque 4		
Estimate Increase (°)	Std. Error	p-value	Estimate Increase (°)	Std. Error	p-value
8.043	3.837	0.046	33.790	1.682	1.0×10^{-58}
Muscle On to Muscle Off			**Immobilized to Contralateral**		
Estimate Increase (°)	Std. Error	p-value	Estimate Increase (°)	Std. Error	p-value
23.790	1.190	3.9×10^{-55}	37.710	1.190	4.3×10^{-95}

Figure 10. Boxplots of Range of Motion Measurements of Buffer-Injected or Xiaflex®-Injected and Corresponding Contralateral Knees Two Weeks Post-Injection and Linear Model with Statistical Analysis. a) Xiaflex® and **b)** buffer groups' boxplots show median ROM plotted for each category; experimental muscle on (Exp-On), experimental muscle off (Exp-Off), contralateral muscle on (ConLat-On), and contralateral muscle off (ConLat-Off). Each box represents the median value and interquartile range. Whiskers indicate the lowest and highest extension angles that are non-outliers. Outliers (outside 1.5 times the interquartile range) are plotted as individual points. **c)** Linear mixed effect model indicates that Xiaflex® injection with 2 weeks remobilization increases ROM by 8.043° (+/- 3.837°) with a p-value of 0.046. There are significant increases in ROM with increase in torque, between muscle on and off, and between experimental and contralateral knees. n=9 X-Inj rats; n=11 B-Inj rats.

3.2.2 Range of Motion – Four Weeks Immobility Followed by Four Weeks Remobilization

Based on the recommended posology for the use of Xiaflex® in the treatment of patients with Dupuytren's contractures (allowing four weeks between injections and follow-ups), four rats per group were allowed four weeks post-injection before outcomes were measured. ROM results of experimental and contralateral legs of rats immobilized for four weeks to induce a knee FC, intra-articularly injected with either Xiaflex® or buffer, and remobilized for 4 weeks are presented in **Figure 11a**. Results presented are descriptive statistics including mean ROM +/- 1 SEM and sample size for each experimental group; four rats were used in each group. Mean values are presented with standard error for all four torques and legs with muscle on and muscle off. Each leg group was assigned a letter for ease of reading the following figures. ROM always increased with increase of torque and with removal of muscle. The contralateral leg was always more mobile than the immobilized leg confirming the presence of a knee FC induced by immobilization. With the muscle off, immobilized legs injected with Xiaflex® had a higher ROM than those injected with buffer (see statistical analysis below). **Figure 11b** displays a graphical representation of the results of X-Inj legs versus B-Inj legs. **Figure 11c** is the calculated value of the difference in ROM between X-Inj and B-Inj legs with muscle off, which compares restriction of motion mainly due to the posterior capsule. The difference between the groups increased with increase in torque. The gain in ROM from removal of muscle was higher in the X-Inj knees.

The experimental legs were also compared to the within-rat contralateral legs, the difference between which can be interpreted as the amount of contracture. **Figures 12a and b** show the comparison for both groups. **Figure 12c** is a graphical representation of the amount of articular restriction remaining in the experimental legs when compared to the matching contralateral legs. Mean differences are presented with standard error. There was no noticeable difference between the treated and untreated knee FCs when compared to the corresponding contralateral knees.

The statistical significance of the ROM measurements was evaluated using statistical modeling. The linear mixed effects model used took into account both fixed and random

a

		Xiaflex (n=4)						Buffer (n=4)					
		Immobilized			Contralateral			Immobilized			Contralateral		
Muscle	Torque	Mean	SEM	Name	Mean	SEM	Name	Mean	SEM	Name	Mean	SEM	Name
On	1	93.8	8.7	i	128.5	7.0	k	101.8	1.9	m	120.4	2.6	o
	2	100.0	9.5		135.9	6.4		107.5	1.7		127.3	2.4	
	3	110.5	11.1		148.4	5.9		116.1	2.1		140.3	2.0	
	4	122.3	13.1		158.3	6.1		125.0	2.9		152.1	2.4	
Off	1	123.4	8.7	j	147.8	4.6	l	116.9	3.1	n	144.4	2.6	p
	2	127.9	8.4		153.3	3.8		120.7	3.1		151.9	2.2	
	3	136.2	7.6		160.7	4.4		126.6	5.2		161.4	2.7	
	4	148.1	4.7		172.8	8.9		138.7	4.8		173.8	2.4	

b

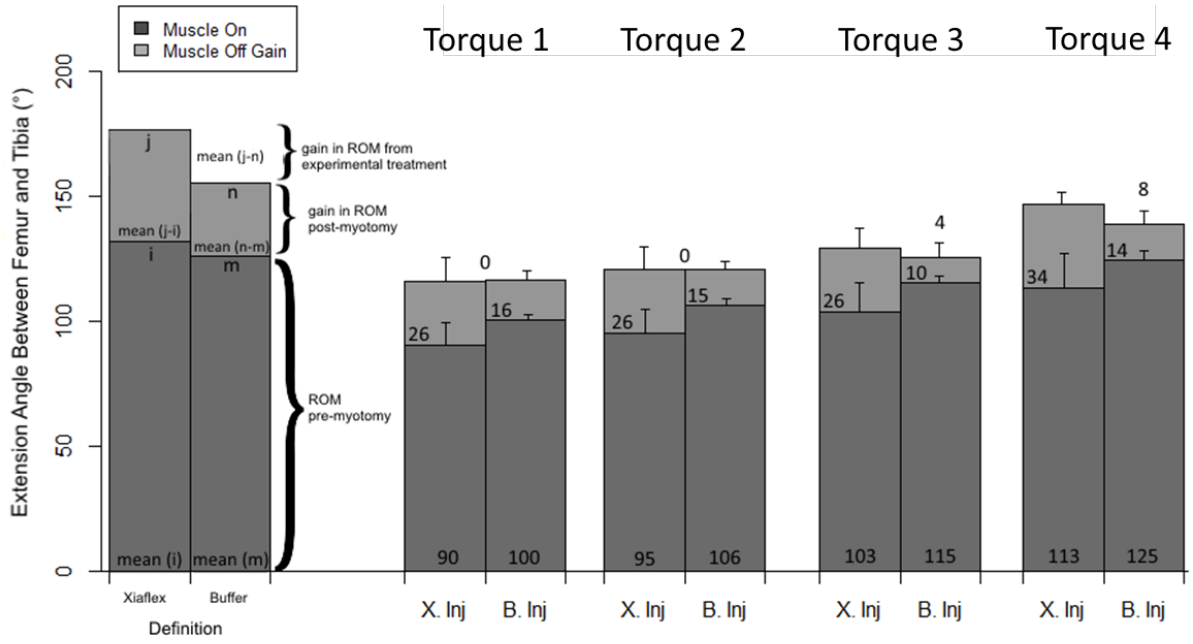

c

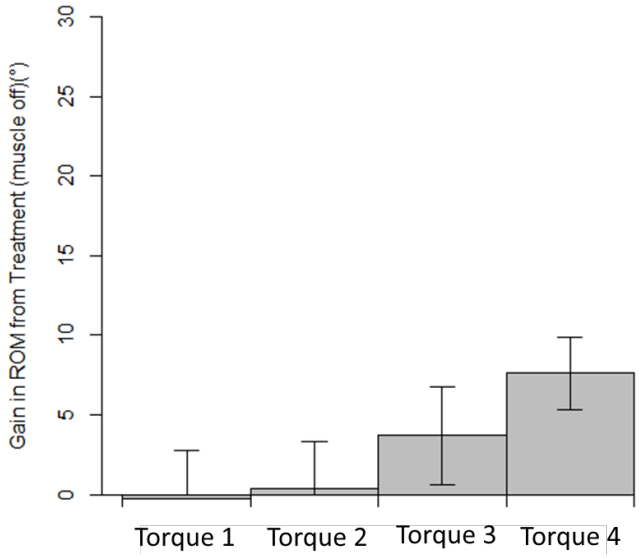

Figure 11. Direct and Calculated Measurements of the Range of Motion of Xiaflex®-Injected and Buffer-Injected Rat Knees After Four Weeks of Immobilization and Four Weeks Recovery at Four Torques. One hind leg of each rat was immobilized at 45° flexion with a plate and screws. After 4 weeks of immobilization, legs were remobilized by surgically removing the immobilization device and knees were intra-articularly injected with either Xiaflex® (50µL, 0.6µg/µL) or buffer (50µL). Rats were brought to end point at 4 weeks post-injection and ROM in extension of both experimental and contralateral legs were measured, first with muscle on and then with the muscles around the joint sectioned. 'Muscle on' reflected the contribution of both muscles and posterior knee capsule in the limitation of ROM while 'muscle off' reflected the contribution of only the capsule. An automatic arthrometer was used at four different torques: 2.5N·cm, 7.5N·cm, 12.5N·cm, and 23.4N·cm. Pictures were captured at each torque and the angle between femur and tibia was measured using ImageJ. **a)** Mean extension angles are presented with standard error. Each group was assigned a letter for ease of interpreting the subsequent figures. **b)** Mean ROM values are given within each bar along with value of the differences between mean buffer-injected (B. Inj) and mean Xiaflex®-injected (X. Inj) extension with muscle off (number above B. Inj bar). Error bars present standard error of direct and calculated measurements. **c)** The difference in degrees between the mean ROM values of X-Inj legs and B-Inj legs without muscle against each of the four different torques shows that at torques 3 and 4, ROM of X-Inj knees was higher than ROM of B-Inj knees.
Calculations:

Gain in ROM post-myotomy calculated by:
(Muscle Off ROM)-(Muscle On ROM); j-i, n-m

Gain in ROM from experimental treatment calculated by:
(Xiaflex® Muscle Off)-(Buffer Muscle Off); j-n

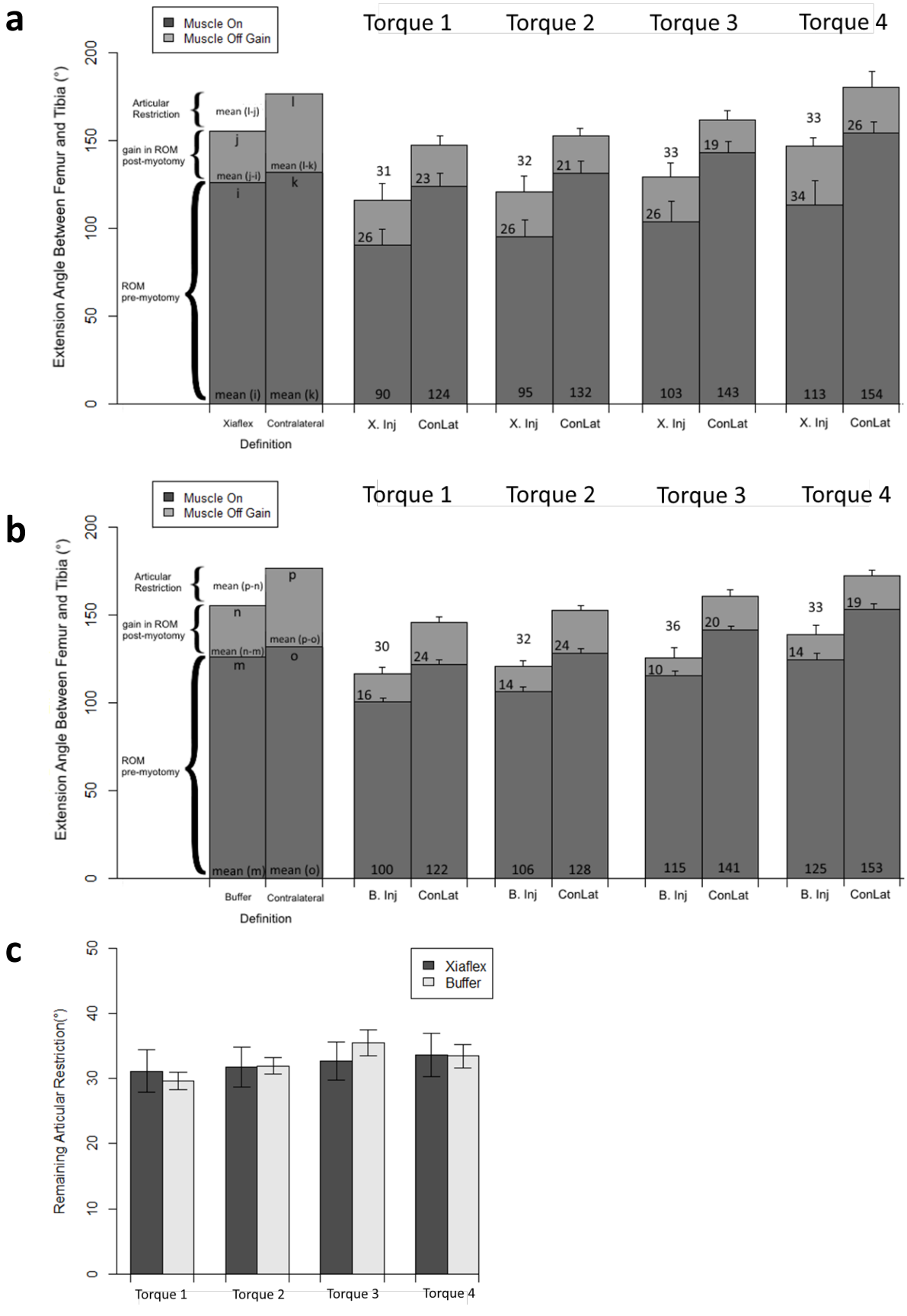
a
Muscle On
Muscle Off Gain
Torque 1
Torque 2
Torque 3
Torque 4
Extension Angle Between Femur and Tibia (°)
Articular Restriction
mean (l-j)
gain in ROM post-myotomy
mean (j-i)
mean (l-k)
ROM pre-myotomy
mean (i)
mean (k)
Xiaflex
Contralateral
Definition
X. Inj
ConLat
b
Muscle On
Muscle Off Gain
Articular Restriction
mean (p-n)
gain in ROM post-myotomy
mean (n-m)
mean (p-o)
ROM pre-myotomy
mean (m)
mean (o)
Buffer
Contralateral
Definition
B. Inj
ConLat
c
Xiaflex
Buffer
Remaining Articular Restriction(°)
Torque 1
Torque 2
Torque 3
Torque 4

Figure 12. Direct and Calculated Measurements of the Range of Motion of Xiaflex®-Injected and Buffer-Injected Rat Knees Against the Within-Rat Contralateral Knees After Four Weeks Post-Injection. Means of ROM are plotted with standard error. Mean ROM values are given within each bar along with value of the differences between mean immobilized (either **a)** X-Inj or **b)** B-Inj) and mean corresponding contralateral knee extension with muscle off (value above bar for injected knee). **c)** These differences are presented with standard error. There is no statistical difference in articular ROM restriction between X-Inj and B-Inj knees.
Calculations:

Gain in ROM post-myotomy calculated by:
(Muscle Off ROM)-(Muscle On ROM); j-I, l-k; n-m, p-o

Articular restriction in the diseased knee calculated by:
(Immobilized Muscle Off)-(Contralateral Muscle Off); l-j; p-n

effects and the repeated ROM measures made for the same knee at the four different torques. Boxplots presented in **Figures 13a and b** show the median values and the interquartile range. X-Inj rats showed more variation in ROM compared to the B-Inj rats, even in the contralateral legs. No mathematical outliers were identified, although two of the four Xiaflex®-treated rats strikingly did not respond to the treatment, and ROM was less than the B-Inj rats. Overall median values in the X-Inj experimental legs were higher than those of the B-Inj legs. The table in **Figure 13c** shows the results of the statistical analysis. The sample size was low (n=4 B-Inj and n=4 X-Inj) and there is no statistical difference in ROM between the Xiaflex® and buffer-injected knees, however trends show an increase in ROM in drug-treated legs

3.2.3 Range of Motion – Comparing Contralateral Legs

Figure 14 compares the ROM of contralateral legs of Xiaflex® treated rats with those of control rats at both remobilization experiments; panel **a** shows rats with 2 weeks remobilization and panel **b** shows the rats with 4 weeks remobilization. In almost all cases, ROM was higher in the contralateral legs of rats with Xiaflex® injected into the experimental leg, both with muscle on and muscle off.

3.2.4 Histology - Collagen I and Collagen III Immunostaining

After the testing mobility function of the knee (ROM), joints were fixed in formalin and decalcified in EDTA solution. Once sufficiently decalcified, knees were embedded in paraffin and 7µm sagittal slides were cut at the medial mid condylar level. Using IHC, slides were stained for collagen proteins, specifically COLI and COLIII. Images of the posterior capsule were captured and brown DAB staining was quantified in ImageJ (**Figure 15a-c**).

In the posterior capsules of rats that had two weeks of remobilization, experimental capsules that had contractures induced showed significantly more staining of COLI than contralateral (**Figure 15d**). Xiaflex®-treated knees showed more COLI staining in posterior capsule than buffer-treated knees, although not statistically significant. Quantification of COLIII staining for the same capsules showed a significant increase in staining in the

a

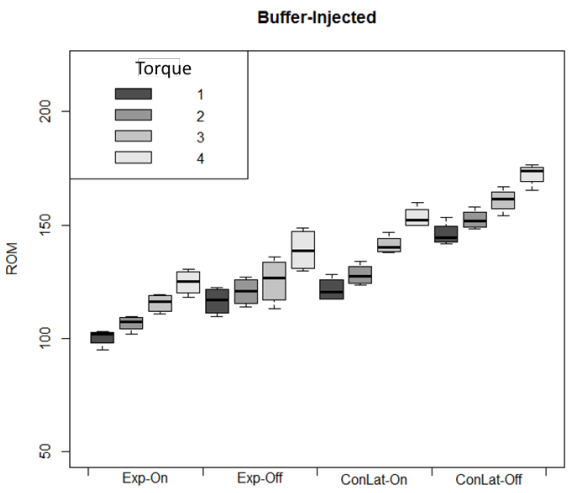

b

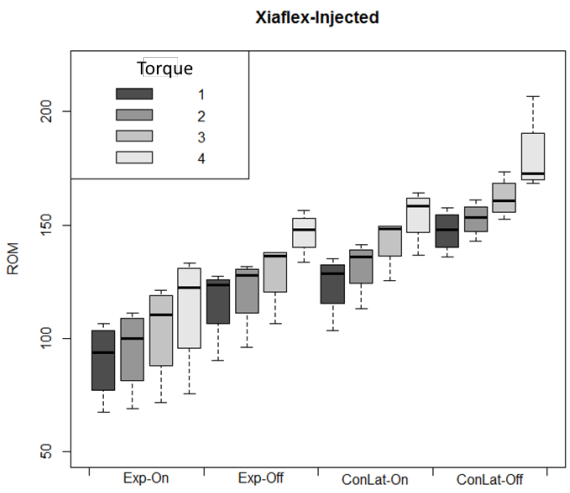

c

Linear model: ROM ~ Injection + Torque + Muscle + Leg + (1 | Rat.ID)

Buffer to Xiaflex®			Torque 1 to Torque 4		
Estimate Increase (°)	Std. Error	p-value	Estimate Increase (°)	Std. Error	p-value
-0.9436	4.502	0.825	27.738	2.263	1.3×10^{-23}
Muscle On to Muscle Off			**Immobilized to Contralateral**		
Estimate Increase (°)	Std. Error	p-value	Estimate Increase (°)	Std. Error	p-value
21.359	1.600	1.9×10^{-24}	31.719	1.600	2.7×10^{-38}

Figure 13. Boxplots of Range of Motion Measurements of Buffer-Injected or Xiaflex®-Injected and Corresponding Contralateral Knees Four Weeks Post-Injection and Linear Model with Statistical Analysis. a) Xiaflex® and **b)** buffer groups' boxplots show median ROM plotted for each category; experimental muscle on (Exp-On), experimental muscle off (Exp-Off), contralateral muscle on (ConLat-On), and contralateral muscle off (ConLat-Off). Each box represents the median value and interquartile range. Whiskers indicate the lowest and highest extension angles that are non-outliers. Outliers (outside 1.5 times the interquartile range) would have been plotted as individual points. **c)** The linear mixed effect model indicates no significant difference between X-Inj and B-Inj knees at four weeks post-injection. There are significant increases in ROM with increase in torque, between muscle on and off, and between experimental and contralateral knees. n=4 X-Inj rats; n=4 B-Inj rats

a

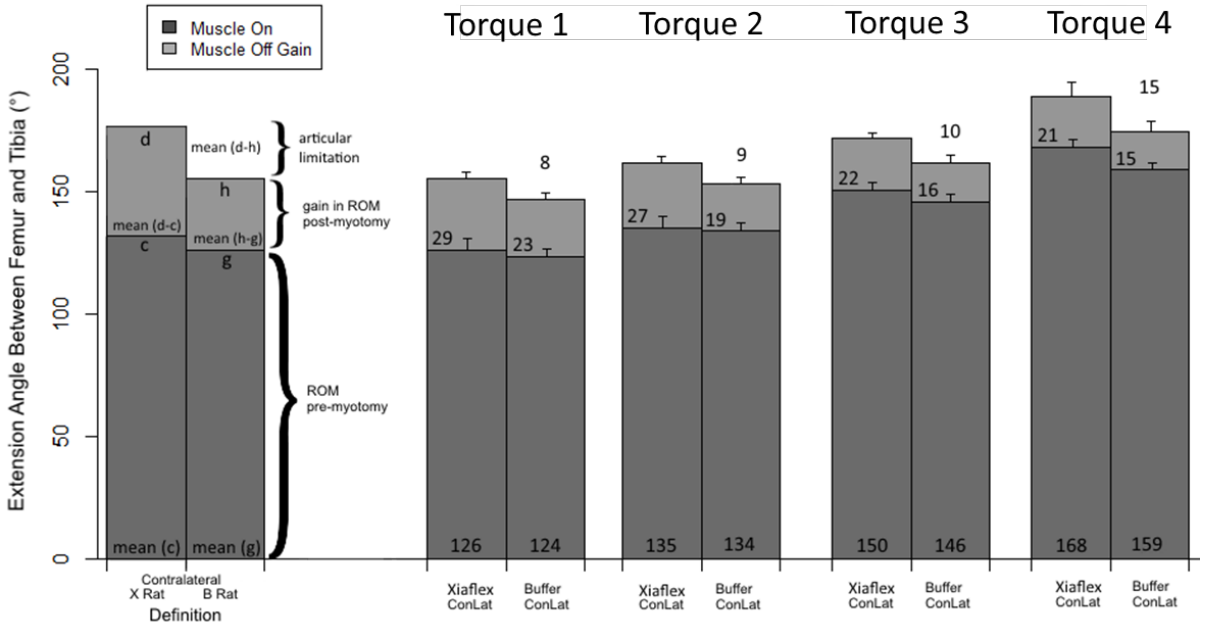
Muscle On
Muscle Off Gain
Torque 1
Torque 2
Torque 3
Torque 4
Extension Angle Between Femur and Tibia (°)
0
50
100
150
200
d
mean (d-c)
c
mean (c)
h
mean (h-g)
g
mean (g)
mean (d-h)
articular limitation
gain in ROM post-myotomy
ROM pre-myotomy
29
23
8
27
19
9
22
16
10
21
15
15
126
124
135
134
150
146
168
159
Contralateral
X Rat
B Rat
Definition
Xiaflex ConLat
Buffer ConLat

b

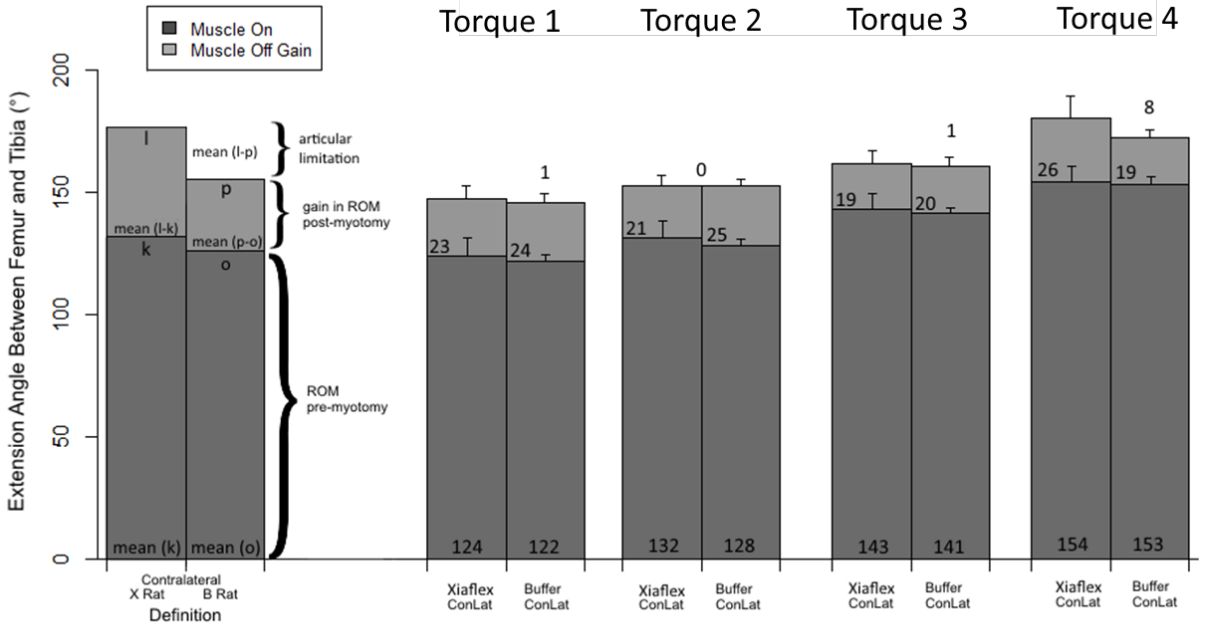
Muscle On
Muscle Off Gain
Torque 1
Torque 2
Torque 3
Torque 4
Extension Angle Between Femur and Tibia (°)
0
50
100
150
200
l
mean (l-k)
k
mean (k)
p
mean (p-o)
o
mean (o)
mean (l-p)
articular limitation
gain in ROM post-myotomy
ROM pre-myotomy
23
24
1
21
25
0
19
20
1
26
19
8
124
122
132
128
143
141
154
153
Contralateral
X Rat
B Rat
Definition
Xiaflex ConLat
Buffer ConLat

Figure 14. Direct and Calculated Measurements of the Range of Motion of Contralateral Knees. ROM of the contralateral legs were measured along with the experimental legs **a)** two weeks or **b)** four weeks post-injection of the experimental knee at four torques. Means of ROM are plotted with standard error. Mean ROM values are given within each bar along with value of the differences between mean contralateral knee extensions with muscle off (above "Buffer ConLat" bar). The contralateral legs of the B-Inj rats show a general trend of less ROM than the treatment rats.
Calculations:

Gain in ROM post-myotomy calculated by:
(Muscle Off ROM)-(Muscle On ROM); d-c, h-g, l-k, p-o

Difference in articular restriction calculated by:
(Contralateral Buffer Rat Muscle Off)-(Contralateral Xiaflex® Rat Muscle Off); d-h, l-p

a **b** **c**

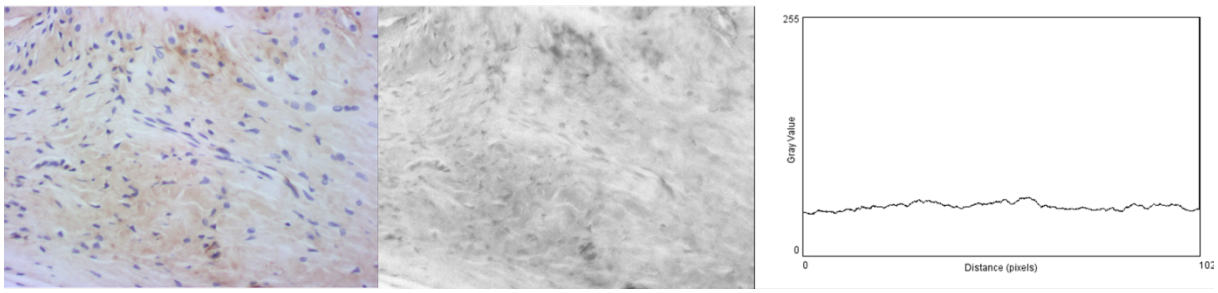

2 weeks remobilized

d **e**

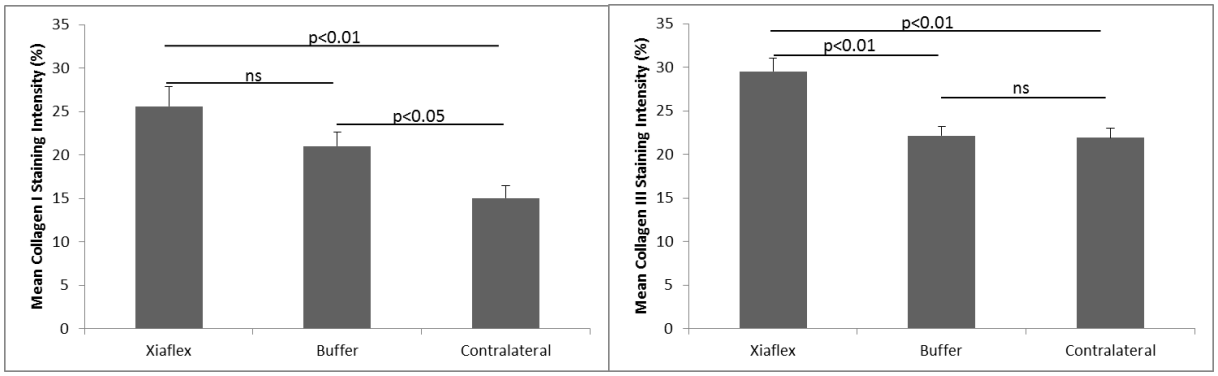

4 weeks remobilized

f **g**

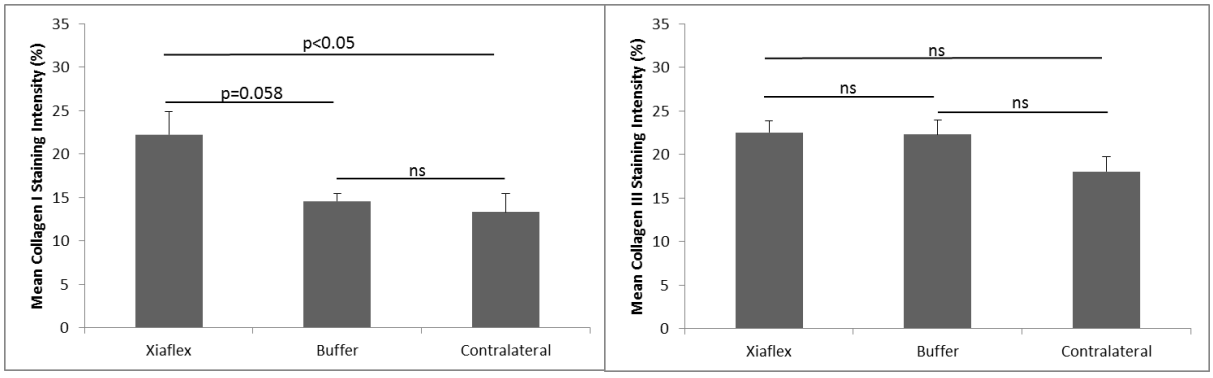

Figure 15. Collagen I and Collagen III Immunostaining in the Posterior Capsule of Immobilized Rat Knees Injected with Xiaflex® or Buffer. After ROM was measured, knees were fixed in formalin and decalcified with EDTA solution. Once sufficiently decalcified, knees were embedded in paraffin and sectioned into 7µm medial mid-condylar sagittal slides. Using primary antibody for COLI or COLIII, secondary HRP antibody, and DAB substrate, slides were immunostained with hematoxylin used as a counter stain. Four fields of the posterior capsule were imaged at 66X with a Marlin F080C digital camera (Allied Vision Technologies) with AVT Smartview 1.5.1 software. **a)** Images were imported into ImageJ for analysis. An example field is presented from a B-Inj knee with four weeks remobilization and stained for COLI. **b)** In ImageJ, the "Blue" channel is selected to isolate brown DAB staining and eliminate the blue hematoxylin staining. **c)** A "Plot Profile" is generated, plotting average pixel brightness intensity per vertical column of pixels. The area under the graph is recorded as staining intensity and the four fields per knee were averaged. Staining intensity is reported as a percentage where total black represents 100%. **d)** Quantification of COLI staining in posterior capsule of experimental legs with contracture (X-Inj or B-Inj) and contralateral legs; four weeks of immobilization followed by two weeks of remobilization. Experimental capsule showed significantly more staining than contralateral. Xiaflex®-treated capsule showed more staining than buffer-treated capsule, although not significant. **e)** Quantification of COLIII staining for the same capsules showed a significant increase in staining in the Xiaflex®-treated capsule compared to buffer-treated and contralateral capsules. n=11 buffer knees, n=9 Xiaflex® knees, and n=16 contralateral knees. **f)** Quantification of COLI staining in posterior capsule of experimental legs with contracture (X-Inj or B-Inj) and contralateral legs; four weeks of immobilization followed by four weeks of remobilization. There was an increase in staining in the Xiaflex®-treated capsule compared to buffer-treated and contralateral capsules, although only comparison to the contralateral capsules was significant. **g)** Quantification of COLIII staining for the same capsules showed no significant differences between groups. n=4 buffer knees, n=4 Xiaflex® knees, and n=4 contralateral knees.

Xiaflex®-treated capsule compared to buffer-treated and contralateral capsules, and there was no significant difference between buffer and contralateral capsules (**Figure 15e**).

For rats with four weeks of remobilization, there was an increase in COLI staining in the Xiaflex®-treated capsule compared to buffer-treated and contralateral capsules, although only comparison to the contralateral capsules was significant (**Figure 15f**). Quantification of COLIII staining for the same capsules showed no significant differences between groups (**Figure 15g**).

3.2.5 Histology - Masson Trichrome

To evaluate overall fibrosis in the posterior capsules of the rat knees, MT staining was used. **Figure 16a** shows an example of MT staining in the posterior capsule of a B-Inj rat knee with two weeks remobilization; collagen stains blue, nuclei stain black, and cytoplasm stains red [72]. After knees were sectioned, slides were stained by the Pathology Department at the University of Ottawa and four fields of the posterior capsule were imaged and imported into ImageJ for quantification. The "Threshold Color" tool was used to isolate and count the number of blue pixels in the field (**Figure 16b**). Results are presented as a percentage of blue pixels from the total number of pixels without including white space. No significant differences were identified between Xiaflex®, buffer, or contralateral legs with either two or four weeks remobilization (**Figure 16c and d**).

3.2.6 Histology – Articular Cartilage Surface

Histological examination was used to detect potential damage to articular cartilage caused by Xiaflex® treatment. The main collagen found in the articular cartilage is type II [55], theoretically susceptible to degradation by the collagenase treatment. Articular cartilage surrounds the surface of the bones and is exposed to the intra-articular space. Contractures induced by immobility are known to cause surface irregularity of the articular cartilage [78], which is exposed to the collagenases that were injected. Representative slides were imaged at 3.3X and 13.2X with Hematoxylin and Eosin (H&E) staining (**Figure 17**). The articular cartilage along the condyles of the contralateral joints is smooth and

a **b**

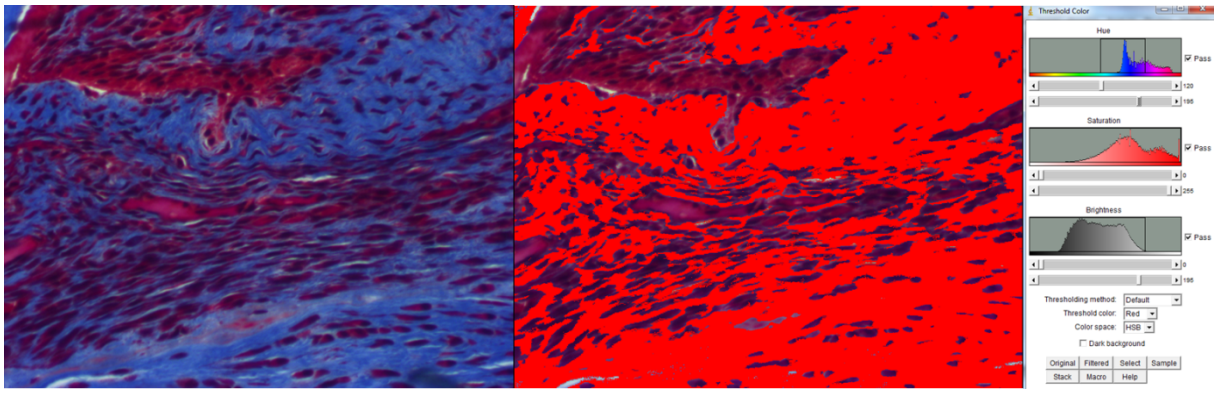

c 2 weeks remobilized

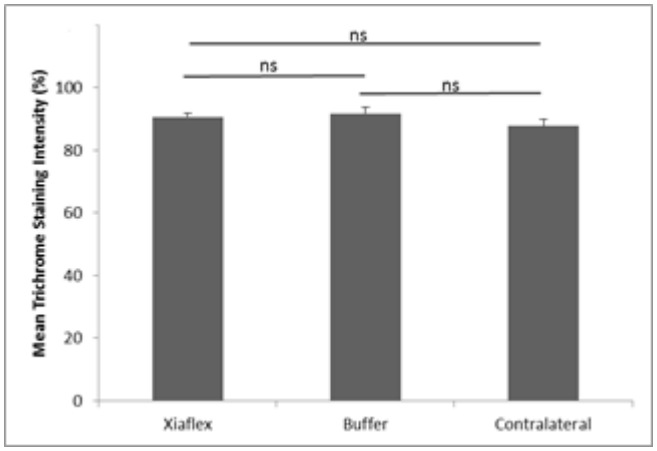

d 4 weeks remobilized

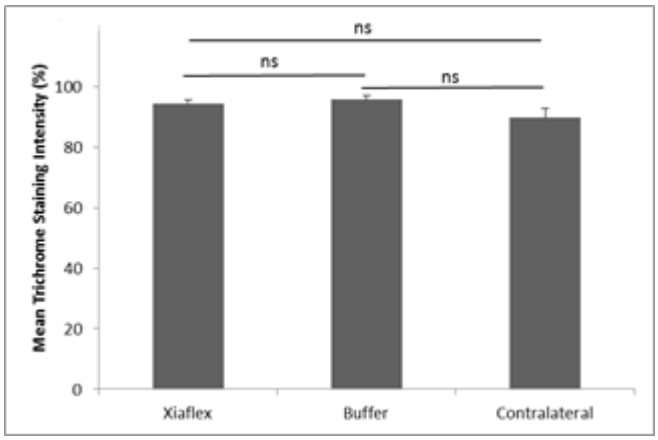

Figure 16. Masson Trichrome Staining in the Posterior Capsule of Immobilized Rat Knees Injected with Xiaflex® or Buffer. a) An example of MT staining in the posterior capsule of a B-Inj rat knee with two weeks remobilization; collagen stains blue, nuclei stain black, and cytoplasm stains red. After knees were sectioned, slides were stained and four fields of the posterior capsule were imaged at 66X with an Olympus BH-2 light microscope and a Marlin F080C digital camera (Allied Vision Technologies) with AVT Smartview 1.5.1 software. **b)** Images were imported into ImageJ for quantification. The "Threshold Color" tool was used to isolate and count the number of blue pixels in the field. Results are presented as a percentage of blue pixels from the total number of pixels without including white space. **c)** Quantification of MT staining in posterior capsule of experimental legs with contracture (X-Inj or B-Inj) and contralateral legs; four weeks of immobilization followed by two weeks of remobilization. No significant differences were identified. n=11 buffer knees, n=9 Xiaflex® knees, and n=16 contralateral knees. **d)** MT capsule staining of rat knees with four weeks of remobilization. No significant differences were identified. n=4 buffer knees, n=4 Xiaflex® knees, and n=4 contralateral knees.

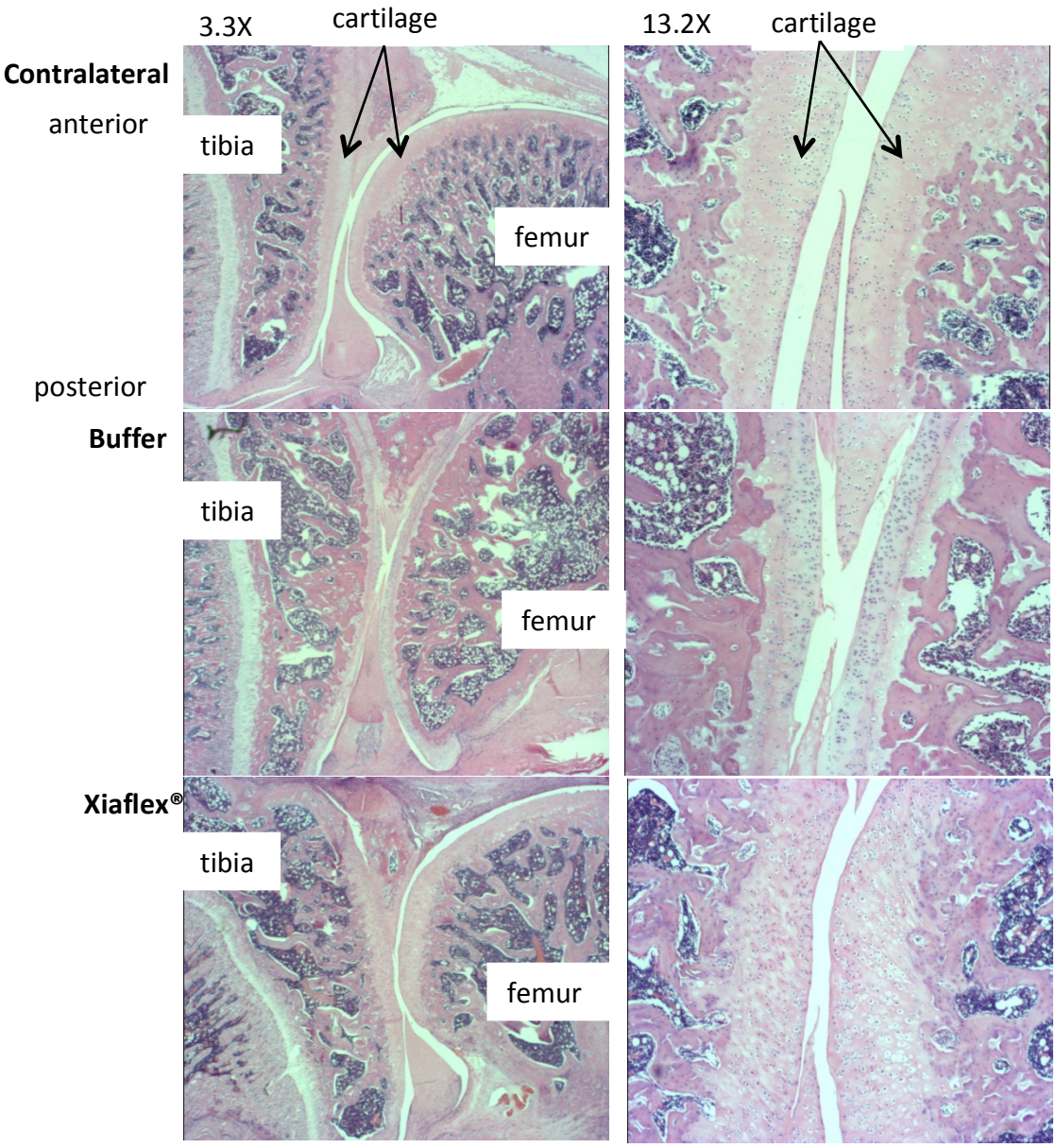
3.3X
cartilage
13.2X
cartilage
Contralateral
anterior
tibia
femur
posterior
Buffer
tibia
femur
Xiaflex®
tibia
femur

Figure 17. Hematoxylin and Eosin Staining of Experimental (Xiaflex® or Buffer Injected) and Contralateral Rat Knees to Detect Damage to Articular Cartilage. After sectioning of the knees, slides were stained with standard hematoxylin and eosin. Images of representative slides were imaged at 3.3X and 13.2X with an Olympus BH-2 light microscope and a Marlin F080C digital camera (Allied Vision Technologies) with AVT Smartview 1.5.1 software. The images are positioned so that the anterior of the joint is at the top and the posterior at the bottom, the femur is on the right and the tibia is on the left. The articular cartilage along the condyles of the contralateral joints is smooth and undamaged. The cartilage of joints with contractures are uneven, however X-Inj knee joints show no further damage compared to the B-Inj joints.

undamaged. The cartilage of joints with contractures is uneven: there is surface irregularity and the cartilage appears less thick, a change previously observed in immobilized rat knee joints over time [78]. The X-Inj knee joints show no further damage compared to the B-Inj joints.

3.3 Collagenase - Capsule Incubations

To further investigate the effect of the collagenase activity in Xiaflex® on posterior capsule, tissue samples of normal rats (n=3) and human diseased (osteoarthritis, with (n=1) and without (n=3) knee FC) were cut in half with one half incubated in Xiaflex® and the other in saline buffer. After 24 hours at 37°C, tissue was removed and embedded for histological analysis and the remaining supernatant was analysed for protein content using protein gel electrophoresis.

3.3.1 Histology – Collagen I and Collagen III Protein Staining

The overall collagen content in capsule sections was evaluated using IHC staining for COLI and COLIII proteins post-incubations and were quantified as intensity of staining divided by overall tissue area. An example of immunostaining of the capsule tissue is shown in **Figure 18a**. The means with standard error are presented in **Figure 18**. The normal rat capsule incubated in Xiaflex® had less staining intensity for both collagen types (**Figure 18b**). The human samples had less staining in the buffer-incubated sample for COLI, but less COLIII staining in the Xiaflex®-incubated sample (**Figure 18c**). The difference in collagen staining between Xiaflex® and buffer was more substantial in the rat samples compared to the human samples. Despite the low sample size, paired t-tests were used and no significant differences between means were found.

3.3.2 Histology – Masson Trichrome

Tissue samples were also stained with MT, which stains all collagen types in blue, nuclei in black, and cytoplasm in red [72] (**Figure 19a**). The incubated rat samples were stained and the number of blue pixels over all pixels of the sample area was quantified as a

a

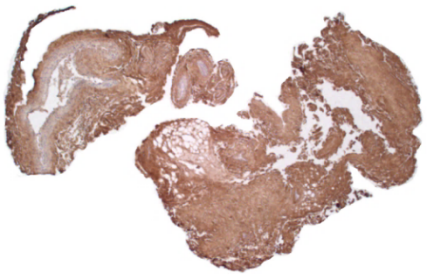

b

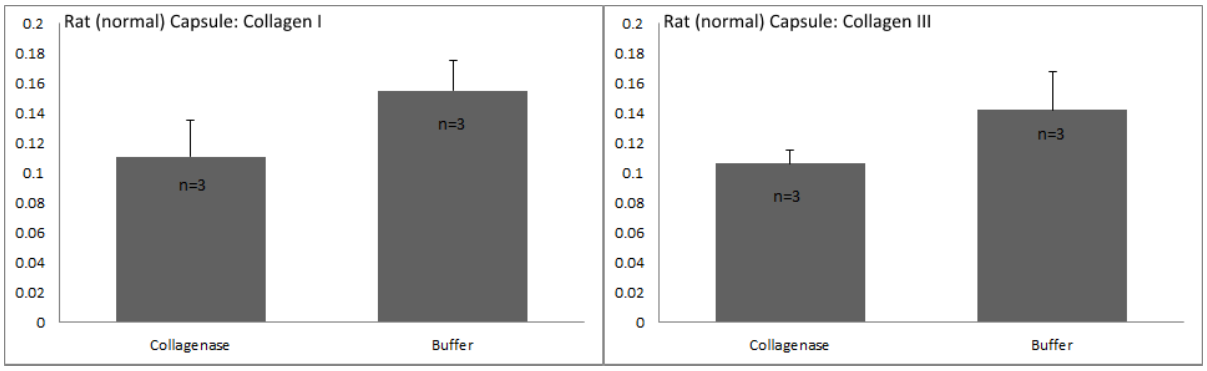
Rat (normal) Capsule: Collagen I
0.2
0.18
0.16
0.14
0.12
0.1
0.08
0.06
0.04
0.02
0
n=3
n=3
Collagenase
Buffer
Rat (normal) Capsule: Collagen III
0.2
0.18
0.16
0.14
0.12
0.1
0.08
0.06
0.04
0.02
0
n=3
n=3
Collagenase
Buffer

c

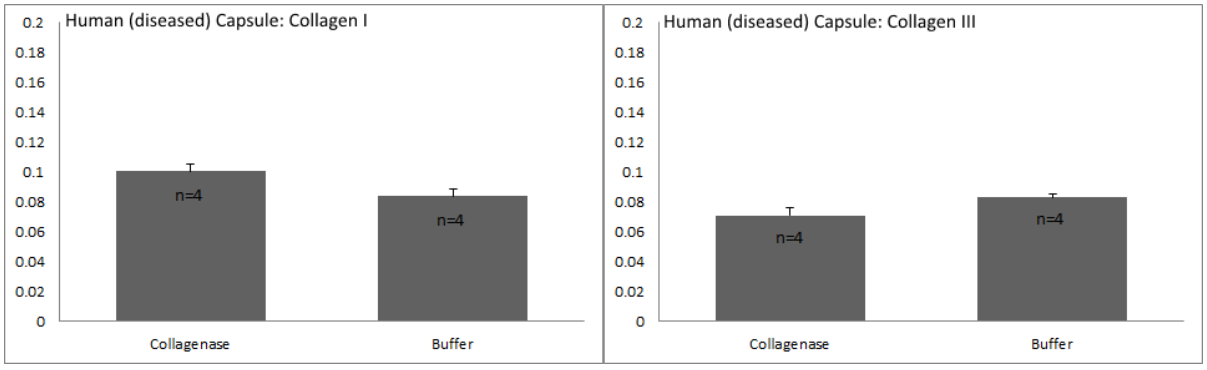
Human (diseased) Capsule: Collagen I
0.2
0.18
0.16
0.14
0.12
0.1
0.08
0.06
0.04
0.02
0
n=4
n=4
Collagenase
Buffer
Human (diseased) Capsule: Collagen III
0.2
0.18
0.16
0.14
0.12
0.1
0.08
0.06
0.04
0.02
0
n=4
n=4
Collagenase
Buffer

Figure 18. Immunohistochemistry Quantification of Collagen I and Collagen III Staining in Rat and Human Posterior Knee Capsule Samples Incubated in Xiaflex® or Buffer. Normal rat posterior knee capsules and samples of diseased (osteoarthritis) human posterior knee capsule were split in half and each half (5-10mg) was incubated at 37°C in either Xiaflex® (1mg/mL, 50 µL) or buffer (50µL) for 24 hours. The OA capsule samples were with (n=3) and without (n=1) contracture. Tissue samples were sectioned at 7µm to slides and stained via IHC for either COLI or COLIII. **a)** An example of rat tissue stained for COLI. Images were captured with an Olympus BH-2 light microscope and a Marlin F080C digital camera (Allied Vision Technologies) with AVT Smartview 1.5.1 software, magnified to 6.6X. HRP-Polymer DAB staining intensity was quantified using density plots in ImageJ and divided by total area of the sample on the slide. The mean values were plotted with standard error. **b)** In rat tissue samples (n=3), both types of collagen were less abundant in Xiaflex®-incubated capsules. **c)** Human samples showed marginal differences in collagen abundance. Paired t-tests found no significant differences between means.

a

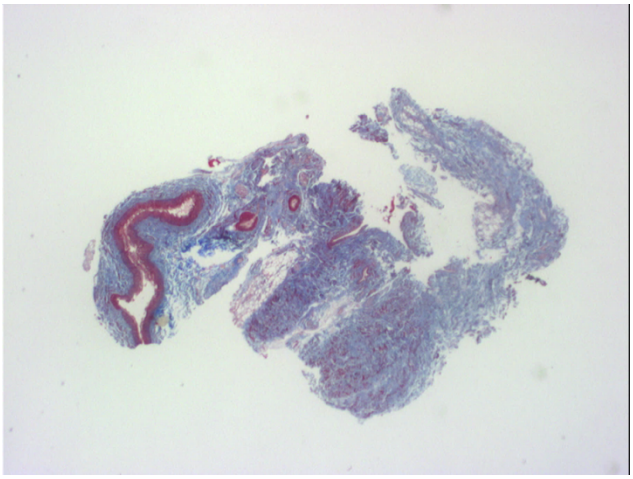

b

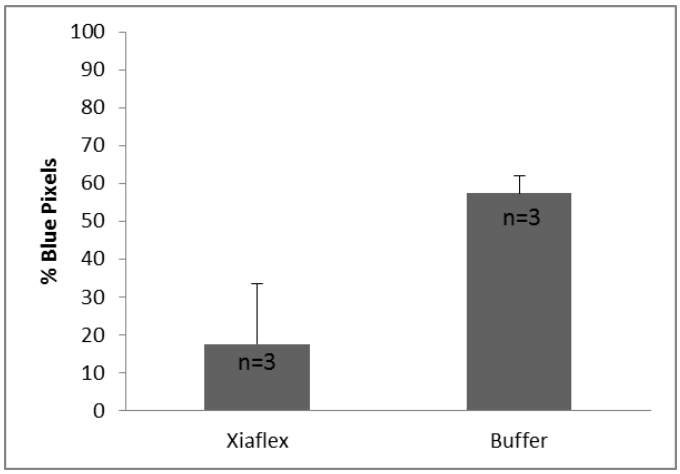

rat capsule

c

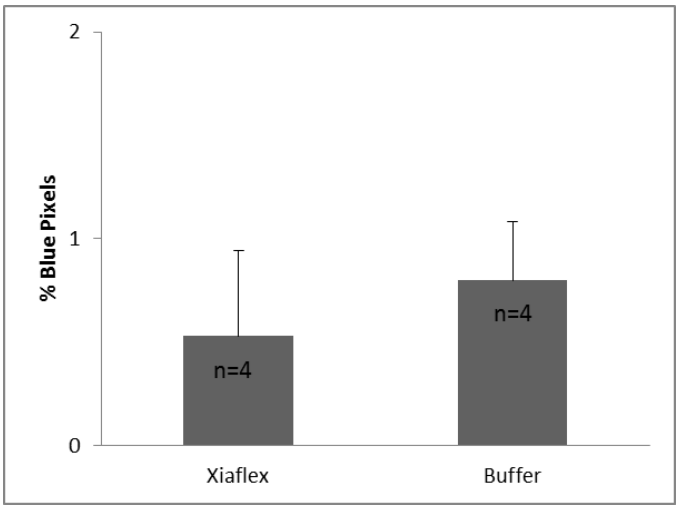

human capsule

Figure 19. Quantification of Fibrosis by Masson Trichrome Staining of Rat Capsule Incubated in Xiaflex® or Buffer. Posterior capsules from normal rat knees and diseased human knees (osteoarthritis) were cut in half and each half (5-10mg) was incubated at 37°C in either Xiaflex® (1mg/mL, 50µL) or saline buffer (50µL) for 24 hours. Samples were sectioned at 7µm to slides and stained with MT, which stains blue for collagen, black for nuclei, and red for cytoplasm. **a)** Images of the entire stained sample were captured with an Olympus BH-2 light microscope and a Marlin F080C digital camera (Allied Vision Technologies) with AVT Smartview 1.5.1 software, magnified to 6.6X. Using ImageJ, blue pixels (collagen) were isolated and counted. A mean percent of blue pixels is plotted with standard error of **b)** rat capsule samples (n=3) and **c)** human capsule samples (n=3 with contracture, n=1 without contracture). Collagen was less abundant in capsule tissue incubated in Xiaflex® compared to buffer. Paired t-tests found no significant differences between means.

percentage. There was a strikingly lower amount of blue staining in two of the three Xiaflex®-incubated samples compared to the buffer-incubated ones (**Figure 19b**), though this difference was not significant due to the high amount of staining in the third Xiaflex® sample (paired t-test). Collagen staining in the human tissue samples was much lower than the rat samples; about 1% compared to 20-60% (**Figure 19c**). Despite the low sample size, paired t-tests were used and no significant differences between means were found.

3.3.3 Protein Gel Electrophoresis – Supernatant

After capsule tissue was incubated in Xiaflex® or control buffer, the remaining supernatant was analyzed for protein content on SDS-PAGE gels. **Figure 20** presents images of the rat samples (panel **a**) and human samples (panel **b**). Protein size was estimated using a standard curve of the ladder (migration distance versus log of known molecular weights) on the rat sample gel created in Excel with an R^2=0.993. The collagenases are likely visualized at about 113kDa, which was expected, labelled with an 'A'. In the rat samples, but not the human samples, three unique and consistent protein bands are found in the Xiaflex® samples (labelled 'B', 'C', and 'D'). Band 'B' was calculated to be approximately 61kDa, 'C' was 52kDa, and 'D' was 42kDa. A few other faint protein bands can be seen, including the buffer-incubated samples, which may be artefacts of tissue incubation.

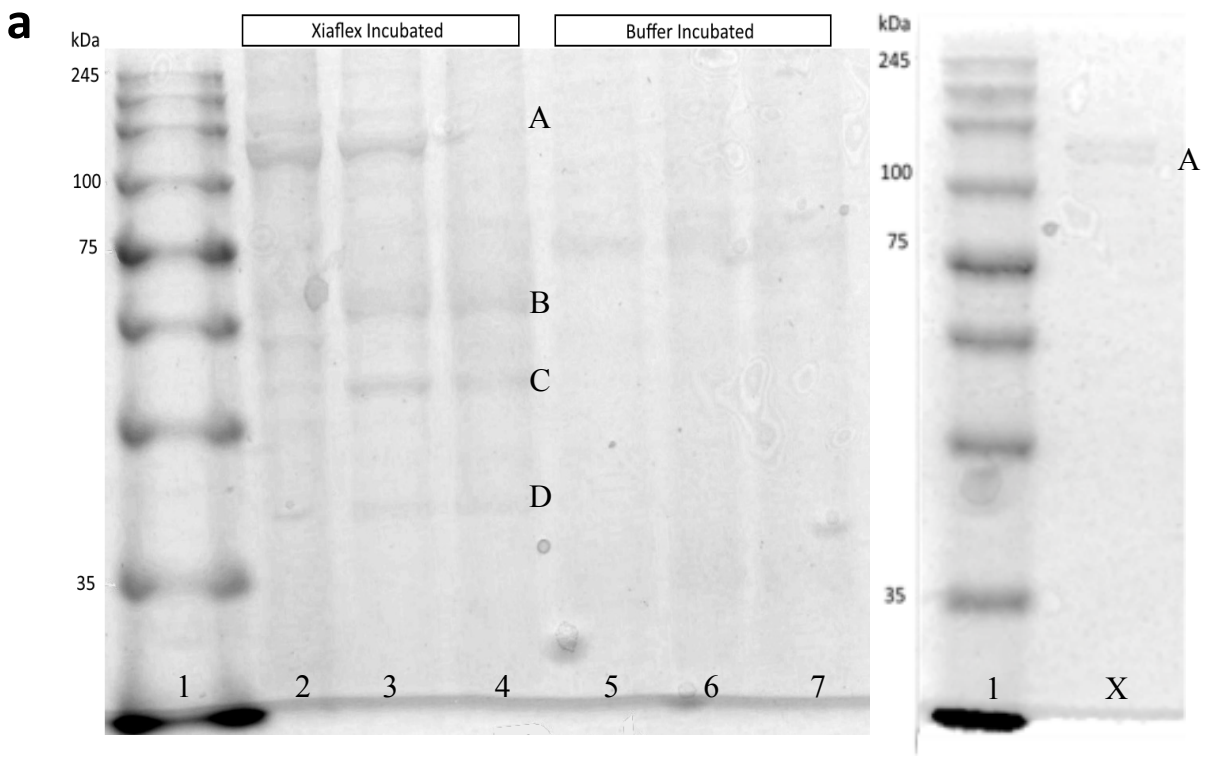
a
kDa
Xiaflex Incubated
Buffer Incubated
245
100
75
35
A
B
C
D
1
2
3
4
5
6
7
kDa
245
100
75
35
A
1
X

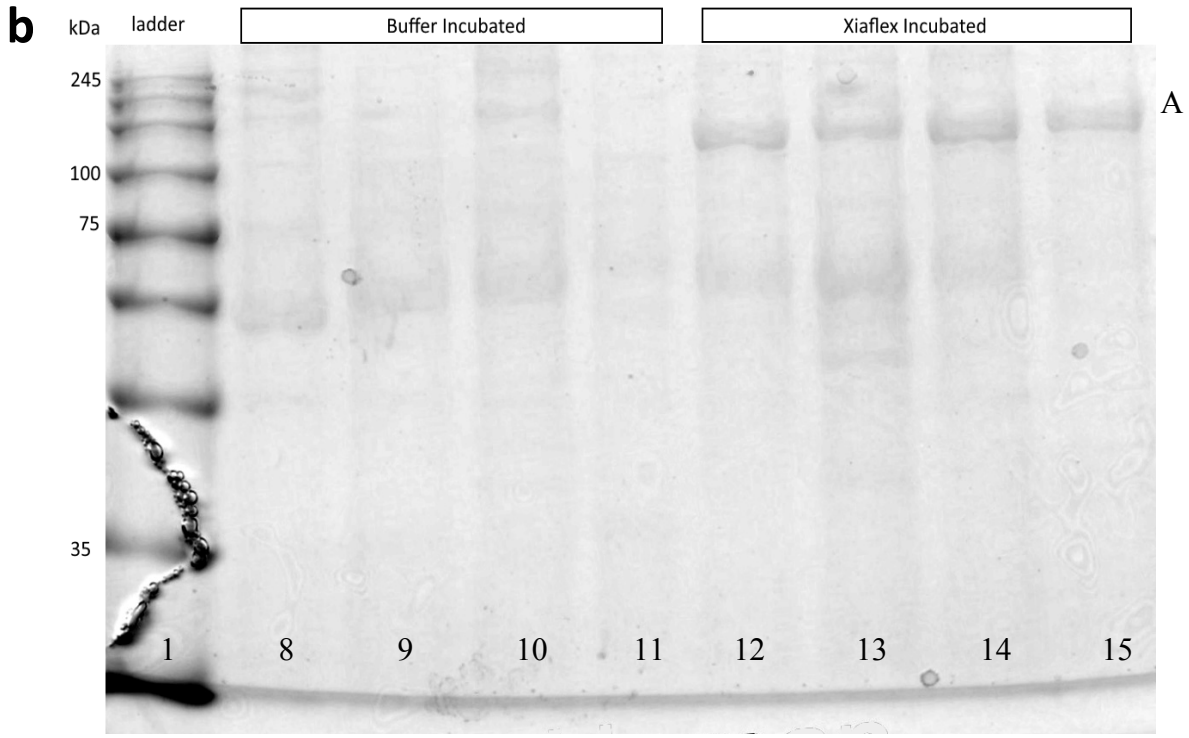
b
kDa
ladder
Buffer Incubated
Xiaflex Incubated
245
100
75
35
A
1
8
9
10
11
12
13
14
15

Figure 20. SDS-PAGE of Supernatant From Normal Rat Posterior Capsule and Diseased Human Posterior Capsule Incubated in Xiaflex® or Buffer. a) Normal rat posterior knee capsules (n=3) and a Xiaflex®-only sample (X) **b)** samples of diseased (osteoarthritis, with (n=3) and without (n=1) contracture) human posterior capsule samples were split in half and each half (5-10mg) was incubated at 37°C in either Xiaflex® (1mg/mL, 50µL) or buffer (50µL) for 24 hours. Tissues were used for histology and the remaining supernatant was analysed by SDS-PAGE in order to attempt to visualize collagen fragments. BLUeye protein ladder (10µL) was used for reference for size determination in lane 1. Gels (12%) were stained with Coomassie blue. Along with 20µL of Laemmli loading buffer, 20µL of sample was loaded and proteins were resolved by gel electrophoresis. Supernatant from Xiaflex®-incubated rat capsule in lanes 2-4, buffer-incubated rat capsule in lanes 5-7; buffer-incubated human capsule in lanes 8-11, and Xiaflex®-incubated human capsule in lanes 12-15. Protein band 'A' is consistent in the lanes loaded with Xiaflex® samples and in the Xiaflex®-only lane. In the rat samples, unique protein bands are found in the Xiaflex® samples ('B', 'C', and 'D'). Using the ladder for a standard curve, molecular weights of these bands are approximately: 113kDa ('A'), 61kDa ('B'), 52kDa ('C'), and 42kDa ('D').

4 DISCUSSION

In this study we focused on the posterior capsule as a major contributing tissue involved in limiting range of motion in a knee flexion contracture. Based on previous studies that showed evidence of a genetic influence on the development of joint contractures and a time-dependent response, a time-series microarray of gene expression in the posterior capsule was carried out in order to deduce the molecular pathways involved during immobilization. Sham-operated rats were chosen as a control in order to account for the effect of surgery.

Overall global fold changes compared to week 1 were examined for both the immobilized and the sham-operated data sets (**Figure 4**). The immobilized data set showed a large number of probe sets with a decrease in expression, which mostly occurs at week 8. The timing of this important decrease in expression could indicate irreversible changes occurring in the connective tissue that leads to articular contractures that are not able to spontaneously recover [34]. Previous biomechanical studies using the same experimental model have shown that ROM gradually decreased up to 8 weeks of immobilization where it thereafter reached a plateau. The reduction in the expression of many genes of the capsule correlated with functional changes of knee mobility and the 8-week time point when no further loss of ROM was measured despite continued immobilization. Additional experiments designed to measure unassisted, spontaneous reversibility established that immobilization for four weeks or more leads to irreversible contractures [14,18,27,34,79]. Homeostasis in synovial joints is known to depend on active and passive mechanical stress [18] for synovial fluid lubrication and transynovial nutrient flow [15]. The lack of joint mobility appears to have an effect on the gene expression in posterior capsule. Gene expression changes were also reflected in the spike of increased transcript levels in the sham-operated data set at 2 and 4 weeks post-operation. It is expected that the rats were less mobile within the few days after surgery (week 1) and a stimulation of gene expression could have occurred once the leg became more mobile at 2 and 4 weeks post-operation.

The Bayesian modelling method of CAGED was used on the microarray data since it took into account the dynamic nature of gene expression over a time course [53]. The longitudinal approach used in our study design generated multiple measurements of gene expression at different time points and CAGED was applied to assess the changes in expression within the immobilized and sham-operated data sets separately. Time series analyses differ from the commonly used static paired design that does not take into account the temporal effects on gene expression. By using an arbitrary 2-fold change in expression as a cut-off value, we were able to eliminate probe sets that did not display a large differential expression in each of the two data sets. Once final lists of differentially expressed genes for the sham-operated and immobilized data sets were generated, common genes were eliminated and a list of 162 genes differentially expressed in the immobilized capsule was further analyzed for biological significance.

Functional analysis revealed three general terms/pathways enriched in the list of differentially expressed genes: muscle contraction, lipids, and extracellular matrix/collagen (**Table 2**). The enrichment of genes in the "cardiomyopathy" pathway was unexpected; however, most of the genes in these clusters are related to muscle contraction including actin, myosins, and troponin. Myosin motors bind to actin filaments via calcium binding to troponin, and a muscle contraction occurs [55]. Expression of these three genes showed mostly down-regulation or variable expression. Actin is a myofibroblast marker and, while fibroblasts do not have a definitive cell marker, intermediate filament and collagen receptor proteins are useful in their identification [80]. *In vitro*, myofibroblasts have been shown to contract collagen gels more than fibroblasts, and expression of actin is required in this process [81]. In previous studies of trauma-related joint contractures, proliferation of myofibroblasts has been reported [32,50]. An increase in myofibroblasts has also been reported in other human fibrotic diseases, including frozen shoulder [51], Dupuytren's disease [11], and elbow contracture [50]. Myofibroblasts are known to be involved in wound healing; stimulation through the inflammation pathway (e.g. with TGFβ and other cytokines) lead to changes in gene expression that causes differentiation of fibroblasts to myofibroblasts [80]. Myofibroblasts actively participate in the inflammatory response to

injury, which coincides more with a contracture model that uses direct trauma to the joint and immobilization [50], but the decrease in related genes discovered through our functional analysis did not coincide with these previous studies. This may be because the rat leg immobilization model we employ decidedly does not cause direct trauma to the joint itself, in particular to the knee posterior capsule, and therefore a wound healing response may not be stimulated.

Lipid pathways were also unexpectedly enriched in the gene list. It is possible that since the posterior capsule is not mechanically stimulated through the stretching and relaxation that occurs through joint movement, there is a reduced requirement for energy and therefore reduced lipid use. Lipid pathways may be down-regulated due to disuse characterizing joint immobilization. Lipids, along with myofibroblasts, have been associated with wound healing, as the phospholipid lysophosphatidic acid has been shown to be an agonist of contraction of myofibroblasts and can be released by cells after stimulation of growth factors [11]. Increased serum lipids have also been associated with Dupuytren's disease [11]. Genes identified as part of triglyceride synthesis in our gene list unique to contractures all clustered together with a decrease in expression over time, emphasizing a consequence of disuse on overall gene expression in the capsule. Interestingly, a case of a patient diagnosed with congenital generalized lipodystrophy type 1 from a mutation in the *AGPAT-2* gene (identified in our gene list) has been reported to have joint contractures [82]. Other lipodystrophies, such as mandibuloacral dysplasia, have also been associated with joint contractures [83]. A decrease in triglycerides has been shown to result in adipocyte lipotoxicity, mitochondrial dysfunction and oxidative stress [84]. A decrease in expression of lipid pathways as a causative role in the development of joint contractures has not yet been explored.

Extracellular matrix, the main component of posterior capsule [36], was, as expected, a biological term found enriched in the gene list. The posterior joint capsule is a connective tissue consisting mostly of fibroblasts surrounded by extensive extracellular matrix that is rich in collagen [37]. CAGED analysis indicated that *Col11a1* (a fibrillar collagen) has a profile of expression that decreased over time. *Col2a1* (found mostly in

hyaline cartilage) and *Col10a1* (hypertrophic cartilage) increased in early time points and decreased in later time points, which may indicate a role in the reversibility of joint contractures in early time points. Previous studies on the spontaneous reversibility of joint contractures using the same rat model showed unassisted reversibility with two weeks of immobilization, and contractures secondary to immobilization of over four weeks were irreversible [27,34]. Chondroadherin (*CHAD*) is clustered by CAGED in the same up-down expression profile. CHAD is a cell-binding protein found in many tissues and is known to strongly associate with collagen, including types I and III [5]. *CHAD* was also identified as differentially expressed in the posterior capsule of osteoarthritis (OA) patients with contracture undergoing total knee arthroplasty (TKA) compared to patients without contracture [5]. Several extracellular matrix degrading matrix metalloproteinases (MMPs) were also enriched in the immobility-only gene list: *MMP3, MMP9*, and *MMP13*. *MMP9*, which specifically degrades type IV and type V collagens [85], showed an increase in expression over time. MMP3 and MMP13 proteins degrade a wide variety of extracellular matrix proteins [86,87], showed a decrease in expression over the time course, possibly influencing collagen homeostasis in the capsule. MMPs have been associated with OA; one study showed an increase in expression of *MMP*s *-1*, *-8* and *-13* in the articular cartilage in patients with advanced OA when compared to normal controls [88]. A rat model that induces OA by cartilage degradation through high intensity running found that intra-articular injections with MMP3 inhibitor protected chondrocytes in the articular cartilage, also signifying that MMPs have an important role in the progression of the disease [86]. *MMP3* is also implicated in rat tendon healing, impairing biomechanical properties of the tendon by remodelling extracellular matrix for angiogenesis [87]. A decrease in MMP3 transcript in our joint contracture model suggests a lower matrix turnover. A more detailed look at the gene expression of MMPs in the joint capsule and the cartilage during immobilization-induced joint contractures may further elucidate their role in the disease.

Cadherin-1 and *cadherin-2*, both up-regulated over time in the immobilized capsule, have important roles in cell adhesion. Adherens junctions, which mediate calcium-dependent inter-cell adhesions, consist of cadherins that extend through the plasma

membrane and also interact intra-cellularly with actin [89]. Interactions between cadherin with actin and myosin are part of the wound healing process, generating the force required for wound closure [90]. Adherens junctions are mechano-sensitive and transmit tension that is known to change the viscoelastic properties of fibroblasts [90]. The lack of mobility during immobilization may be effecting the expression and function of adherens junctions in the posterior capsule. In a previous study using the immobilization rat model, the length of the synovial intima of joints with contractures was significantly shorter than sham-operated and contralateral knees [33]. The potential increase in capsule cell adhesion could explain the shortening of synovial intima length [33]. The folded conformation that the posterior capsule takes when in flexion (**Figure 1a**) may adhere and fuse [33].

In order to validate some of the microarray results, immunohistochemistry was used to compare the transcript and protein levels of *Agpat9, Pck1, P4hb,* and *Hsp47*. Protein levels are more functionally relevant than mRNA levels and the correlation between the two is not always accurate [91]; up to about 60% of the variation in protein levels cannot be explained by mRNA expression [92]. Current high-throughput transcript expression experiments such as microarray contain noise in the analysis. Combined with regulation of translation and protein turnover, there can be low correlation between transcript and protein levels [91]. The collagen-related proteins showed loose correlation between mRNA and protein levels. *HSP47* is a chaperone for collagen folding that interacts with procollagen in folding, assembly, and transport from the endoplasmic reticulum [39,77]. Since collagen is the primary protein found in joint capsule, *HSP47* is important for capsule structure and function. *P4HB* is a post-translational modifier of collagen that provides proline hydroxylation to create the highly prevalent hydroxyproline residues (about 10% of all residues) in collagen [55,76]. Both of these collagen-modifying genes showed overall lower levels both protein and transcript in the immobilized capsule compared to the sham, suggesting that normal folding and post-translational modification of collagen was interrupted in immobilized capsule.

Xiaflex®, a purified mixture of collagenases from the prokaryote *Clostridium histolyticum*, is currently available to patients with fibrosis-related Dupuytren's and

Peyronie's diseases. *C. histolyticum* collagenases have broad-substrate specificity and will degrade many types of collagen into small peptides [54,57]. Purified Xiaflex®, however, has been shown to spare the collagen type IV which composes the basement membrane of neurovasculature [59]. This makes the drug clinically relevant, since the posterior capsule contains nerves and blood vessels [5] that are important for function and cannot be compromised. We tested the use of Xiaflex® in the rat knee model with intra-articular injections after four weeks of immobilization. The treatment significantly increased the range of motion in rat knees given two weeks of remobilization, compared to rats injected with buffer. Some rats were allowed four weeks of remobilization in order to mimic the clinical injection-follow up timeline, however no significant difference was found between drug-injected and buffer-injected legs. The lower sample size of this group and the higher proportion of non-responder rats influenced the results. Non-responder rats were also present in the two weeks remobilization group. The lack of response of some animals could be attributed to the injection missing the intra-articular compartment, which is much smaller and easier to miss in rat knees compared to human knees. Injections were conducted blindly (with no marker) using an anterior-lateral approach and the collagenases may not have reached the posterior capsule. Differences in genetics between the rats would not be an issue since all rats were from an inbred strain and purchased at the same time. Despite the lower response in some of the Xiaflex®-treated knees, there were no other noticeable differences in the biomechanical (ROM) or histological analyses between rats given two or four weeks of remobilization.

The most difference between Xiaflex® and buffer injected knees was apparent at torque 4 (**Figure 8**). Testing of biomechanical outcomes (ROM) was purposefully designed to go from low torque to high torque to reduce error from damaging structures in the leg and subsequently increasing the ROM. Forced motion with the testing of ROM may have caused physical disruption of the large structures of the joint (such as capsular release) or the crosslinking of collagen [41]. This has not been tested with our rat model or electronic arthrometer. One way to do so would be to compare ROM in rat legs measured at only low torques with those measured at only high torques. In clinical uses of Xiaflex®,

manipulations, stretches, and exercises are used post-injection and throughout the 4-6 weeks before follow-up appointment in order to disrupt the fibrous cords; the amount of force applied is determined by the physician and the patient. [93]. The rats in our experiment were left to spontaneously recover; lower torque testing of ROM may have simulated the exercises given to patients by disrupting the weakened collagen framework and therefore allowing a higher ROM in the higher torque, assuming that the destabilization of the extracellular matrix from degradation of collagen by the collagenases at the time of injection was not reversed. Perhaps if the rats were given post-injection exercises, the difference in ROM between treated and untreated knees would be more apparent. Exercises similar to rehabilitation may have also helped in recovery of ROM. By combining collagenase treatment of the soft tissue with physical therapy of the joint, a further increase in ROM may be observed along with improvement in mobility. While posterior capsule contributes the most to the irreversibility of contractures, it is also important to treat the myogenic component of contractures in order to achieve the best possible recovery [27]. Experimental preventative treatment with losartan, an angiotensin II antagonist commonly used to treat high blood pressure, has been shown to prevent loss of muscle mass in hind limb immobilized mice through the IGF-1/Akt/mTOR signalling cascade and promotes muscle remodelling in Marfan syndrome and dystrophin-deficient Duchenne muscular dystrophy mouse models [28]. Interestingly, Marfan syndrome is a hereditary disorder of connective tissue caused by mutations in the *fibrillin* gene, and there has been a case of a neonatal Marfan syndrome patient with flexion contractures described in the literature [94].

Of note, the Xiaflex®-treated rats showed more variation in ROM, including in the contralateral knees (**Figure 10b**). The contralateral knees of Xiaflex®-treated rats showed more ROM than the contralateral knees of the buffer-treated rats (**Figure 14**). The contralateral leg has been previously validated as a suitable control [9]; however evidence in a rabbit model has shown that the contralateral leg of an immobilized animal also develops contracture compared to legs of unoperated rabbits [95]. In patients with OA, those with knee flexion contracture had reduced extension of the contralateral leg,

compared with OA patients without contracture [17]. Contralateral legs are also overworking, making up for the lack of function in its diseased partner. Rat legs are naturally in habitual flexion and when one leg is immobilized, the contralateral leg may compensate by increasing the amount of flexion. It is possible that the increased ROM in Xiaflex®-treated knees allowed for increased mobility in the contralateral leg, and therefore less of a contracture compared to the contralateral legs of the buffer-treated rats. The increased ROM in the contralateral legs of Xiaflex®-treated rats may be indicative of the increased ROM in the experimental legs.

Since collagen is the main component of joint capsule and should be degraded by collagenase treatments, immunohistochemistry was used to visualize COLI and COLIII in the rat knees. Collagen is an extracellular matrix protein; therefore counting positively stained cells is not an appropriate method to determine the change in collagen due to collagenase treatment, especially since ECM in the capsule is much more abundant compared to cells. A quantitative method was used to measure the intensity of collagen I and III staining in the entire field. Compared with the contralateral legs, there was an increase in staining in both groups of experimental legs (buffer or Xiaflex® injected). This may be due to changes in the collagen metabolism resulting from immobilization and drug treatment: increased collagen synthesis, decreased collagen degradation, or an increase in collagen disorganization resulting in exposure of epitopes. The exact epitopes recognized by the ColI and ColIII primary antibodies used are not specified by the manufacturer, however they are related to the triple helical structure [96,97]. There is more collagen staining in posterior capsule of knees treated with Xiaflex® compared with knees injected with buffer. The interpretation of an increased amount of collagen deposition in the drug-treated capsule is incongruous with ROM results. In another explanation, the broad substrate spectrum of the bacterial collagenases, which cleave tropocollagen at many points along the molecule [66], may have disturbed the highly organized collagen fibrils, exposing more collagen epitopes revealed by immunostaining.

The *in vitro* incubations of posterior capsules in Xiaflex® revealed mostly inconclusive results from analyses of both the tissues and the remaining supernatant.

Differences between rat and human samples may be attributed to the use of fresh, normal rat capsules compared to the diseased (osteoarthritis, with and without contracture) human samples that were collected for a different study and had been frozen for a longer period in RNAlater® (Ambion, Inc.) tissue storage solution. The protein gels for analysis of the supernatant revealed fragments of 61kDa, 52kDa, and 42kDa. ColH is known to cleave Type I collagen into 62kDa, 59kDa, and 35kDa, similar to the bands found in the Xiaflex® capsule lanes. Since ColG and ColH work synergistically together to degrade collagen into many small peptides, other fragments may have been small enough to exit the gel or may not have been in high enough concentration to be visualized with Coomassie.

A concern with using collagenase treatments for joint contractures is that there is possible degradation of collagen in the articular cartilage. The main type of collagen in the articular cartilage is type II [55] which distinguishes cartilage from the capsule composed mostly of collagen types I and III [37]. The collagenases in Xiaflex®, however, theoretically do not distinguish between these three types of collagen. Intra-articular injection of *Clostridium histolyticum* ColH (type 2) collagenase has been used in a rabbit model to successfully induce osteoarthritis, however the dose used was much higher (1mg compared to 30µg in our Xiaflex® model) and the injection is performed twice at day 1 and day 4 [98]. A larger volume is used (500µL [98] compared to 50µL), since rabbits are larger than rats and therefore have a larger joint space. Immobility-induced contractures are already known to cause deterioration of articular cartilage [18,78,99]. The most notable change in this rabbit OA model was an increase in surface irregularity [78,100]. Visual examination of the cartilage of the X-Inj and the B-Inj knees show surface irregularity but there does not appear to further degradation with the addition of collagenases. These results were not quantified. If damage to the cartilage is still a concern for use of Xiaflex® in human treatment of joint contractures, there are still potential applications in patients undergoing tri-compartmental knee arthroplasty where the knee, including the articular cartilage, is replaced with artificial parts. For patients who present contractures at TKA surgery, the likelihood of having a post-operative contracture is high [12]. Patients with inoperable end

stage “bone-on-bone” knee joints also do not have cartilage sensitive to collagenase. The use of Xiaflex® would be an option to treat contractures in these patients.

The preclinical data provided in this research shows the potential of the use of Xiaflex® to treat knee flexion contractures. There are many possible avenues for further research. The drug dosage and the timing of treatment (for example, testing collagenase use as a prophylactic) can be adjusted and studied in our rat model. The composition of Xiaflex® as a 1:1 ratio of ColG and ColH [101] could also be adjusted to find a more efficient ratio. Recently a patent has been published that claims a higher ColH to ColG ratio is more efficient, since ColH has higher activity [101]; this could be tested in knee flexion contractures. Clinical trials and preclinical research for the use of Xiaflex® are ongoing for many different conditions, including frozen shoulder syndrome, canine and human lipomas, cellulite, uterine fibroids, and glaucoma [102]. This thesis presents promising data in the future testing of Xiaflex® in clinical trials to treat knee flexion contractures.

In this study, focus was given to the posterior capsule based on previous evidence of its involvement in limiting the ROM in knee flexion contractures. Temporal gene expression in the capsule was examined and pathways relating to extracellular matrix and collagen were prominently enriched. Collagenase treatments currently available to patients with other types of contractures seemed to be an appropriate pharmacological intervention to target collagen in the capsule. Treatment of knee flexion contracture with intra-articular Xiaflex® injections has shown promising results in this rat model. While our study focused on the posterior capsule, other soft tissues may be involved in the development of a contracture and also may have interacted with the Xiaflex® treatment. Overall, there was an increase in range of motion in rat knees with contracture when treated with Xiaflex® and differences in the staining of COLI and COLIII in the posterior capsule. In combination with rehabilitation, this non-surgical option has the potential to improve mobility in patients with contractures.

REFERENCES

[1] M Campbell, N Dudek, and G Trudel, "Joint Contractures," in *Essentials of Physical Medicine and Rehabilitation: Musculoskeletal Disorders, Pain, and Rehabilitation*. Philadelphia, PA: Elsevier Saunders, 2014, pp. 651-655.

[2] R K R Prabhu, N Swaminathan, and L A Harvey, "Passive movements for the treatment and prevention of contractures (Review)," *Cochrane Database Syst Rev*, vol. 12, p. CD009331, 2013.

[3] W P Bevan et al., "Arthrogryposis Multiplex Congenita (Amyoplasia)," *J Pediatr Orthop*, vol. 27, no. 5, pp. 594-600, 2007.

[4] O M Katalinic, L A Harvey, and R D Herbert, "Effectiveness of Stretch for the Treatment and Prevention of Contractures in People With Neurological Conditions: A Systematic Review," *Phys Ther*, vol. 91, no. 1, pp. 11-24, 2011.

[5] T M Campbell, G Trudel, K K Wong, and O Laneuville, "Genome Wide Gene Expression Analysis of the Posterior Capsule in Patients with Osteoarthritis and Knee Flexion Contracture," *J Rheum*, vol. 41, pp. 2232-2239, 2014.

[6] M. Offenbacher et al., "Contractures with Special References in Elderly: Definition and Risk Factors: A Systematic Review with Practical Implications," *Disabil Rehabil*, vol. 36, no. 7, pp. 529-538, 2014.

[7] M R Chen and J L Dragoo, "Arthroscopic Releases for Arthrofibrosis of the Knee," *J Am Acad Orthop Surg*, vol. 19, no. 11, pp. 709-716, 2011.

[8] H Clavet, P C Hebert, D Fergusson, S Doucette, and G Trudel, "Joint contracture following prolonged stay in the intensive care unit," *CMAJ*, vol. 178, no. 6, pp. 691-697, 2008.

[9] G Trudel, H K Uhthoff, and M Brown, "Extent and Direction of Joint Motion Limitation After Prolonged Immobility: An Experimental Study in the Rat," *Arch Phys Med Rehabil*, vol. 80, pp. 1542-1547, 1999.

[10] H J Appell, "Muscular atrophy following immobilisation. A review," *Sports Med*, vol. 10, no. 1, pp. 42-58, 1990.

[11] A J Thurston, "Dupuytren's Disease," *J Bone Joint Surg Br*, vol. 85, no. 4, pp. 469-477, 2003.

[12] M A. Ritter et al., "The Role of Flexion Contracture on Outcomes in Primary Total Knee Arthroplasty," *J Arthroplasty*, vol. 22, no. 8, pp. 1092-1096, 2007.

[13] M P Steultjens, J Dekker, M E van Baar, R A Oostendorp, and J W Bijlsma, "Range of joint motion and disability in patients with osteoarthritis of the knee or hip," *Rheumatology*, vol. 39, no. 9, pp. 955-961, 2000.

[14] E E Peacock, "Some Biochemical and Biophysical Aspects of Joint Stiffness: Role of Collagen Synthesis as Opposed to Altered Molecular Bonding," *Ann Surg*, vol. 164, no. 1, pp. 1-12, 1966.

[15] W H Akeson, D Amiel, M F Abel, S R Garfin, and S L-Y Woo, "Effects of Immobilization on Joints," *Clin Orthop Rel Res*, vol. 219, pp. 28-37, 1987.

[16] A Ando et al., "Distribution of Type A and B Synoviocytes in the Adhesive and Shortened Synovial Membrane during Immobilization of the Knee Joint in Rats," *Tohoku J Exp Med*, vol. 221, pp. 161-168, 2010.

[17] T M Campbell, G Trudel, and O Laneuville, "Knee Flexion Contractures in Patients with Osteoarthritis: Clinical Features and Histologic Characterization of the Posterior Capsule," *PM R*, p. [Epub ahead of print], 2014.

[18] S Lee et al., "Tissue stiffness induced by prolonged immobilization of the rat knee joint and relevance of AGEs (pentosidine)," *Connect Tissue Res*, vol. 51, no. 6, pp. 467-477, 2010.

[19] D Fergusson, B Hutton, and A Drodge, "The Epidemiology of Major Joint Contractures: A Systematic Review of the Literature," *Clin Orthop Rel Res*, vol. 456, pp. 22-29, 2006.

[20] H Clavet, S Doucette, and G Trudel, "Joint contractures in the intensive care unit: quality of life and function 3.3 years after hospital discharge," *Disabil Rehabil*, p. [Epub ahead of print], 2014.

[21] A J Skalsky and C M McDonald, "Prevention and management of limb contractures in neuromuscular diseases," *Phys Med Rehabil Clin N Am*, vol. 23, no. 3, pp. 675-687, 2012.

[22] S T. Goudie, A H. Deakin, A Ahmad, R Maheshwari, and F Picard, "Flexion Contracture Following Primary Total Knee Arthroplasty: Risk Factors and Outcomes," *Orthopedics*, vol. 34, no. 12, pp. e855-e859, 2011.

[23] P Woratanarat, K W Dabney, and F Miller, "Knee capsulotomy for fixed knee flexion contracture," *Acta Orthrop Traumatol Turc*, vol. 43, no. 2, pp. 121-127, 2009.

[24] G Trudel, "Differentiating the myogenic and arthrogenic components of joint contractures. An experimental study on the rat knee joint," *Int J Rehabil Res*, vol. 20, no. 4, pp. 397-404, 1997.

[25] K A Hildebrand, M Zhang, and D A Hart, "Myofibroblast upregulators are elevated in joint capsules in posttraumatic contractures," *Clin Orthop Relat Res*, vol. 456, pp. 85-91, 2007.

[26] C A Reynolds, G S Cummings, P D Andrew, and L J Tillman, "The effect of nontraumatic immobilization on ankle dorsiflexion stiffness in rats," *J Orthop Sports Phys Ther*, vol. 23, no. 1, pp. 27-33, 1996.

[27] G Trudel, O Laneuville, E Coletta, L Goudreau, and H K Uhthoff, "Quantitative and Temporal Differential Recovery of Articular and Muscular Limitations of Knee Joint Contractures: Results in a Rat Model," *J Appl Physiol*, vol. 117, no. 7, pp. 730-737, 2014.

[28] T N Burks et al., "Losartan Restores Skeletal Muscle Remodeling and Protects Against Disuse Atrophy in Sarcopenia," *Sci Transl Med*, vol. 3, no. 82, p. 82ra37, 2011.

[29] A Ando et al., "Remobilization Does Not Restore Immobilization-Induced Adhesion of Capsule and Restricted Joint Motion in Rat Knee Joints," *Tohoku J Exp Med*, vol. 227, pp. 13-22, 2012.

[30] E Chimoto, Y Hagiwara, A Ando, and E Itoi, "Progression of an arthrogenic motion restriction after immobilization in a rat experimental knee model," *Ups J Med Sci*, vol. 112, no. 3, pp. 347-355, 2007.

[31] Y Hagiwara et al., "Expression of type I collagen in the capsule of a contracture knee in a rat model," *Ups J Med Sci*, vol. 112, no. 3, pp. 356-365, 2007.

[32] F Li, S Liu, and C Fan, "Lentivirus-Mediated ERK2 siRNA Reduces Joint Capsule Fibrosis in a Rat Model of Post-Traumatic Joint Contracture," *Int J Mol Sci*, vol. 14, pp. 20833-20844, 2013.

[33] G Trudel, M Jabi, and H K Uhthoff, "Localized and Adaptive Synoviocyte Proliferation Characteristics in Rat Knee Joint Contractures Secondary to Immobility," *Arch Phys Med Rehabil*, vol. 84, pp. 1350-1356, 2003.

[34] G Trudel, J Zhou, and H K Uhthoff, "Four Weeks of Mobility After 8 Weeks of Immobility Fails to Restore Normal Motion," *Clin Orthop Relat Res*, vol. 466, pp. 1239-1244, 2008.

[35] M De Maeseneer et al., "Normal Anatomy and Pathology of the Posterior Capsular Area of the Knee: Findings in Cadaveric Specimens and in Patients," *Am J Roentgenol*, vol. 182, no. 4, pp. 955-962, 2004.

[36] J R Ralphs and M Benjamin, "The joint capsule: structure, composition, ageing and disease," *J Anat*, vol. 184, no. Pt 3, pp. 503-509, 1994.

[37] F Kleftogiannis, C J Handley, and M A Campbell, "Characterization of Extracellular Matrix Macromolecules from Bovine Synovial Capsule," *J Orthop Res*, vol. 12, pp. 365-374, 1994.

[38] F Matsumoto, G Trudel, and H K Uhthoff, "High collagen type I and low collagen type III levels in knee joint contracture," *Acta Orthop Scand*, vol. 73, no. 3, pp. 335-343, 2002.

[39] S Ricard-Blum, "The Collagen Family," in *Extracellular Matrix Biology*. Cold Spring Harbor, NY: Cold Spring Harbor Laboratory Press, 2012, pp. 45-63.

[40] M Abate, C Schiavone, V Salini, and I Andia, "Management of limited joint mobility in diabetic patients," *Diabetes Metab Syndr Obes*, vol. 6, pp. 197-207, 2013.

[41] S L-Y. Woo, J V. Matthews, W H. Akeson, D Amiel, and F R Convery, "Connective Tissue Response to Immobility," *Arthritis Rheum*, vol. 18, no. 3, pp. 257-264, 1975.

[42] J Hall, "Arthrogryposis (multiple congenital contractures): Diagnostic approach to etiology, classification, genetics, and general principles," *European Journal of Medical Genetics*, p. [Epub ahead of print], 2014.

[43] G Trudel, H K Uhthoff, and O Laneuville, "Prothrombin gene expression in articular cartilage with a putative role in cartilage degeneration secondary to joint immobility," *J Rheumatol*, vol. 32, no. 8, pp. 1547-1555, 2005.

[44] G Trudel, N Desaulniers, H K Uhthoff, and O Laneuville, "Different levels of COX-1 and COX-2 enzymes in synoviocytes and chondrocytes during joint contracture formation," *J Rheumatol*, vol. 28, no. 9, pp. 2066-2074, 2001.

[45] G Trudel, A Recklies, and O Laneuville, "Increased Expression of Chitinase 3-like Protein 1 Secondary to Joint Immobility," *Clin Orthop Rel Res*, vol. 456, pp. 92-97, 2007.

[46] G Trudel, H K Uhthoff, and O Laneuville, "Knee joint immobility induces Mcl-1 gene expression in articular chondrocytes," *Biochem Biophys Res Comm*, vol. 333, no. 1, pp. 247-252, 2005.

[47] O Laneuville, J Zhou, H K Uhthoff, and G Trudel, "Genetic Influences on Joint Contractures Secondary to Immobilization," *Clin Orthop Rel Res*, vol. 456, pp. 36-41, 2006.

[48] K A Hildebrand, M Zhang, and D A Hart, "High Rate of Joint Capsule Matrix Turnover in Chronic Human Elbow Contractures," *Clin Orthop Relat Res*, vol. 439, pp. 228-234, 2005.

[49] Y Hagiwara et al., "Expression of transforming growth factor-beta1 and connective tissue growth factor in the capsule in a rat immobilized knee model," *Ups J Med Sci*, vol. 113, no. 2, pp. 221-234, 2008.

[50] K A Hildebrand, C Sutherland, and M Zhang, "Rabbit knee model of post-traumatic joint contractures: the long-term natural history of motion loss and myofibroblasts," *J Orthop Res*, vol. 22, no. 2, pp. 313-320, 2004.

[51] J Lewis, "Frozen shoulder contracture syndrome – Aetiology, diagnosis and management," *Man Ther*, vol. 20, no. 1, pp. 2-9, 2015.

[52] Affymetrix. (2005) GeneChip® Microarrays: Student Manual. [Online]. http://www.affymetrix.com/estore/about_affymetrix/outreach/educator/microarray_curricula.affx

[53] M Ramoni, P Sebastiani, and I S Kohane, "Cluster analysis of gene expression dynamics," *PNAS*, vol. 99, no. 14, pp. 9121-9126, 2002.

[54] U Eckhard et al., "Biochemical characterization of the catalytic domains of three different clostridial collagenases," *Biol Chem*, vol. 390, no. 1, pp. 11-18, 2009.

[55] D Voet and J G Voet, *Biochemistry*. Hoboken, NJ: Wiley, 2004.

[56] T Toyoshima et al., "Collagen-Binding Domain of a Clostridium histolyticum Collagenase Exhibits a Broad Substrate Spectrum Both in vitro and in vivo," *Connect Tissue Res*, vol. 42, no. 4, pp. 281-290, 2001.

[57] U Eckhard, P Huesgen, H Brandsetter, and CM Overall, "Proteomic protease specificity profiling of clostridial collagenases reveals their intrinsic nature as dedicated degraders of collagen," *J Proteomics*, vol. 100, pp. 102-114, 2014.

[58] H A Bird, "Joint Hypermobility," *Musckuloskeletal Care*, vol. 5, no. 1, pp. 4-19, 2007.

[59] F Syed et al., "In Vitro Study of Novel Collagenase (XIAFLEX(R)) on Dupuytren's Disease Fibroblasts Displays Unique Drug Related Properties," *PLoS ONE*, vol. 7, no. 2, p. e31430, 2012.

[60] G Garaffa, L W Trost, E C Serefoglu, D Ralph, and W J G Hellstrom, "Understanding the Course of Peyronie's Disease," *Int J Clin Pract*, vol. 67, no. 8, pp. 781-788, 2013.

[61] clinicaltrials.gov. (2014, October) Clinical Trials. [Online]. https://clinicaltrials.gov/ct2/show/NCT02006719?term=xiaflex&rank=17

[62] L N Brunengraber, F L Jayes, and P C Leppert, "Injectable Clostridium Histolyticum Collagenase as a Potential Treatment for Uterine Fibroids," *Reprod Sci*, vol. 21, no. 12, pp. 1452-1459, 2014.

[63] R K Davidson et al., "Expression profiling of metalloproteinases and their inhibitors in synovium and cartilage," *Arthritis Res Ther*, vol. 8, no. 4, p. R124, 2006.

[64] S T L Philominathan, T Koide, O Matsushita, and J Sakon, "Bacterial collagen-binding domain targets undertwisted regions of collagen," *Protein Sci*, vol. 21, no. 10, pp. 1554-1565, 2012.

[65] A G Breite, R C MaCarthy, and F E Dwulet, "Characterization and Functional Assessment of Clostridium Histolyticum Class I (C1) Collagenases and the Synergistic Degradation of Native Collagen in Enzyme Mixtures Containing Class II (C2) Collagenase," *Transplant Proc*, vol. 43, no. 9, pp. 3171-3175, 2011.

[66] M F French, K A Mookhtiar, and H E Van Wart, "Limited Proteolysis of Type I Collagen at Hyperreactive Sites by Class I and II Clostridium histolyticum Collagenases: Complementary Digestion Patterns," *Biochemistry*, vol. 26, no. 3, pp. 681-687, 1987.

[67] D W Huang, B T Sherman, and R A Lempicki, "Systematic and integrative analysis of large gene lists using DAVID bioinformatics resources," *Nat Protoc*, vol. 4, no. 1, pp. 44-57, 2009.

[68] P D'Eustachio, "Reactome Knowledgebase of Human Biological Pathways and Processes," *Methods Mol Bio*, vol. 694, pp. 49-61, 2011.

[69] R Core Team. (2014) R: A language and environment for statistical. [Online]. http://www.R-project.org/

[70] C A Schneider, W S Rasband, and K W Eliceiri, "NIH Image to ImageJ: 25 years of image analysis," *Nat Methods*, vol. 9, pp. 671-675, 2012.

[71] D Bates, Maechler, M, B Bolker, and S Walker. (2014) lme4: Linear mixed-effects models using Eigen and S4. [Online]. http://CRAN.R-project.org/package=lme4

[72] M Lamar Jones. (2010) Mastering the Trichrome Stain. [Online]. http://www.dako.com/28829_2010_conn14_trichrome_stain_jones.pdf

[73] Affymetrix. (2007) Data Sheet: GeneChip® Rat Genome 230 Arrays. [Online]. http://media.affymetrix.com/support/technical/datasheets/rg230arrays_datasheet.pdf

[74] G Dennis Jr et al., "DAVID: Database for Annotation, Visualization, and Integrated Discovery," *Genome Biol*, vol. 4, p. R60, 2003.

[75] K I Kivirikko and J Myllyharju, "Prolyl 4-hydroxylases and their protein disulfide isomerase subunit," *Matrix Biol*, vol. 16, no. 7, pp. 357-368, 1998.

[76] R Wilson, J F Lees, and N J Bulleid, "Protein disulfide Isomerase Acts as a Molecular Chaperone during the Assembly of Procollagen," *J Biol Chem*, vol. 273, no. 16, pp. 9637-9643, 1998.

[77] M Tasab, M R Batten, and N J Bulleid, "Hsp47: a molecular chaperone that interacts with and stabilizes correctly-folded procollagen," *EMBO J*, vol. 19, no. 10, pp. 2204-2211, 2000.

[78] G Trudel, K Himori, L Goudreau, and H K Uhthoff, "Measurement of Articular Cartilage Surface Irregularity in Rat Knee Contracture," *J Rheum*, vol. 30, pp. 2218-2225, 2003.

[79] G Trudel, H K Uhthoff, L Goudreau, and O Laneuville, "Quantitative analysis of the reversibility of knee flexion contractures with time: an experimental study using the rat model," *BMC Musculoskelet Disord*, vol. 15, p. 338, 2014.

[80] J Baum and H Duffy, "Fibroblasts and Myofibroblasts: What are we talking about?," *J Cardiovasc Pharmacol*, vol. 57, no. 4, pp. 376-379, 2011.

[81] J J Tomasek, G Gabbiani, B Hinz, C Chaponnier, and R A Brown, "Myofibroblasts and mechano-regulation of connective tissue remodelling," *Nat Rev Mol Cell Bio*, vol. 3, no. 5, pp. 349-363, 2002.

[82] A Haghighi et al., "Identification of a novel nonsense mutation and a missense substitution in the AGPAT2 gene causing congenital generalized lipodystrophy type 1," *Eur J Med Genet*, vol. 55, no. 11, pp. 620-624, 2012.

[83] A Garg, "Clinical review: Lipodystrophies: genetic and acquired body fat disorders," *J Clin Endocrinol Metab*, vol. 96, no. 11, pp. 3313-3325, 2011.

[84] C Vigouroux, M Caron-Debarle, C Le Dour, J Magré, and J Capeau, "Molecular mechanisms of human lipodystrophies: from adipocyte lipid droplet to oxidative stress and lipotoxicity," *Int J Biochem Cell Biol*, vol. 43, no. 6, pp. 862-876, 2011.

[85] D Ulrich, F Ulrich, A Piatkowski, and N Pallua, "Expression of matrix metalloproteinases and their inhibitors in cords and nodules of patients with Dupuytren's disease," *Arch Orthop Trauma Surg*, vol. 129, no. 11, pp. 1453-1459, 2009.

[86] G-X Ni et al., "Matrix metalloproteinase-3 inhibitor retards treadmill running-induced cartilage degradation in rats," *Arthritis Res Ther*, vol. 13, no. 6, p. R192, 2011.

[87] H Sahin, N Tholema, W Petersen, M J Raschke, and R Stange, "Impaired biomechanical properties correlate with neoangiogenesis as well as VEGF and MMP-3 expression during rat patellar tendon healing," *J Orthop Res*, vol. 30, no. 12, pp. 1952-1957, 2012.

[88] T Aigner, A Zien, D Hanish, and R Zimmer, "Gene Expression in Chondrocytes Assessed with Use of Microarrays," *JBJS Am*, vol. 85A(Suppl 2), pp. 117-123, 2003.

[89] J S Verhoekx et al., "Isometric contraction of Dupuytren's myofibroblasts is inhibited by blocking intercellular junctions," *J Invest Dermatol*, vol. 133, no. 12, pp. 2664-2671, 2013.

[90] K S Ko, P D Arora, and C A G McCulloch, "Cadherins Mediate Intercellular Mechanical Signaling in Fibroblasts by Activation of Stretch-sensitive Calcium-permeable Channels," *J Biol Chem*, vol. 276, pp. 35967-35977, 2001.

[91] D Greenbaum, C Colangelo, K Williams, and M Gerstein, "Comparing protein abundance and mRNA expression levels on genomic scale," *Genome Biol*, vol. 4, no. 9, p. 117, 2003.

[92] C Vogel and E M Marcotte, "Insights into the regulation of protein abundance from proteomic and transcriptomic analyses," *Nat Rev Genet*, vol. 13, no. 4, pp. 227-232, 2012.

[93] Auxillium Pharmaceuticals. (2013, December) Xiaflex Prescribing Information and Medication Guide. [Online]. https://www.xiaflex.com/assets/XIAFLEX-PI-and-MedGuide-Combined-20131206-ver-e.pdf

[94] J Sutherell et al., "Novel fibrillin 1 mutation in a case of neonatal Marfan syndrome: the increasing importance of early recognition," *Congenit Heart Dis*, vol. 2, no. 5, pp. 342-346, 2007.

[95] M P Abdel et al., "Effects of joint contracture on the contralateral unoperated limb in a rabbit knee contracture model: a biomechanical and genetic study," *J Orthop Res*, vol. 30, no. 10, pp. 1581-1585, 2012.

[96] GeneTex. Collagen I antibody. [Online]. http://www.genetex.com/Collagen-I-antibody-GTX20292.html

[97] Bioss Antibodies. RABBIT ANTI-COLLAGEN III POLYCLONAL ANTIBODY. [Online]. http://biossusa.com/store/bs-0549r.html

[98] T Kikuchi, T Sakuta, and T Yamaguchi, "Intra-articular injection of collagenase induces experimental oesteoarthritis in mature rabbits," *Osteoarthritis Cartilage*, vol. 6, no. 3, pp. 177-186, 1998.

[99] T Matsuzaki, S Yoshida, S Kojima, M Watanabe, and M Hoso, "Influence of ROM Exercise on the Joint Components during Immobilization," *J Phys Ther Sci*, vol. 25, pp. 1547-1551, 2013.

[100] G Trudel, K Himori, and H K Uhthoff, "Contrasting Alterations of Apposed and Unapposed Articular Cartilage During Joint Contracture Formation," *Arch Phys Med Rehabil*, vol. 86, pp. 90-97, 2005.

[101] Juan Ramón Muñoz Montano, "Collagenase g and collagenase h compositions for the treatment of diseases involving alterations of collagen," US 20130287759 A1, 2013.

[102] Biospecifics Technologies Corp. (2015, March) Events and Presentation. [Online]. http://investors.biospecifics.com/index.php?s=63

CONTRIBUTIONS OF COLLABORATORS

Dr. Odette Laneuville: Thesis supervisor – project direction and guidance; lead the genome-wide expression project as outlined in the Methods section; collaborator in quantification of cell staining; collaborator in immobilization and remobilization surgeries.

Génome Québec: performed microarray hybridization after receiving isolated RNA.

Dr. Paola Sebastiani and Dr. Fangui Sun: CAGED analysis of genome-wide expression time-series data

Winnie Nie: Participated in measuring range of motion with arthrometer; paraffin embedding of knee joints; sectioning some of the knee joints to slides; sectioning capsule tissue to slides

Animal Care Facility: Care of animals post-surgery; Eileen Franklin and Kim Yates for assistance during surgeries

Dr. Ana Giassi and the members of the Histology Core Lab: tissue processing; capsule embedding in agar; Masson trichrome staining

CURRICULUM VITAE

Kayleigh Wong

Education

2012-2015	**Master of Science** (Biochemistry) University of Ottawa
2007-2012	**Bachelor of Science** with Honours, CO-OP, *summa cum laude* Major Biochemistry, Minor Theatre University of Ottawa

Awards and Honours

2013-2014	**Ontario Graduate Scholarship**, University of Ottawa and Government of Ontario *Merit-based scholarship for support in graduate studies ($15,000)*
2012-2013	**Queen Elizabeth II Graduate Scholarship in Science and Technology**, University of Ottawa and Government of Ontario *Merit-based scholarship for support in graduate studies in science and technology disciplines ($15,000)*
2012-2014	**Excellence Scholarship**, University of Ottawa *Awarded to students with excellent academic records (tuition)*
2007-2012	**Dean's Honour List**, University of Ottawa *Awarded to undergraduate students who demonstrate academic excellence*
2007-2012	**Admission Scholarship**, University of Ottawa *Awarded to matriculating high school students who exhibit and maintain an excellent academic record ($16,000)*
2010	**Undergraduate Research Opportunity Program**, University of Ottawa *Awarded to undergraduate students to participate in research with a faculty sponsor ($1,000)*
2007	**Governor General's Bronze Medal**, Rideau Hall *Awarded to the student who achieves the highest average upon graduating from a secondary school*

Research

Published:

Campbell TM, Trudel G, **Wong KK**, Laneuville, O. 2014. *Genome wide Gene Expression Analysis of the Posterior Capsule in Patients with Osteoarthritis and Knee Flexion Contracture*. The Journal of Rheumatology 41(11):2232-9.

Submitted:

Wong K, Sun F, Sebastiani P, Trudel G, Laneuville O. *Temporal Gene Expression Profiling of the Rat Knee Joint Capsule During Immobilization-Induced Joint Contractures*. Under review at BioMed Central: Musculoskeletal Disorders.

Wong K, Trudel G, Laneuville O. *Noninflammatory Joint Contractures Arising From Immobility: Animal Models to Future Treatments.* Under review for Special Issue on "Physiopathology of Noninflammatory Diseases of the Musculoskeletal System: From Basic Biology to Therapy," BioMed Research International: Cell Biology.

In Preparation:

Wong K, Laneuville O. *Collagenase Intervention Increases Range of Motion in Knee Flexion Contractures*. In preparation for submission to Journal of Orthopaedic Research

Presentations:

2014 *Pharmacological intervention targeting collagen degradation increases range of motion in rat knee flexion contractures*
Wong K, Laneuville O. Seminar Presentation, Biology, Microbiology and Immunology Seminar Day, University of Ottawa

2013 *Lipid and collagen pathways in the posterior capsule of rat knee joints with contractures secondary to immobilization*
Wong K, Laneuville O. Poster Presentation, Biology, Microbiology and Immunology Poster Day, University of Ottawa

2011 *Do Deamidated Product-Related Impurities Reduce Shelf-Life for Therapeutic Protein Drugs Like Interferon?*
Wong K, Smith S, Hefford MA, Poster Presentation, Health Canada Science Forum

2010 *Revisiting Morgan: Spatial Control of Fin Growth in Danio rerio (zebrafish)*
Wong K, Rolland-Lagan AG, Akimenko MA. Poster presentation, Undergraduate Research Opportunity Program Symposium, University of Ottawa

Work

2015	Technician Level 2 Bone and Joint Lab, Faculty of Medicine, University of Ottawa *Short-term contract, participating in various research projects including optimization of protocols for experiments involving the ISS (NASA) and bed rest studies (ESA)*
2013-2014	Teaching Assistant – Lab Demonstrator Faculty of Science, University of Ottawa *Conducted teaching labs and corrected lab reports for undergraduate biochemistry and molecular biology courses*
2012	Teaching Assistant – Exam Proctor and Corrector Faculty of Science, University of Ottawa *Proctor and corrector of exams for undergraduate molecular biology*
2011	Co-op Student – Research Assistant Health Canada Centre for Vaccine Evaluation *Conducted protein drug stability research in a lab under the supervision of Dr. Mary Hefford*
2010	Co-op and UROP Student – Research Assistant University of Ottawa *Conducted fin regeneration research in a developmental biology lab under the supervision of Dr. Anne-Gaëlle Rolland-Lagan*
2009	Co-op Student – Junior Prevention Officer Environment Canada Environmental Emergencies Division *Contributed to a database of chemicals and their properties through intensive research of information found online and in print*

Leadership and Extracurricular Activities

2012-2014	**Member-at-large**, Department of Biochemistry, Microbiology and Immunology Graduate Student Association, University of Ottawa *Organized a day trip to Montreal for students, organized a social night for student recruitment day, participated in organization of various student events*
2012-2014	**Writer**, Department of Biochemistry, Microbiology and Immunology Bulletin, University of Ottawa *Wrote "Mythbusters" column for the departmental newsletter, debunking popular trends in science and health*

2011-2015 **Volunteer**, Live Work Play, Ottawa
Companion for a person with an intellectual disability and volunteer for weekly evening activities

2008-2014 **Volunteer Server/Bartender**, Ottawa Bluesfest and Ottawa Folk Fest
Serving patrons at The Winery/Beer Tent. The Winery volunteer of the year for 2012

2010-2013 **Actor**, Ottawa Storytellers
Performer and production assistant for annual murder mystery at the Billings Estate

2009-2013 **Volunteer Server/Bartender,** Magnetic North Theatre Festival, Ottawa
Serving patrons at the festival bar and assisted in a performance of Portage *(2009)*

2011-2012 **Volunteer**, Canadian AIDS Society, Ottawa
Completed administrative and clerical tasks; assisted with and participated in World AIDS Day Gala 2012

Skills

Laboratory skills: nucleic acid and protein extraction and purification, immunohistochemistry, H&E staining, paraffin embedding and microtomy, microscopy, Western blotting, circular dichroism spectroscopy, PCR, fluorescence spectroscopy, chromatography (FPLC, HPLC, immobilized metal affinity, thin layer), research with animals (rat and zebrafish).

Computer skills: bioinformatics tools such as FlexArray and BLAST, microarray, statistical analysis and figure building using the R environment, ImageJ, experience with MATLAB, basic computer skills including Microsoft Office applications, CorelDraw.

Other Interests

Film and Television
Gastronomy
Group Fitness
Make-up and Beauty
Theatre
Travel